Ontario

Ontario Geological Survey
Open File Report 5998

Mineral Potential of Proterozoic Keweenawan Intrusions: Implications of Major and Trace Element Geochemical Data from Bimodal Mafic and Felsic Volcanic Sequences of Mamainse Point and the Black Bay Peninsula, Ontario

1999

Ontario

ONTARIO GEOLOGICAL SURVEY

Open File Report 5998

Mineral Potential of Proterozoic Keweenawan Intrusions: Implications of Major and Trace Element Geochemical Data from Bimodal Mafic and Felsic Volcanic Sequences of Mamainse Point and the Black Bay Peninsula, Ontario

by

P.C. Lightfoot, R.P. Sage, W. Doherty, A.J. Naldrett, and R.H. Sutcliffe

1999

Lightfoot, P.C., Sage, R.P., Doherty, W., Naldrett, A.J. and Sutcliffe, R.H. 1999. Mineral potential of Proterozoic Keweenawan intrusions: implications of major and trace element geochemical data from bimodal mafic and felsic volcanic sequences of Mamainse Point and the Black Bay Peninsula, Ontario; Ontario Geological Survey, Open File Report 5998, 57p.

Open File Reports of the Ontario Geological Survey are available for viewing at the Mines Library in Sudbury, at the Mines and Minerals Information Centre in Toronto, and at the regional Mines and Minerals office whose district includes the area covered by the report (see below).

Copies can be purchased at Publication Sales and the office whose district includes the area covered by the report. Although a particular report may not be in stock at locations other than the Publication Sales office in Sudbury, they can generally be obtained within 3 working days. All telephone, fax, mail and e-mail orders should be directed to the Publication Sales office in Sudbury. Use of VISA or MasterCard ensures the fastest possible service. Cheques or money orders should be made payable to the *Minister of Finance.*

Mines and Minerals Information Centre (MMIC) Macdonald Block, Room M2-17 900 Bay St. Toronto, Ontario M7A 1C3	Tel:	(416) 314-3800 1-800-665-4480(toll free inside Ontario)
Mines Library 933 Ramsey Lake Road, Level A3 Sudbury, Ontario P3E 6B5	Tel:	(705) 670-5615
Publication Sales 933 Ramsey Lake Rd., Level A3 Sudbury, Ontario P3E 6B5	Tel: Fax: E-mail:	(705) 670-5691(local) 1-888-415-9847(toll-free) (705) 670-5770 pubsales@ndm.gov.on.ca

Regional Mines and Minerals Offices:

Kenora - Suite 104, 810 Robertson St., Kenora P9N 4J2

Kirkland Lake - 10 Government Rd. E., Kirkland Lake P2N 1A8

Red Lake - Box 324, Ontario Government Building, Red Lake P0V 2M0

Sault Ste. Marie - 70 Foster Dr., Ste. 200, Sault Ste. Marie P6A 6V8

Sioux Lookout - Box 3000, Queen and Fourth, Sioux Lookout P8T 1C6

Southern Ontario - P.O. Bag Service 43, Old Troy Rd., Tweed K0K 3J0

Sudbury - Level B3, 933 Ramsey Lake Rd., Sudbury P3E 6B5

Thunder Bay - Suite B002, 435 James St. S., Thunder Bay P7E 6S7

Timmins - Ontario Government Complex, P.O. Bag 3060, Hwy. 101 East, South Porcupine P0N 1H0

Toronto - MMIC, Macdonald Block, Room M2-17, 900 Bay St., Toronto M7A 1C3

Cette publication est disponible en anglais seulement.

Lightfoot, P.C., Sage, R.P., Doherty, W., Naldrett, A.J. and Sutcliffe, R.H. 1999. Mineral potential of Proterozoic Keweenawan intrusions: implications of major and trace element geochemical data from bimodal mafic and felsic volcanic sequences of Mamainse Point and the Black Bay Peninsula, Ontario; Ontario Geological Survey, Open File Report 5998, 57p.

Contents

FIGURES

TABLES

Abstract

A 0-30km thick, 1.1 Ga sequence of basaltic volcanic rocks and clastic sediments fill the aborted North American Midcontinent Rift system in the Lake Superior region. We report major- and trace-element data for stratigraphical sequences of lavas from the 6 km thick Mamainse Point Volcanic Group (MPVG) at Mamainse Point, and the 3km thick Osler Volcanic Group (OVG) exposed on the Black Bay Peninsula. The OVG flows belong to at least two different magma types. The OVG Lower Formation is a high-Ti series, whereas the OVG Central and Upper Formations are a low-Ti series. The high-Ti series lavas are high-Cr lavas with very low Al_2O_3 and have elevated Gd/Yb, Zr/Y, Ti/Y and Ce/Nb but low La/Sm. The most primitive and least contaminated Central and Upper Formation OVG lavas belong to a high-Al, low-Cr series with low Ti/Y and variable Ce/Nb and characteristically have low La/Sm and Gd/Yb.

The MPVG lavas include members which broadly resemble the Lower Formation of the OVG lavas; these include lavas of Groups 1 and 2a. However, the MPVG lavas of Groups 1 and 2a have lower Zr/Y, La/Lu and Gd/Yb than Lower Formation flows of the Osler Group. Groups 6 and 7 of the Upper Division of MPVG lavas are low-Cr, -La/Sm, -Gd/Yb, and -La/Lu flows, which belong to a high-Al series. Lavas of Groups 2b, 3, and 9 are all probably contaminated versions of either Group 1+2a type magma, or Group 6+7 type magma. Only Group 5 of the MPVG lavas is entirely different in composition, with remarkably low Gd/Yb, Zr/Y, La/Lu, Cr, Zr, but variable MgO and La/Sm.

The rhyolites of the MPVG and OVG occur at discrete horizons in the stratigraphy and appear to be compositionally quite different at the two locations. Major and trace element data suggest that the basal members of the OVG and MPVG are represented by and probably evolved from high-Mg primitive liquids, whereas the remainder of the stratigraphy records lavas of essentially tholeiitic composition. Partial melting appears to have occurred deeper in the earlier lavas whereas the degree of source melting appears to have achieved a maximum in the Group 5 lavas at Mamainse Point. Trace element data indicate that the Osler Series lavas have seen significantly more crustal contamination than the MPVG lavas, whereas the Upper Division of the MPVG series record evidence for protracted polybaric fractionation, perhaps much like the North Shore Volcanic Group (NSVG). Assimilation coupled to fractional crystallisation is recognised in Group 5 of the MPVG and possibly also in the Central and Upper Formations of the OVG. However, as the amount of fractional crystallisation relative to the amount of crustal contamination is low in the Central and Upper Formation lavas of the Osler, we suggest that the variation more likely reflects mixing between mantle-derived tholeiitic magmas and rhyolitic melts of crustal derivation.

The trace element signatures of the Lower Formation OVG and lower Division MPVG lavas are similar to those of young uncontaminated asthenospheric-mantle-derived oceanic basalts from above mantle plumes although others speculate that a contribution from the continental lithospheric mantle can be recognized in the earliest MPVG lavas (Shirey et al 1994). In the Group 5 MPVG lavas, elemental signatures of enriched MORB-type lavas are recognised. The trace element signatures of least-contaminated Central and Upper Formation Osler lavas and Upper Division MPVG lavas are essentially similar to Phanerozoic within-plate basalts, and probably sample wide-spread asthenospheric mantle and domains of stable continental lithospheric mantle.

Compositionally, the Lower Formation of the OVG and the Lower Division of the MPVG series are similar to the primitive rocks of the Nipigon Plate, whereas the Central and Upper Formations of the Osler series and the Upper Division of the MPVG series have compositions similar to the Fe-Ti transitional basalts of the NSVG and may be extrusive equivalents of the Logan diabase sills.

Geological, petrological, and geochemical similarities exist between the Noril'sk Region of the Siberian Trap and the Keweenawan Midcontinent Rift. These have mineral potential implications. Both have lava sequences which appear to represent a transition from plume–induced rifting to lithospheric extension; both sequences record evidence of crustal contamination, and although the evidence is not as strong in the Keweenawan (especially the MPVG lavas), both show variable degrees of Ni and Cu depletion which have been attributed to sulphide segregation (Naldrett & Lightfoot 1993). These features, together with the very large number of Keweenawan intrusions in the Nipigon Plate cutting the OVG lavas, and the presence of mineralised intrusions such as the Duluth Complex and the Crystal Lake Gabbro, suggest that exploration models should not dismiss the possibility that the Keweenawan Midcontinent Rift hosts a giant Noril'sk type Ni–Cu–PGE sulphide deposit.

Mineral Potential of Proterozoic Keweenawan Intrusions: Implications of Major and Trace Element Geochemical Data from Bimodal Felsic and Volcanic Sequences of Mamainse Point and the Black Bay Peninsula, Ontario

P.C. Lightfoot[1], R.P. Sage[2], W. Doherty[3], A.J. Naldrett[4], and R.H. Sutcliffe[5]

[1] Inco Limited, Exploration Office, Highway 17 W, Copper Cliff, Ontario, P0M 1N0, CANADA.

[2] Precambrian Geoscience Section, Ontario Geological Survey, 933 Ramsey Lake Road, B7, Sudbury, Ontario, P3E 6B5, CANADA.

[3] Geological Survey of Canada, 601 Booth Street, Ottawa, Ontario, K1A OE8, CANADA.

[4] Department of Geology, University of Toronto, Toronto, Ontario, M5S 1A1, CANADA.

[5] Sutcliffe Geological Consultants Inc., 793 William Street, London, Ontario, N5Y 2R7, CANADA.

Introduction

THIS STUDY

This study was designed to determine whether any similarities exist between the rocks of the Keweenawan Midcontinent Rift and the Siberian Trap at Noril'sk. We document evidence for crustal contamination and limited chalcophile element depletion in the Keweenawan lavas and compare these chemical signatures with the Permotriassic Siberian Trap lavas of the Noril'sk Region, Russia (Naldrett et al., 1992; Naldrett and Lightfoot, 1993; Lightfoot et al., 1990, 1993, 1994; Brugmann et al., 1993, Hawkesworth et al., 1995) where comagmatic intrusions host the giant Ni-Cu-platinum group element (PGE) deposits.

This study, begun in 1987, was not intended to reproduce the results of recent academic geochemical studies on the Mamainse Point Volcanic Group (MPVG) stratigraphy (Berg and Klewin, 1988; Klewin and Berg, 1990, 1991; Klewin, 1989; Shirey et. al., 1994). Rather, we built on these results by presenting new geochemical data for the MPVG, comparing and contrasting these data with the more extensive and better exposed Osler Volcanic Group (OVG), and evaluate the nature of the source regions of both tholeiitic and rhyolitic magmas. This comparison examines volcanic rocks proximal (OVG) to the proposed plume initiated triple junction (Burke and Dewey, 1973) and volcanic rocks distal to the proposed mantle plume (MPVG). Stratigraphic controlled ratios of incompatible trace elements together with other geochemical criteria provide a window whereby we can "see through" the effects of alteration, shallow-level fractional crystallisation and various degrees of melting of the mantle source. We attempt to investigate the mechanism(s) by which continental crust has contributed to bi-modal volcanism and then compare and contrast the magma types from sections of the stratigraphy in two different sub-basins of the Keweenawan Midcontinent Rift. Using criteria developed in Phanerozoic settings, we investigate whether the geochemical data provide any evidence for a contribution from the deep asthensopheric mantle in the form of a plume, and speculate regarding the relative roles of mantle plumes versus regional lithospheric extension in the formation of the Midcontinent Rift. Finally, we note the similarity in setting, geology, petrology and geochemistry of the Keweenawan Midcontinent Rift to part of the Siberian Trap.

MANTLE PLUMES AND LITHOSPHERIC RIFTING

The importance of mantle plumes in the generation of Continental Flood Basalts (CFB), and as possible causes of crustal extension, remains rather controversial. At issue is whether plumes initiate partial melting and contribute to continental break-up (Campbell and Griffiths, 1990), or whether they play a passive role where continental magmatism is a response to crustal extension over an area of anomalously hot mantle (Peate et al., 1990). The different melting regimes within these two settings have different implications for mineral potential. In this study we look at the extent to which uncontaminated asthenospheric mantle (? plume source), shallow convecting mantle mid-ocean ridge basalt (MORB-type source), and remobilised lithospheric mantle or continental crust have contributed to the observed volcanism in the Keweenawan Midcontinent Rift. Of specific importance is whether these lavas record geochemical evidence for: 1. A deep mantle plume component such as that seen in the Deccan Trap CFB (Cox and Hawkesworth, 1984, 1985; Lightfoot and Hawkesworth, 1988) and Siberian Trap CFB (Lightfoot et al., 1993, 1994), and 2. Whether they record geochemical evidence for shallow melting in an intracratonic rift zone by lithospheric extension such as that seen in the Parana Flood Basalt Province (Peate et. al., 1992). In the former case, this would imply that the evolution of the Proterozoic Midcontinent Rift is driven by a deep mantle event such as those recorded in Phanerozoic oceanic and continental settings. In the later case, it would imply that the Midcontinent Rift magmas are derived from relatively shallow depths in the mantle and reflect regional tectonic forces giving rise to lithospheric extension. Recent work suggests that the geochemical signatures of rocks generated in response to mantle plumes versus those resulting from lithospheric extension may be distinguished (Gallagher and Hawkesworth, 1992; Bradshaw et al., 1993).

STRATIGRAPHICALLY CONTROLLED GEOCHEMICAL STUDIES OF CFB

Stratigraphic studies have an important role in the investigation of CFB provinces in relating internal structure and sequential development of the lava pile (e.g. Columbia River Basalts: Hooper, 1982, Deccan Trap: Cox and Hawkesworth, 1985; Devey and Lightfoot, 1986; Beane et al., 1986, Siberian Trap: Lightfoot et al, 1990, 1993, 1994; Naldrett et al., 1992; Hawkesworth et al., 1995). A 0-30km thick, 1.1 Ga sequence of CFB basaltic volcanic rocks and clastic sedimentary rock fills the aborted North American Midcontinent Rift system in the Lake Superior region (Cannon et al., 1989) (Fig. 1). Exposed thicknesses of lavas and clastic sedimentary rocks, located in Fig 2a, exceed 8km in the North Shore Volcanic Group (NSVG; Green, 1982; 1983), exceed 3km in the Osler Volcanic Group (OVG; Lightfoot et al., 1991a), and are probably greater than 6 km in the Mamainse Point Volcanic Group (MPVG; Massey, 1980; Annells, 1973; Lightfoot et al., 1989; Shirey et. al., 1994). The basalts appear to occupy nine or more separate basins (Green, 1983) beneath Lake Superior. We report and discuss new major and trace element data for stratigraphic sequences of lavas from the margins of two of these basins: the thick (approximately 5000 m) MPVG lavas exposed on a small area of Ontario called Mamainse Point on the eastern margin of the SE limb of the rift, and the laterally far more extensive (approximately 3000 m thick) OVG lavas exposed on the Black Bay Peninsula (Figs. 1 and 2a,b) at the northern margin where the SW and SE limbs meet at the supposed Nipigon Plate aulacogen (Burke and Dewey, 1973; Sutcliffe, 1987).

Chemostratigraphic studies of the Osler Volcanic Group suggest that at least two different magma types are recorded (Lightfoot et. al., 1991a). The lower Formation is more primitive and similar to magmas derived from the asthenospheric mantle as sampled above mantle hot spots. The upper two Formations show a variable tendency to be SiO_2, large-ion-lithophile element (LILE), and light rare earth element (LREE) enriched, perhaps due to crustal contamination (Lightfoot et al., 1991a) or the incorporation of melts from an enriched lithospheric mantle source containing contributions from recycled continental crust (c.f. Lightfoot et. al., 1993). Geochemical data for the NSVG lavas record evidence for protracted fractional crystallisation of one or more magma types (Basaltic Volcanism Study Project, 1981; Brannon, 1984) and the compositions of the Logan sills are similar to the least contaminated Central and Upper Formation lavas. Data for the MPVG suggest a number of different magma types. The Lower Division of the Mamainse Point Group contains picritic and tholeiitic basalts which record evidence of different amounts of partial melting at decreasing depth, periodic replenishment and tapping of magma chambers, crustal contamination and polybaric fractional crystallisation (Klewin and Berg, 1991; Shirey et. al., 1994). These are compositionally more like the Osler series Lower Formation flows. The Upper Division of the MPVG contains tholeiites which record evidence of extensive fractional crystallisation and vigorous eruption of >2000 m of lavas which essentially belong to one magma series (Klewin and Berg, 1991; Shirey et. at., 1994).

Geological Setting

The Keweenawan lavas of the Lake Superior area, along with their associated mafic intrusions (Fig. 1), are the igneous expression of the North American midcontinent gravity high. This gravity high extends from Lake Superior southwest into Kansas, and southeast to south through Michigan into Kentucky. It is interpreted to be an aborted continental rift (Wold and Hinze, 1982; Van Schmus and Hinze, 1985). The lavas rest unconformably on stable Archean and Lower Proterozoic crust. In common with many other continental flood basalt (CFB) sequences, most of the feeder dykes appear to be buried beneath lavas or younger sediments. As many as nine eruptive centres have been recognised (Green, 1977), each with several kilometres thickness of lava.

Seismic studies show that the Moho is 50-55km deep below the central part of Lake Superior. A thin attenuated granitic crust (<10km thick) may be beneath the deepest part of the basin. The on-shore portion of the basin rests on thick crust (25-30km) which is broadly granitic in composition. Seismic profiling of the Lake Superior basin shows that the rift system consists of a series of linked half-grabens of

alternating structural polarity with up to 30 km of volcanics and sediments beneath the lake (Cannon et al., 1989).

The volcanic sequences that we have studied lie unconformably on the Archean and Proterozoic basement along the north shore of Lake Superior. The sequences are marginal to different sub-basins. The OVG is located close to the Nipigon plate area which may be an embryonic triple junction at the northern margin of the main rift (Fig.2a; Sutcliffe, 1987). The MPVG is located on the northern margin of the main rift over 500km to the east (Figs. 2a and 2b). As both sampled sections are located at the margin of two different sub-basins, and as they are dominantly represented by compound flow units, there may be a bias in composition towards the more prolific eruptive events and a bias away from lavas which were erupted in more central areas of the sub-basins.

The paleomagnetic polarity of the OVG lavas records early reversed polarity and later normal polarity with the break corresponding to a point roughly 2900m above the base of the stratigraphy on the Black Bay Peninsula in the Upper Formation (Halls and Pesonen, 1982; Lightfoot et al, 1991a). The MPVG lavas also have reversed followed by normal polarity and Halls and Pesonen (1982) correlate these lavas with the Portage Lake Volcanics of the Keweenawan Peninsula in Michigan rather than the NSVG and OVG lavas. Palmer (1970) and Klewin and Berg (1990) confirmed that the Lower Division flows at Mamainse Point show reverse-normal-reverse polarity and the Upper division has normal polarity (Fig. 4). These lavas correlate with the lower portion of the OVG (Halls and Pesonen, 1982).

GEOLOGY OF THE MAMAINSE POINT VOLCANIC GROUP

The MPVG unconformably overlie Precambrian basement northwest of Sault Ste. Marie, Ontario (Fig. 2a). The flood basalt lavas (Green, 1992) are interbedded with coarse conglomerates and injected by rhyolite and felsite bodies (Fig. 2b). Olivine-rich high-MgO basalts occur near the base of the section (Annells, 1973; Massey, 1980; Berg and Klewin, 1988; Klewin and Berg, 1990; Klewin and Berg, 1991; Shirey et. al., 1994) below the "Great Conglomerate" in a sequence of flows referred to as the Lower Division. Berg and Klewin (1988) use geochemical and textural evidence to suggest that the Mg-rich Lower Division flows were dominantly high-Mg lavas rather than olivine cumulates.

The flows dip 30-55ºW to WSW into Lake Superior, and are cut by numerous NW-SE trending faults. The dip declines from 55º at the base of the sequence to 30º at the top of the sequence. In many places the concordant flows are disrupted by small rhyolite and felsite intrusive and extrusive centres (Annells, 1973).

The sequence of volcanics and clastic sedimentary rocks is estimated to be about 6000 m thick (Fig. 4) along the shoreline section, but the degree of possible repetition by faulting is unclear from field evidence. Of particular concern is the Hibbard Bay fault (Fig. 2b) which may offset the upper part of the stratigraphy, and on which there is no field control on the displacement or throw. About 300 flows make up the entire sequence, and range in thickness from 1.5 to 30m. Many of the flows have lower and upper vesicular zones and some develop ropy pahoehoe surfaces (Annells, 1973). Olivine phyric flows occur within the Lower Division, making up to 20% of the sequence. Coarser-grained ophitic basalts make up the remainder of the Lower and Upper Divisions. The flows carry phenocrysts of plagioclase and pseudomorphed olivine, and rarely the plagioclase crystals are concentrated in flows developing radiating clusters of glomeroporphyritic plagioclase (the "Daisystone" flow; Annells, 1973).

All of the rocks have undergone low-grade hydrothermal metamorphism. Olivine is pseudomorphed by saponite and hematite in all of the flows sampled. Plagioclase is frequently zeolitised, and augite is often entirely altered to chlorite. Alteration minerals are arranged in a crude stratigraphic zonation, similar to that observed in Iceland (e.g. Kristmannsdottir and Tomasson, 1978). Zeolites, and in particular, heulandite and stilbite, are characteristic of the flows above the Great Conglomerate horizon, whereas prehnite and pumpellyite are more common in the underlying flows. Epidote is restricted to highly permeable vesicular zones towards the base of the sequence and to major crosscutting veins and fissures (Richards and Spooner, 1989). In the vicinity of the abandoned Copper Corp Mine property, there is evidence for

magmatic-meteoric fluids mixing to form the chalcocite-rich mineralised fissure veins (Richards and Spooner, 1989); these areas of fluid mixings are localised close to faults and were avoided in this study. The presence of this mineralization perhaps suggest the presence of a deeper Cu-rich? body.

The felsic bodies are composed of quartz porphyry, felsite and flow banded rhyolite. With the exception of the quartz porphyry, they are phenocryst poor rocks, and are compositionally like quartz latites of the Minnesota NSVG (Green, 1971). The thickest stratiform bodies, such as those exposed at Pancake Point, are pale grey to pink, fine-grained, compact rhyolite with some flow banding and scattered feldspar phenocrysts. The quartz porphyries occur as small plugs or thin intrusive sheets. In places, composite sheets of felsic and mafic material are developed which suggest that felsic and mafic lavas were simultaneously mobile (Annells, 1973).

Coarse terrigenous sedimentary rocks comprise 24% of the stratigraphy at Mamainse Point (Klewin and Berg, 1991; Fig. 2b). These include at least three major conglomeratic horizons, one of which is present in the Lower Sequence and carries basaltic clasts (Basaltic Clast Conglomerate; Annells, 1973), and most of which carry clasts of Archean country rocks. The Great Conglomerate separates the Lower and Upper Divisions. Annells (1973) suggests that these conglomerates were deposited in an alluvial fan environment, and on this interpretation, Klewin and Berg (1991) suggest that the conglomerates were derived from local uplifted areas of Archean highlands to the NE.

The deposition of the Great Conglomerate horizon (550m thick in the Mamainse Point road and coastal sections) followed Group 5c, and marks a sudden change in the chemistry of the lavas to an Upper Division characterised by low-Mg-number (0.36-0.48 in Groups 6a and 6b), and very high TiO_2 (1.9-3.2 wt.%) lavas quite different from those of the Lower Division of the MPVG. This break correlates with a change from normal magnetic polarity below the Great Conglomerate, to reversed magnetic polarity within the flow hosted by the Great Conglomerate, to normal magnetic polarity in Group 6 (Halls and Pesonen, 1982).

GEOLOGY AND GEOCHEMISTRY OF THE OSLER VOLCANIC GROUP, BLACK BAY PENINSULA

The OVG lavas of the Black Bay peninsula (Fig. 2a and Lightfoot et. al., 1991a) unconformably overlie Sibley Group sedimentary rocks, and dip gently (10-20^o) southwards into Lake Superior (McIlwaine and Wallace, 1976; Wallace, 1972; 1981; Lightfoot et. al., 1991a). The sequence has been subdivided into Lower, Central, and Upper Formations based on petrographic variations; major, and trace element geochemistry (Lightfoot et al., 1991a). The Lower Formation is porphyritic, containing pseudomorphs of olivine and pyroxene, and mineralogically broadly resembles the Lower Division olivine-phyric flows at Mamainse Point (Berg and Klewin, 1988). The Central and Upper Formation flows are plagioclase porphyritic, and broadly resemble the more plagioclase-porphyritic flows of the Lower and Upper Divisions at Mamainse Point.

A number of major faults are developed parallel to the rift margin and strike direction of the flows. The displacement on these faults is not known, but geochemical data suggest that there is no evidence for major repetition of the basalt stratigraphy (Lightfoot et al., 1991a). These faults may have been formed in response to the lithostatic loading imposed by the eruption of large volumes of dense magma within the rift zone, with concomitant subsidence (Sutcliffe, 1987). Major trans-rift faults have been recognised, and of these, the Thiel Fault may have controlled the location of the Coldwell Complex (Fig. 2a) (Klasner et. al., 1982). Others may have controlled the distribution of gabbro and diabase dikes and ring complex gabbros cutting the OVG (Lightfoot et. al., 1991a).

There are a limited number of sedimentary rock horizons in the lower part of the stratigraphy (composing <4% of the entire exposed stratigraphy). The rocks include mudstones, arkose, and conglomerate units with graded bedding (Giguere, 1975). As with many other Keweenawan interflow sedimentary rocks, these are relatively fine-grained and may have been deposited in an alluvial fan environment (Merk and Jirsa, 1982).

The Lower Formation consists of augite-olivine porphyritic lavas with elevated MgO, SiO_2, TiO_2, Gd/Yb, and Sr/Yb, but low La/Sm. The overlying Central Formation flows are either aphyric or plagioclase porphyritic; they have low MgO, SiO_2, and La/Sm, and Gd/Yb declines upwards through the Central Formation. The Upper Formation flows are either aphyric or plagioclase porphyritic, and define a range of element ratios which is slightly different compared to the Central Formation. The most mafic flows of each formation were used by Lightfoot et. al. (1991a) to characterize the mafic end member composition of the Formation. More strictly defined Formations are now possible based on stratigraphic and geochemical criteria utilised in a similar way to that which Cox and Hawkesworth (1984) used to characterize the stratigraphy of the Deccan Trap tholeiitic lavas. Therefore, the allocation of these lava suites to various formations identified by Lightfoot et. al. (1991a) is now warranted.

Sampling, Sample Preparation, Analysis, Sensitivity and Results

Approximately 1 kg samples of basalt and rhyolite were collected systematically through the MPVG in the 1987 field season (Fig. 2b), and the OVG on the Black Bay Peninsula in the 1986 field season (see Lightfoot et al., 1991a). The freshest samples were collected from the least altered and least vesicular (and most massive and blocky) lower portions of each exposed flow (Brannon, 1984; Nicholson and Shirey, 1990; Hellman et. al., 1979). Samples were taken from the cores of pillows or the centres of columnar jointed flows. Samples were cleaned of altered or weathered surfaces, jaw-crushed using steel plates, and milled in a 99.98% pure alumina P5 planetary ball mill (Ontario Geological Survey, 1990; Lightfoot et al., 1991b).

Powders were analyzed for the major element oxides by wavelength dispersive X-ray fluorescence analysis, loss on ignition (LOI) was determined gravimetrically, S and CO_2 by infra-red analysis, Ba and Cr by flame atomic absorption, Sc, V, Ni, Cu, Co, Zn and Sr by inductively coupled plasma optical emission spectroscopy, and the rare earth elements, Y, Zr, Nb, Ta, Hf, Rb, and Cs by inductively coupled plasma mass spectrometry (Ontario Geological Survey, 1990). In the case of the petrogenetically important trace elements determined by ICP-MS, the Ru-Re internal standardisation scheme (Doherty, 1989a), and an HF solution stabilization method were used (Doherty, 1989b; Doherty et al., 1990). Considerable care was taken to ensure that precision and accuracy could be quoted at the 5% RSD (2σ), or better, confidence level. None of the analytes of interest approached 6 sigma determination limits of the analytical methods used. Additional effort was taken to ensure that decompositions of powders was complete and no residues remained. Quality control results for a compositionally-similar and blind in-house reference standard MRB-29 (Lightfoot et al., 1991b) are given in Table 1 and representative data acquired during the analysis of MPVG lavas are given in Table 2. Data and quality control results for the OVG sequence are given in Lightfoot et al. (1991a).

Specific care was paid to the determination of analytes which might be considered present in insoluble mineral phases, or unstable in solution during a classical wet chemical digestion (Ontario Geological Survey, 1990), such as the REE, Y, Zr, Nb, Ta, and Hf. The procedure of stabilising the solution in the presence of dilute HF has been documented by Doherty et al. (1990), and used in the preparation of samples for determination of the REE, Y, Zr, Nb, Ta, Hf, Rb, and Sr. A comparison of Y data determined by ICP-MS and XRF indicated a correlation coefficient of 0.95623 (p=0.0001) for 110 samples; the regression line has a slope of 1.0081 (s. err.=0.0297) and an intercept of 3.2 (s. err=0.766). Likewise, for Zr determined by ICP-MS and XRF, the correlation coefficient of 0.99576 (p=0.0001) on 59 determinations; the regression line has a slope of 0.910 (s. err=0.011) and an intercept of 12.9 (s. err.=1.7). The high intercept on the XRF axis presumably reflects the elevated determination limit of this method. These data indicate that Zr and Y are not retained in insoluble phases and are determined on stable solutions. Nb determinations by XRF at low abundance levels make a comparison difficult, but for samples with >10ppm Nb, XRF and ICP-MS determinations are well correlated r=0.99477 (p=0.0001) on 57 determinations. Finally, Ta/Nb and Hf/Zr for all basalts analysed for these elements (n=60) have typically chondritic ratios (0.0632 and 43.32, respectively) which suggests that the determination of these analytes by ICP-MS is based on equal extraction of Ta+Nb and Hf+Zr.

Compositional variations within a single flow were monitored by: 1. Sampling vertically through a 17 m thick simple flow close to the base of the MPVG (660 m above the unconformity), and 2. By sampling for a distance of 2000m along strike in a separate 5 m thick flow. The results (given in Table 1 as an average and %RSD(1σ) for a single flow) suggest that for some elements, there is a considerable variation within the flow, whereas for other analytes, the results are very uniform. Compared to the standard deviation of MRB-29, the analytes Na_2O, K_2O, Ba, Sr, and Cu are all significantly more variable (>3 times) than the precision based on MRB-29.

Fig. 3a and Table 1 show that for many elements (e.g: Na_2O, K_2O, Ba, Rb), the intraflow variation is very large. Unless these elements behave differently in other parts of the lava package, it is unlikely that meaningful petrogenetic information may be gleaned from them. For some elements, petrogenetic interpretations may proceed with some caution (e.g. Sr, Cu). For most of the high field strength (HFS) elements, the rare earth elements (REE), the base metals (Ni, Cr, Sc, V, Zn, Co), and the less mobile major element oxides, the degree of intraflow variation (%RSD (1σ)) is less than four times the analytical uncertainty (%RSD (1σ)), and is small compared with the interflow compositional range. This is illustrated for a representative sample from a single flow collected from the base to the top in the Lower Division of the MPVG (Fig. 3b). Analytical data for samples collected along strike within a single simple flow unit are summarised in Fig. 3c. In both cases, the chondrite-normalised (Thompson, 1982) abundance patterns are all essentially identical in shape and similar in abundance levels. In Fig. 3d, the variation in selected immobile major and trace elements are shown as a function of vertical distance through a single flow. There is no systematic change in MgO, Al_2O_3, Ni, Ce, or Yb through the flow. In contrast, Ba, a mobile element, shows an overall increase in abundance upwards through the flow, reaching a maximum in the most amygdaloidal portion of the flow top. It is suggested that the absence of any slight shift in the concentrations of the immobile elements indicate that either the remobilization processes (which appear to influence Ba) or the in-situ crystallisation processes, have not produced any significant intraflow variation (Table 2).

CHEMOSTRATIGRAPHY OF THE MPVG LAVAS

Stratigraphic Field-based subdivisions of the MPVG lavas are difficult to establish due to the rapid alternation between fine- and coarse-grained basalts and the lack of laterally persistent marker horizons (Annells, 1973). On the basis of petrographic and limited chemical data, Annells (1973), subdivided the group into two main Divisions separated by the Great Conglomerate unit (GC) (Fig 4). The Lower Division is about 2500 m thick and with the exception of the Basaltic Clast Conglomerate (BCC) is devoid of conglomerates, but contains many distinctive olivine porphyritic flows. These rocks have reverse-normal-reverse magnetic polarity (Palmer, 1970). The breaks in polarity correlate approximately with the positions of the BCC and the GC on Fig. 4, and presumably record significant time intervals separating the generation of different batches of magma. The Upper Division consists of about 3000m of plagioclase porphyritic flows with normal polarity (Palmer, 1970).

More recently, geochemical studies of the MPVG by Massey (1980) have characterised the flows of Mamainse Point, and permitted stratigraphically controlled trends to be recognised in the sequence. Massey (1983) identified five major groups of flows, and Klewin and Berg (1991) further subdivided the sequence into seven Groups. The break between the Lower and Upper Division occurs stratigraphically at the break between Groups III and IV (Massey, 1983), and Group 5 and 6 (Klewin and Berg, 1991), but the similarities in the subdivisions presented in these two papers appear to extend no further than this.

Our data collected systematically through the basalt stratigraphy, provide additional detail to further refine the stratigraphy of Klewin and Berg (1991), to characterise the flows in each subdivision, and to erect a stratigraphy (e.g. Cox and Hawkesworth, 1984; Devey and Lightfoot, 1986). For ease of comparison with the study of Klewin and Berg (1991), we have chosen to retain their stratigraphic subdivision which we emphasise is based not only on relative stratigraphic position, but also on geochemical parameters. Fig. 5 shows the vertical variation in selected analyte abundances through the MPVG lavas. The samples have been allocated to the equivalent stratigraphic height based on the position

of marker horizons most recently summarised in Klewin and Berg (1991) and based on Annells (1973). Specifically, the variations in Mg-number and MgO, TiO_2, Al_2O_3, Ni, Cu, Sr, Ce, Yb, Zr, Gd/Yb, and Ti/Y versus stratigraphic position are reproduced in Fig. 5a-k. Stratigraphically-controlled variations in the abundances and ratios of selected analytes provide a good basis for the subdivision and classification of the flows.

CLASSIFICATION OF THE MPVG AND OVG LAVA FLOWS AND DEFINITION OF MAGMA TYPES

Table 3 shows the petrographic, stratigraphic and geochemical criteria which discriminate the different Formations and Groups; the geochemical variations are summarised in Figures 6a-f. If a criterion is not required to classify a flow or is not diagnostic when compared with other criteria, it has been omitted from Table 3 to achieve clarity.

The OVG flows belong to at least two different magma types (Lightfoot et al., 1991a). The Lower Formation is a high-Ti series (1.5-3.2 wt.%), whereas the Central and Upper Formations are low-Ti series (1.0-1.5 and 1.3-2.4 wt.%, respectively; Fig 6a). The high-Ti series lavas are also characterised by very low Al_2O_3 (7-12 wt.%) and elevated Gd/Yb (3.2-4.3), Zr/Y(>6), Ti/Y (>500) and Ce/Nb but low La/Sm (2-3.8; Figs. 6c-e); they are high-Cr lavas. The most primitive and least contaminated Central and Upper Formation OVG lavas have low La/Sm and Gd/Yb; they belong to a high-Al, low-Cr series with low Ti/Y and variable Ce/Nb. Lightfoot et al. (1991a) give a more detailed discussion of the characteristics and origin of the contaminated lavas from the Central and Upper OVG Formations.

The MPVG lavas include flows which broadly resemble the Lower Formation of the OVG; these include lavas of Groups 1 and 2a. However, the MPVG lavas of Groups 1 and 2a have lower Zr/Y (5.8-7.0), La/Lu and Gd/Yb (2.0-3.1) than Lower Formation flows of the OVG. Groups 6 and 7 of the Upper Division of MPVG lavas, and the least contaminated Central and Upper Formation OVG lavas (Lightfoot et. al., 1991a) are low-Cr, -La/Sm, -Gd/Yb, and-La/Lu flows which belong to a high-Al series. Lavas of Groups 2b, 3, and 9 are all probably contaminated versions of either Group 1+2a type magma, or Group 6+7 type magma. Only Group 5 of the MPVG lavas is entirely different in composition to the other MPVG and OVG lavas and this is characterized by remarkably low Gd/Yb (1.0-1.3), Zr/Y (2.8-3.5), Cr, Zr, but variable MgO, La/Lu, and La/Sm.

Importantly, the rhyolites of the MPVG and OVG occur dominantly at discrete horizons in the stratigraphy, and as shown later, these appear to be compositionally quite different at the two locations.

FEATURES OF THE MAMAINSE POINT BASALTS

1. The MPVG Lower Division

The Lower Division has been subdivided by Klewin and Berg (1991) into five flow groupings; although we have followed their nomenclature as far as possible, we have further subdivided the groups and recognise lava compositions which were not documented by them. Group 1 basalts include the high-MgO picritic basalts of Klewin and Berg (1991), and although we have sampled no basalts with such extreme MgO contents (18-19 wt.% MgO) as those identified by them, we see similar chemical traits in the less primitive olivine-phyric lavas. Our olivine-phyric basalts have Mg-number=0.64-0.70 and TiO_2=1.1-1.3 wt.%. These flows are separated from an overlying group (2a) of olivine-phyric basalts by a plagioclase glomeroporphyritic basalt (the daisystone flow). Group 2a flows have high Mg-number (0.64-0.66) and moderate TiO_2 (1.6-2.0 wt.%). In the overlying flows of group 2b, Ce, Yb, and Zr reach a maximum in the Lower Division, and in Group 2c, Ce, Yb, and Zr decline as Mg-number and TiO_2 continue to fall (Fig. 4).

Berg and Klewin (1988) suggested that the picritic flows of Groups 1 and 2 are primary liquids and not olivine accumulates. They supported this suggestion with evidence pointing to the skeletal nature of the

olivine phenocrysts and the observation that the flow compositions do not lie along an olivine control line. The reason for the elevated MgO content is ascribed by Klewin and Berg (1991) to melting at deeper levels within the mantle, perhaps at 15–30 kbar to yield liquids with 13–18 wt. % MgO (McKenzie and Bickle, 1988). Klewin and Berg (1991) noted the difference in trace element compositions between Groups 1 and 2. In detail, Group 2b (Fig. 6a–f) consists of flows which are compositionally quite different compared to Groups 1 and 2, but most flows of Groups 1 and 2 have broadly similar geochemical compositions. However, as noted by Klewin and Berg (1991), flows of Groups 1 and 2 with similar MgO have a wide range in TiO_2 content (Fig. 6a). Group 1 flows have lower Gd/Yb than Group 2, and this might be consistent with different degrees of partial melting of the source, and this would be consistent with the lower Ni contents of Group 2 flows compared with Group1 flows (Klewin and Berg, 1991). However, these variations are accompanied by a range in La/Sm and Ce/Nb between Groups 1 and 2 which can not be ascribed to simple partial melting. The models of Berg and Klewin (1988) for Group 2 suggest that much of the variation within the Group is explained by two stages of fractional crystallisation (first stage: olivine, clinopyroxene, and spinel; second stage: olivine, clinopyroxene, and plagioclase). This applies to the flows grouped as 2a and 2c, but the different La/Sm, Gd/Yb and Ti/Y ratios of Group 2b flows make any fractionation relationship between these flows and the remainder of Group 2 difficult to achieve. The elevated La/Sm ratios of some of the lowermost MPVG flows suggest a contribution from a LREE enriched source, such as the continental lithosphere mantle or crust. This is supported by the very negative CHR end of the most basalt MPVG flows (Shirey et. al., 1994). The viability of a crustal contamination model is dismissed by Shirey et. al. (1994) based on the Th/La ratio.

In the overlying plagioclase phyric basalts of Group 3a, TiO_2 continues to fall to 1.2 wt.% as Al_2O_3 increases and Zr decreases (Fig. 4). Overlying Group 3a flows is the BCC horizon, which contains two flows allocated to Groups 3b and 3c. Flows from Group 3a have low Ni contents (80–110ppm), and many of the flows have exceptionally low Cu contents (10–70ppm; Fig. 4) compared with more typical CFB (e.g: the Deccan Trap lavas typically have 120–350 ppm Cu (Lightfoot, 1985). The Group 3 flows all have elevated La/Sm (Fig. 6c) compared with Groups 1 and 2.

Klewin and Berg (1991) analysed over 45 flows from Group 3 and suggested that the variations within Group 3 are consistent with a physical model of replenished, tapped, and fractionated (RTF) magma chambers (O'Hara, 1977). Our data, combined with those published by Klewin and Berg (1991) suggest that all Group 3 flows have elevated La/Sm (Fig. 6c) and have a chemical contribution from old large ion lithophile element (LILE) and light rare earth element (LREE) enriched sources.

Group 4 flows of Klewin and Berg (1991) were not identified during our sampling or analysis. Group 5 flows overlie the Basalt Clast Conglomerate, and define the entry of ophitic basalts after a series of more phenocryst–rich flows (Figs 3 and 4). Group 5 flows all have quite low TiO_2 (<1.5 wt.%) but trace element variations indicate that there are three groups. Group 5a flows have high Ce (45–50ppm) and Yb (2.8–3.1ppm), whereas Group 5b basalts have very low Ce (10–20ppm) and Yb (1.8–2.1ppm). Group 5b basalts have very low Ti/Y (210–360). Group 5 basalts contrast strongly with Groups 1–3 in that they have remarkably low Ti/Y. Group 5 flows are characterised by very low Gd/Yb and have variable Ce/Yb. All Group 5 flows have low Ni (<60ppm for most samples) and low Cu (20–130ppm).

The most primitive Group 5a flows have moderate Mg–numbers, low TiO_2, and very similar low Gd/Yb ratios compared to the other flows of the Lower Sequence. Klewin and Berg (1991) suggest that high degrees of partial melting (approaching 25% melting) would be required to eliminate clinopyroxene from their source. Group 5 basalts range from 30 to 110 ppm Zr, which could represent 73% fractional crystallisation; however, this is accompanied by a wide range in La/Sm (Fig. 6c), which is not explicable in terms of conventional models involving fractionation of olivine, plagioclase, and/or pyroxene(s). The range in compositions between Groups 5a and c are modelled by Klewin and Berg (1991) in terms of assimilation (A) coupled with fractional crystallisation (FC) following DePaolo (1981). Their models require an r value (ratio of mass assimilated to mass fractionated) of 0.3 to 0.5 and up to 50% fractional crystallisation is required to explain the entire compositional range of Group 5. Modelling of the Central Formation of the OVG is best achieved by AFC, and these models require an r value of 0.8–0.9 with <8% fractionation of plagioclase, clinopyroxene, and olivine (Lightfoot et al., 1991a). In AFC models, an important requirement is that the value of r does not become unreasonably large, otherwise the latent heat of crystallisation would

need to be supplemented with an additional source of superheat in order to assimilate large amounts of crust (DePaolo, 1981). Perhaps the presence of a mantle plume would provide some of this heat, but the alternative model of mixing overcomes this difficulty. In the case of the OVG and MPVG, the r values do reach unreasonable magnitudes, and therefore if contamination does play a major part in the evolution of the lava series, much of this contamination must be by mixing of magmas rather than by an AFC-type processes. It is unlikely to be a coincidence that the eruption of voluminous rhyolites accompanies the emplacement of the most contaminated lava series in the Black Bay Peninsula and Mamainse Point areas.

SUMMARISING THE KEY FEATURES OF THE MAIN BASALT GROUPS IN THE MPVG LOWER DIVISION

A. Groups 1 and 2a have essentially high Mg-numbers, TiO_2, and Gd/Yb with low CaO and Al_2O_3, and represent a group with many of the features of the olivine-phyric high-MgO lavas of Groups 1 and 2 identified by Berg and Klewin (1991) generated at 15-30 kbar (Figs. 4,6).

B. Groups 2b and 3 are displaced to lower MgO and TiO_2 compared with Groups 1 and 2a, and have lower Gd/Yb but high La/Sm, Al_2O_3, and CaO (Figs. 4,6). The compositions of these flows appear to be controlled by polybaric fractional crystallisation and limited amounts of crustal contamination.

C. Group 5a-c flows are characterised by very low TiO_2 with a wide range in MgO (Fig. 4). These rocks are essentially low in Gd/Yb (like the rhyolites of Mamainse Point) with a wide range in La/Sm. These are presumably very large degree melts of shallow mantle, and the magmas appear to have been modified in composition by addition of crustal melts in a direct mixing of mantle- and crustal-derived magmas.

D. Lavas of Groups 1-3c most resemble the more primitive Lower Formation of the OVG. However, some of the lavas may record interaction with the lithospheric mantle (Shirey et. al., 1994), unlike the Osler Lower Formation flows (Fig. 6).

E. Group 5 lavas have no volumetrically important compositional analogues in the OVG.

F. Lavas of Group 5 are very Ni poor, and have moderate to low Cu (Fig. 4). Some Group 5 lavas are displaced to high La/Sm (Fig. 6c) and these rocks also have elevated silica contents (Table 2). They are associated spatially with the dominant phase of rhyolitic magmatism.

FEATURES OF THE MPVG UPPER DIVISION

Group 6 lavas include 3 units of diabasic to fine-grained aphyric basalt which all have high Yb (2.3-5.7 ppm), high TiO_2 (1.8-3.4 wt.%) and low Mg-number (0.30-0.48). Unit 6a has low uniform Ce, Yb and Zr; unit 6b has uniform higher Ce, Yb, and Zr, whereas unit 6c has variable and high Ce, Yb, and Zr (Fig. 7a). Units 6a, 6b, and 6c appear to interdigitate throughout the stratigraphy, although we are uncertain whether local fault repetition may be the cause of this feature (Fig. 5). Group 6 flows have remarkably constant and low Ni (<60 ppm), and have the lowest Mg-numbers of the entire sequence which make them different from the Lower Division and the overlying flows of groups 7-9. The Ni content of Group 6 flows is uniformly low (<60 ppm) (Fig. 7b), but the Cu content is high (>100 ppm) (Fig. 7c).

Group 7 flows are diabasic to ophitic tholeiites which belong to two main units. The lower unit (7a) has elevated Mg-number (0.62-0.70), low TiO_2 (0.9-1.2 wt.%), and low abundances of the incompatible elements (e.g: Ce=15-20 ppm). This marks a shift to Mg-numbers similar to flows of the Lower Division, but these rocks have higher Al_2O_3 and lower Ce than the Lower Division. Overlying Group 7b flows have lower Mg-number (dominantly 0.52-0.60), and higher TiO_2 (1.3-1.9 wt.%), and have elevated incompatible element abundances (Ce=20-25 ppm). Units 7c and 7d are represented by only one flow of each, and are different in that they are higher in Ce (65ppm and 120 ppm, respectively).

Group 7 flows generally have elevated Ni (>75 ppm), but quite low Cu (dominantly less than 100ppm), and incompatible element content (TiO_2=0.9 wt.%). These flows are compositionally like many other primitive Keweenawan high-Al olivine tholeiites (Green, 1972; Brannon, 1984; Paces, 1988; Lightfoot et al., 1991a), which are commonly thought to be derived by partial melting of spinel lherzolite at 8-12 kbar (Green, 1982). In contrast, Group 6 flows are strongly evolved in character, and Klewin and Berg (1991) suggest that they may be linked to Group 7 by extensive (80%) fractional crystallisation of olivine, clinopyroxene, and plagioclase. The similarity in trace element ratios (Fig. 6c,d,e) are consistent with this model. However, the presence of evolved flows lower in the stratigraphy than the more primitive flows poses a problem for a simple closed system model. This trace element distribution pattern is also observed in the NSVG (Brannon, 1984). The reversal may require fractionation at two levels in the crust with the rifting process controlling the tapping of the evolved (higher level) magma chambers before the deeper more primitive ones (Klewin and Berg, 1991) or tectonic juxtaposition. In groups 6 and 7, Zr ranges from 40 to 300 ppm, which corresponds to 87% crystallisation.

We do not recognise Group 8 in our samples, but we do identify two samples of diabasic textured tholeiite with elevated Ce (120-130ppm) and high TiO_2 (3.6-3.7 wt.%). Group 9 flows are not recognised by Klewin and Berg (1991), but we type them with elevated TiO_2, Ce, Yb, Zr, and low Mg-number, Al_2O_3, and Ni. These flows also have elevated La/Sm and high LILE and LREE which indicate that they may contain a contribution from the continental crust.

SUMMARISING THE FEATURES DESCRIBED ABOVE FOR THE MPVG UPPER DIVISION

A. Upper Division flows all have moderate Ti/Y=400-570 and Gd/Yb=1.6-2.2 (in between the low and high Ti/Y Lower Sequence flow types with the exception of 3 samples). Unlike the Lower Sequence flows, the difference between Upper Division flows is not so much in the ratios of incompatible elements, but their absolute abundances.

B. Group 6 flows are dominantly high-Ti and Cu with low Ni and Mg-number, whereas Group 7 flows are dominantly low-Ti and Cu flows with high Ni and Mg-numbers. The difference between Upper Division flows therefore appears to reflect more protracted fractionation, whereas the difference between Lower Division flows must be attributed to processes involving more than one source component.

C. Group 9 flows are clearly different when compared to Groups 6 and 7, and can not be linked by fractional crystallisation. These rocks may contain contributions from the continental crust.

D. Flows from Groups 6 and 7 broadly resemble the least contaminated basalts of the Central Formation of the OVG stratigraphy.

E. Despite very low Ni abundances in Group 6 lavas, the Cu contents of these rocks are very high. These lavas are also the most fractionated in terms of Mg-number (Fig. 4) and are high-Ti. We therefore suggest that the variation in Ni is a function of the fractionation of silicates and not sulphide liquid (c.f. Lightfoot et al., 1990 where a similar high-Ti series is described in the Deccan Trap lavas).

Looking at the stratigraphy of the MPVG as a whole, the variations in Ce versus Zr (Fig. 7a) are related along a single array corresponding to a 1:1 line for most of the samples; this contrasts with the behaviour of Y versus Zr (Fig. 7b), where at least three different trends are evident. The fractionation of Y/Zr and Y/Ce reflects the involvement of a phase into which Y readily partitions, and that the changing Y/Zr ratios then reflect the retention of this phase in the source or the removal of this phase during fractional crystallisation. The removal of augite has a small, yet measurable effect on the Y/Zr ratio ($D_Y$augite=0.5; D_{Zr}augite=0.1; Pearce and Norry, 1979). However, different amounts of augite would have to be removed from each of the magmas to produce the three trends, and this would not easily explain the three trends on the TiO_2 versus Mg-number plot, unless the TiO_2 content of the augite is very high (and D_{TiO2}augite=0.3; Pearce and Norry, 1979). Differential degrees of partial melting of a garnet lherzolite, where there is residual garnet,

would explain the different Y/Zr ratios of each of the lava series ($D_Y$garnet=2; Pearce and Norry, 1979), and would go a long way to explaining the range in Gd/Yb (D_{Gd}garnet=2.1,5.2; D_{Yb}garnet=4-53; Henderson, 1982; p.91). Low pressure fractionation of plagioclase, pyroxene, and/or olivine would then explain the range in absolute Zr and Y abundances. In detail, however, to produce the much steeper geochemical trends found in the Lower Division flows would require very small amounts of partial melting, and this might be deemed inconsistent with the very significant volume of relatively uninterrupted basaltic magmatism in the Lower Division at MPVG and the Lower Formation of the OVG.

The extent to which the MPVG lavas are contaminated by ancient crust or melts of older rocks is of some importance in evaluating the likelihood that these magmas have fractionated sulphide (e.g. Naldrett et al., 1992). There is no strong enrichment of Ce relative to Zr above the 1:1 enrichment line shown in Fig. 7a for samples with low La/Sm; those displaced above this array include Groups 2b, 3, 5a-c, and 9. These are volumetrically substantial in thickness (combined thickness of <1000 m). Importantly, with the exception of Group 5 flows, these contaminated flows retain some similar trace element ratio signatures to the ~1000m cyclical sequence of contaminated Central and Upper Formation flows of the OVG (Lightfoot et al., 1991a). Interestingly, the flows of the Upper Division of the MPVG stratigraphy (with the exception of Group 9) show the most evidence of polybaric fractional crystallisation (up to 87% fractionation), yet these flows appear to be largely devoid of evidence for crustal contamination.

COMPARATIVE GEOCHEMISTRY OF MPVG AND OVG RHYOLITES

The possibility that the rhyolites from the MPVG and OVG are derived from melting of the continental crust and therefore possible crustal contaminants in the genesis of the mafic volcanics warrants some investigation. They appear to be directly interposed in the stratigraphy of the lavas proximal to the most contaminated basaltic flows.

Six samples of rhyolite were collected from the MPVG sequence (See Fig. 2b for sample locations and Table 5 for analyses). These are high silica (72-81. wt.%) rhyolites with elevated Al_2O_3 (11-15wt.%) (e.g. Annells, 1973). On a chondrite plot (Fig. 8a), they are distinguished by steep patterns with a moderately positive Nb+Ta, and, throughly negative troughs at P, Ti, and Eu. They show a wide range in HREE abundances and a more narrow range in LREE and HFSE abundances. The Gd/Yb ratio increases with absolute Yb concentration.

The MPVG rhyolites are compositionally different from the nearby rhyolites of the Archean bimodal Michipicoten Greenstone Belt (MGB) (Cycles 1, 2 and 3; Fig. 8b: Sage, 1994; Sage et al., 1996), in that A) the rhyolites have a marked positive Ta+Nb anomaly (whereas the Michipicoten felsic volcanic rocks have a Ta+Nb trough), B) the slopes of the MPVG rhyolite patterns are flatter than felsic volcanic rocks from the Michipicoten Greenstone Belt, and C) the relative degree of incompatible element enrichment is significantly less than that shown by the Michipicoten Greenstone Belt felsic volcanic rocks (Fig. 8b).

Compositionally, the average of post-Archean terrestrial shales (PATS) (Taylor and McLennan, 1985; page 28, analysis 1) is similar to the Michipicoten Greenstone Belt felsic volcanic rocks, and different compared to the MPVG rhyolites. Sage et al. (1996) suggest that the similarity of PATS to Michipicoten rhyolites may be attributed to the derivation of these rhyolites from sialic crust by partial melting. The MPVG rhyolites are more similar to the small sialic volcanic complexes found in other CFB such as the Salsette Island suite north of Bombay, India, in the Deccan Trap (Sethna and Battiwala, 1980; Lightfoot et al., 1987) than to the nearby, Archean age, Michipicoten Greenstone Belt felsic volcanic rocks (Fig. 8a). Lightfoot et al. (1987) suggest that the Deccan Trap rhyolites are derived by partial melting of basaltic crust based on their isotope systematics. Sage et al. (1996) note the lower Ta/La, and higher La/Sm and Th/Zr of nearby Archean Michipicoten Greenstone Belt felsic volcanic rocks compared with felsic volcanic rocks of the Abitibi Greenstone Belt suggesting that Michipicoten felsic volcanic rocks were derived from sialic crust by partial melting. These variations suggest that the MPVG rhyolites were either derived by partial melting of more mafic sources than the Michipicoten Greenstone Belt rhyolites or generated by fractional crystallisation of basic magmas. The MPVG rhyolites have high Nb/La, La/Sm, and a wide range of

incompatible element abundance which makes these rocks more like the Noranda rhyolites of the Abitibi Greenstone Belt, and these have traditionally been explained by the melting of basaltic crust with subsequent fractional crystallisation (e.g: Ujike and Goodwin, 1987). The range in incompatible element abundance presumably reflects differential amounts of polybaric fractional crystallisation of the felsic magma. The negative Ti and P anomalies are consistent with titanomagnetite apatite and fractionation respectively, and the low K_2O, Ba, Sr, and Eu presumably reflect control by feldspars. However, Al_2O_3 is relatively high in these rocks, and this places some limitation on the amount of plagioclase fractionation.

The MPVG rhyolites are unlikely to be melts of sialic upper crust as they have a positive Nb+Ta anomaly on the chondrite-normalised variation diagram (Fig. 8a), but their high silica content is inconsistent with derivation from a mantle source. The high silica content of these rhyolites compared to the tholeiitic lavas makes it difficult to relate them compositionally by only low pressure fractional crystallisation. This mechanism has no obvious way of explaining the marked bimodal composition of the lavas. Furthermore, there appears to be a significant volume of felsic magmatism, and we see no obvious process which would explain the absence of cumulates or magmas of intermediate composition. Rather, we propose that these rhyolites are the product of melting of pre-existing basaltic crust, and possibly melting of slightly older solidified Keweenawan lavas. The melting may have been initiated by lithostatic loading of the crust and subsequent adiabatic melting of the deeper crust. Alternatively, the production of melts from the crust by heating during transfer of magma and crystallisation of deeper magma chambers may have provided enough heat to generate local melts of pre-existing crust.

In the OVG, rhyolite magmatism is developed at the top of the Central Formation, and Lightfoot et al. (1991a) use this rhyolite in their contamination models. Table 4 includes two analyses of rhyolites from the Black Bay Peninsula (88-ARS-2024; 88-ARS-2027), and these are shown in Fig. 8b. In contrast to the MPVG rhyolites, they demonstrate much steeper chondrite-normalised plots; the trends cross-cut those of the MGB rhyolites and therefore it is suggested that these are melts of sialic crust rather than mafic crust. Support for this proposition is provided by the U-Pb geochronology of zircons from these rhyolites which indicate the presence of inherited Archean zircons (Davis and Sutcliffe, 1985). The broad similarity to the felsic volcanic rocks of the Michipicoten Greenstone Belt and to post-Archean shales suggests that a crustal source for these rhyolites is reasonable.

SUMMARISING THE MAIN CONCLUSIONS FROM THE ABOVE DATA

1. There are at least three different magma series in the MPVG and the OVG (Fig. 7b). These correspond to: A. The Lower Formation of OVG rocks and the compositionally similar, but not identical, Groups 1-2a of the MPVG. B. The least contaminated lavas of the Central and Upper Formations of the OVG, which correspond broadly to the most primitive members of MPVG Groups 6 and 7. C. Group 5 lavas of the MPVG, which may be represented by a limited number of OVG flows (2971m in the OVG section; sample 7). Samples from the Central and Upper Formations of the OVG and MPVG 2b, 3, 5b-c, and 9 are not recognised as different magma types as they are likely generated by crustal contamination of magmas derived from one of the above three groups.

2. There is evidence for protracted fractional crystallisation with no significant crustal contamination within the Upper Division flows at Mamainse Point, but there is limited evidence for protracted fractional crystallisation with major AFC in the Central and Upper Formations of the OVG.

3. Geochemical variations are consistent with the progressive tapping of shallower levels of a garnet lherzolite to spinel lherzolite mantle.

4. Open system RTF processes are well developed in the Lower Division of MPVG lavas. AFC is well developed in Group 5 Lower Division flows of the MPVG, but is a very insignificant process in the Central and Upper Formations of the OVG.

5. The Lower Formation OVG rocks and the lower part of the MPVG stratigraphy contain olivine-phyric rocks which have higher MgO contents, lower Al_2O_3, and higher Gd/Yb than the overlying tholeiites.

These magmas are similar in composition in both locations, and are presumably derived from a similar source material with differential amounts of partial melting and subsequent fractional crystallisation. These are not high-Al basalts in the context of the NSVG (Klewin, 1989), and are clearly part of a different cycle of activity, which Lightfoot et al. (1991a) place in the same episode as the emplacement of the picritic intrusions of the Nipigon Plate (Sutcliffe, 1987).

6. Green (1982) shows that the MPVG and OVG flows belong to two different sub-basins of the Midcontinent Rift, with Osler volcanics retaining dominantly a reversed magnetic polarity followed by normal polarity. In contrast, the Mamainse Point rocks retain essentially a reverse-normal-reverse-normal polarity.

7. The OVG and MPVG rhyolites are compositionally different. Group 5 MPVG lavas have compositions which appear to be influenced by the rhyolites which occur stratigraphically at the same level (Figs. 2b, 4), whereas the Central Formation of the OVG has compositions which can be modelled by AFC involving the rhyolites emplaced between the Central and Upper Formations or mixing between basaltic and rhyolitic magmas (Lightfoot et al., 1991a).

Chondrite-normalised spider diagram (LILE and HFSE from Thompson, 1982, REE from Nakamura, 1974) variations in the incompatible trace element abundances are shown in Figs. 9a-i. The diagrams show representative analyses of lavas from each of the groups using only data for immobile elements determined in this study.

The spider diagrams for the OVG lavas are given in Figs. 9i-k. The Lower Formation is characterised by very steep patterns with weak Ta+Nb and P troughs, and a slight positive Ti anomaly (Fig. 9i). Many of the Lower Formation rocks have sub-parallel patterns which are consistent with low pressure fractional crystallisation of gabbroic minerals. The patterns of the Central Formation have a limited range in HFSE and HREE abundances, but fan-upwards towards elevated LILE and LREE, with the development of progressively more pronounced negative Ti, Ta+Nb and P anomalies (Fig. 9j). The patterns of the Central Formation cut across those of the Lower Formation. Most Upper Formation lavas resemble the Central Formation, but develop more pronounced negative Ti and Ta+Nb anomalies (Fig. 9k). A limited number of flows presently grouped in the Upper Formation are clearly different (Fig. 9c, analysis of sample 2971), and these flows are evidently not of the same magma type as other Upper Formation flows and require further investigation.

The spider diagram for the Lower Division MPVG flows (Fig 9a-e) shows a number of features of petrogenetic significance. Perhaps most importantly, Groups 1 through 3 have much steeper profiles than Group 5b (Figs. 9a,d, e). Group 1 flows and the Daisystone flow are similar in shape and are slightly less steep, and have lower overall levels than the overlying Group 2a flows. The overall shape is similar to the Lower Formation of the OVG. Groups 2b, 2c, and 3 have steep slopes presumably because of interaction with crust. Group 5a flows are slightly more enriched in most of the incompatible elements compared with Group 2b, but develop more pronounced negative P anomalies, small negative Ti anomalies, and also have lower Eu, Ta and Nb abundances (Fig. 9e). Group 5b flows are entirely different in character to the underlying flows and have a flatter profile with sub-chondritic Zr/Yb. The overlying Group 5c flows plot with a similar shape, but have much elevated overall Eu, Ta and Nb abundances and higher LILE abundances, presumably because of the mixing process discussed above.

The Upper Division flows are shown in Fig. 9f-h. Group 6a and 6b flows have similar shapes, and 6a has lower abundances than 6b. Flows of Group 6c show slight overall enrichment of the LREE, Ti, Nb and Ta relative to Group 6b (Fig. 9f). Groups 7a and 7b fall on similar plots where 7a is depleted relative to 7b. The shapes of these profiles is similar to Group 6a. Group 7c shows an enrichment in the LREE relative to Group 7a, and Group 7d shows the same feature, only it is more extreme. All of the Group 6 and 7 flows are essentially similar in pattern to the most primitive Central and Upper Formation flows of the OVG. Patterns for Group 6 and 7 flows cut across the patterns of the Lower Formation OVG and Lower Division MPVG flows (Fig. 7f,g,i).

Group 9 is similar in shape to Group 6c, and also develops a negative P anomaly, but no Ta+Nb trough. The different slopes of the LREE-MREE end of the plot reflect the addition of small amounts of

LILE-enriched materials such as continental crust. LREE mobility has been eliminated as a possible cause by the alteration screening described above.

COMPARISON OF KEWEENAWAN LAVAS WITH PHANEROZOIC OCEANIC BASALTS AND CONTINENTAL FLOOD BASALTS

Chondrite-normalised plots of the average Group 2a Mamainse Point and average most primitive Lower Formation OVG lavas are shown in Fig. 10a. Also shown are the compositional averages of normal-type MORB (N-MORB) and ocean island basalt (OIB) taken from Sun and McDonough (1989). There is a clear similarity in the abundance of all of the incompatible elements (except Nb+Ta) between OIB and the Lower Formation OVG flows. The Group 2a Mamainse Point flows have a pattern which is similar in shape to OIB, but displaced to lower concentrations, and these flows also have small negative Nb+Ta anomalies. This may reflect a contribution from the lithosphere mantle (see Shirey et al, 1994). The average of Group 5a is shown in Fig. 10b compared to N-type MORB and enriched-type MORB (E-MORB). There is a marked similarity in the abundance of the incompatible elements between Group 5b flows and E-MORB. On a discrimination diagram developed by Pearce and Norry (1979) for oceanic and within plate basalts (not shown), most of the Group 5 basalts are displaced to very low Zr and Zr/Y, and overlap with the field of N-MORB, whereas the remainder of the flows all fall close to the field of within-plate basalts. Those lavas with low Zr/Y appear to be dominantly those from lithospheric mantle, whereas those with elevated Zr/Y appear to contain contributions from deeper asthensopheric mantle, and may include plume-type chemical contributions. Thus, the Lower Division MPVG and Lower Formation OVG flows may be derived from oceanic mantle with the earlier flows carrying a pronounced mantle-plume signature; a very few flows in Group 5 of the MPVG have a geochemical signature similar to E-type MORB (Fig. 10b).

Recent studies of the chemostratigraphy of Siberian Trap lavas of the Noril'sk Region suggest that picritic and tholeiitic lavas are derived from both: 1. asthenospheric mantle source, and 2. two compositionally different mantle lithosphere sources (Lightfoot et al., 1993). The basalts of the upper sequence (Nd through Mk; Table 6) show a progressive decline in the amount of contamination by ancient continental crust (Lightfoot et al., 1990). The most contaminated Siberian Trap lavas are strongly depleted in Ni, Cu and the platinum group elements (Lightfoot et al., 1990; Naldrett et al., 1992; Brugmann et al., 1993) and this led Naldrett et al. (1992) to suggest that these lavas had equilibrated with magmatic sulphides. Naldrett and Lightfoot (1993) used data for the OVG lavas (Lightfoot et al., 1991a) to argue that some of the most contaminated lavas are slightly depleted in Ni and Cu, thereby recording evidence for equilibration with magmatic sulphides. A more detailed comparison of the Keweenawan and Noril'sk lavas suggests that some important similarities exist in their geochemical compositions.

Chondrite-normalised plots of the most primitive Central Formation OVG flows, and average Group 6a and 7a MPVG flows are shown in Fig. 10d compared to the compositional averages of CFB derived from lithospheric mantle sources (Lightfoot et al., 1993). The average Mokulaevsky Formation lavas of the Siberian Trap, which Lightfoot et al. (1993) ascribe to an uncontaminated mantle lithosphere source, are compositionally similar to average primitive least contaminated Central Formation OVG flows and the average Group 6a MPVG flows (Fig. 10d). The more evolved Group 7 flows are presumably more primitive equivalents of Group 6. The most contaminated Central Formation OVG lavas have compositions which are very similar to the most contaminated Nadezhdinsky flows of the Nd_1 unit (Lightfoot et al., 1991a, 1994) (Fig. 10c), which Lightfoot et al., (1993) argue originated by contamination of magmas derived from the continental lithospheric mantle.

Figures 11a-j compare, amongst other parameters, the Nb/La versus La/Sm ratios of Keweenawan lavas with Siberian Trap lavas (data from Lightfoot et al., 1990; 1993, 1994; and unpublished data). Compositionally, few of the Keweenawan lavas are displaced to such high La/Sm as the Ivakinsky (Iv), Syverminsky (Sv), and Gudchichinsky (Gd) lavas, but there are still many Lower Formation OVG and Groups 1+2a MPVG lavas which have low La/Sm and high Nb/La signatures that resemble the earlier phase of Siberian Trap lavas represented by the Iv-Gd lavas. Few Keweenawan lavas resemble the Tuklonsky (Tk) lavas of the Siberian Trap. The contaminated Central and Upper Formation flows of the

Keweenawan OVG have low La/Sm and elevated La/Sm like the Nd unit lavas of the Siberian Trap, but the majority of Keweenawan MPVG Upper Division lavas anchor the array of the contaminated flows at high Nb/La and low La/Sm, very much like the Mokulaevsky lavas do in the Siberian Trap. This suggests that only one type of mantle lithosphere contribution existed in the Keweenawan Midcontinent Rift, whereas at least two types are represented in the Siberian Trap (Lightfoot et al., 1993).

Figures 11a-e show the variations in selected major element oxides, trace elements and trace element ratios for the samples of Keweenawan lavas from the MPVG and the OVG. Figures 11f-j show comparable data for samples from the Siberian Trap (Lightfoot et al., 1990; 1993; 1994). These diagrams illustrate a number of points: Comparison of the SiO_2 versus MgO plots in Figs. 11a and 11f shows that samples from the OVG Central Formation are displaced to elevated SiO_2 like the Nd lavas from the Noril'sk sequence. Comparison of the Ni and Cu versus MgO variations in Figs. 11b-c and 11g-h demonstrates that the Central Formation lavas are displaced to low Ni like the Nd lavas from Noril'sk. However, there is no marked shift to low Cu in the Central Formation of the OVG; this may be due to the fact that most of the rocks have suffered sub-greenschist facies metamorphism, and Cu is known to be mobile under these conditions (Livnat et. al., 1983). The fall in Ni in the Central Formation OVG is accompanied by a slight shift to lower MgO content, and this would be consistent with some silicate fractionation. In detail, however, the change in Ni/MgO is not explained by silicate fractionation alone (Naldrett and Lightfoot, 1993).

Variations in La/Sm versus Gd/Yb and Nb/La versus La/Sm reveal a number of similarities between OVG and Noril'sk lavas (Figs. 11d-e, i-j). 1. The Gudchikhinsky lavas from the Noril'sk Region and the Lower Formation OVG and Groups 1, 2, and 3 of the MPVG display to high Gd/Yb and Nb/La but low La/Sm. 2. These data are consistent with the model suggested by Lightfoot et al. (1993) where the Lower Sequence lavas of the Ivakinsky through Gudchichinsky in the Siberian Trap have a chemical contribution from a deep mantle plume. The contaminated Central Formation lavas of the OVG and the Nadezhdinsky lavas are displaced to high La/Sm and low Nb/La and Gd/Yb. The less contaminated MPVG lavas of Groups 6 and 7 which have experienced extreme polybaric fractionation are displaced to moderate La/Sm and Nb/La at low Gd/Yb, very much like the less contaminated Upper Sequence lavas of the Mokulaevsky Formation of the Siberian Trap. Extension of this argument to the Keweenawan rocks would appear to suggest that lavas from both the base of the succession in the MPVG and the OVG have a similar chemical contribution from a deep plume source. Central Formation lavas of the OVG appear to be chemically linked to the Group 5 and 6 MPVG lavas. It has been established that the Group 6 and 7 MPVG lavas are extensive, and represent a major magma type not unlike that responsible for the Logan sills (Lightfoot et al., 1991a, based on the least contaminated Central Formation OVG lavas). The least contaminated lavas of the Central Formation OVG and the Group 6 and 7 MPVG lavas are chemically similar to the Mokulaevsky lavas of the Siberian Trap.

In summary, the sequence of petrogenetic processes, and the implications for variations in the degree of crustal contamination and source characteristics are summarised in Table 6.

Implications for Tectonic Evolution of the Midcontinent Rift

In continental areas it is often difficult to establish the cause of intraplate magmatism. However, in some young CFB there are contributions of lavas with dominantly the signatures of deep oceanic mantle as sampled in oceanic hot spots, and lavas with essentially the trace element signatures of lithospheric mantle. In some cases the plume contributions clearly predate the lithospheric contributions (e.g. Siberian Trap - Lightfoot et al., 1993), and this is consistent with studies which have suggested the link between Siberian Trap magmatism and the Permotriassic location of the Jan Meyen hot spot (Morgan, 1981). This suggests that at least some CFB are triggered by mantle plumes rather than by lithospheric extension (Gallagher and Hawkesworth, 1992).

The presence of OIB-like minor and trace element patterns in some CFB might be regarded as evidence for a mantle plume. In detail, however, many such cases will simply reflect small degrees of

partial melting of the asthenospheric upper mantle, and this melting could be triggered by either a plume or lithospheric extension. In order to link the OIB-like minor and trace element patterns directly to a mantle plume, more evidence is needed than just geochemical data. Specific knowledge is required as to whether there is a link between continental magmatism and associated hot spot traces, whether large volumes of magma have been erupted with plume-like geochemical signatures, and finally whether there have been chemical changes with time which reflect the migration of the mantle hot spot under the magmatic province (Gallagher and Hawkesworth, 1992).

The idea of a mantle plume origin for the Keweenawan Midcontinent Rift is not new (Burke and Dewey, 1973; Nicholson and Shirey, 1990; Klewin and Shirey, 1992), and more recently, the Nipigon Plate - Midcontinent Rift has been proposed as one site of this mantle plume (Sutcliffe, 1987); the OVG being erupted at roughly the point of a triple junction between the main Midcontinent Rift and what has been interpreted as an aulacogen comprising the Nipigon Plate intrusions (Burke and Dewey, 1973). Indeed, the genesis of the igneous rocks in the Nipigon Plate and Osler areas have been attributed to the underplating of large volumes of basaltic magma derived from the asthenospheric mantle (Sutcliffe, 1987), at a location corresponding to the crust-mantle interface as proposed by Cox (1980). The OVG is therefore likely to record the earliest and most proximal magmatic record of this plume. Although there is good evidence that the Nipigon Plate may be the failed arm of an aulacogen, there is no obvious evidence recorded on land or beneath Lake Superior for the trace of a corresponding hot spot. However, the geochemical evidence presented above suggests that the Keweenawan lavas record a transition from lavas with plume-like chemistries to those with N-MORB signatures through the Lower Division. It is unlikely that these signatures, recorded in vast volumes of lava, could be generated by very low degrees of mantle melting.

Geologic Settings of Selected CFB Provinces

Within the Deccan CFB province of Western India, Formations of compositionally distinctive basalts onlap the basement from north to south, becoming progressively younger to the south (Devey and Lightfoot, 1986). It is inferred from this relationship that sites of magmatism have migrated with time, and such rates and directions of movement are similar to those associated with mantle plumes (Watts and Cox, 1989). Lightfoot et al. (1993) and Naldrett et al. (1992) studied the Siberian Trap lavas of the Noril'sk Region and suggested that whereas there was a broad migration of magmatic activity to the east-north-east, the dominant control on the site of emplacement of the lavas was deep crustal faults which penetrate the mantle such as the North Kharaelakh, Noril'sk-Kharaelakh, and Imangda faults. The eastward migration of volcanism appears to be inconsistent with the migration of the Siberian Craton over the Jan Meyen mantle plume. However, much of the volcanism may have been triggered along secondary rifts parallel to the northern margin of the Siberian Platform, and therefore activity may have changed from plume-induced melting in the Noril'sk region to rift-related magmatism towards the east.

In the Parana CFB Province, Peate et al. (1992) show that the inferred northern movement of magmatism is at a high angle to the Tristan hot spot, and therefore they suggest that the Parana magmatism was associated with the northward rifting of South America over an area of anomalously hot mantle, but that the Parana volcanic edifice was not initiated by the arrival of the Tristan mantle plume.

Magmatism within the Keweenawan Midcontinent Rift has been focussed into a number of basins along the length of the rift. The earliest basin appears to have been occupied by the OVG and subsequent evolution appears to have been marked by the migration of volcanic centres along the rift arms beneath what is now Lake Superior. On these grounds, the possibility that plume activity initiated rifting in the Nipigon Plate region, much like activity at Noril'sk appears to have triggered the eruption of the Siberian Trap lavas, is worth additional examination.

Comparison of Siberian Trap and Keweenawan Midcontinent Rift: Implications for Mineral Potential of the Keweenawan Midcontinent Rift

Recent studies of the intrusions which host the Ni-Cu-PGE deposits at Noril'sk (e.g. Naldrett et al., 1992; Lightfoot et al., 1994), and the associated continental flood basalt sequence (e.g. Lightfoot et al., 1990, 1993, 1994; Hawkesworth et al., 1995) have highlighted the importance of the intrusive episodes of CFB magmatism as important hosts for Ni-Cu-PGE deposits. Exploration activity for Ni-Cu-PGE mineralisation has focussed largely on the CFB and the Keweenawan Midcontinent Rift has attracted some interest based on a number of similarities documented by Naldrett and Lightfoot (1993).

The new data presented for the MPVG and the comparative data for the OVG (see also Lightfoot et al., 1991a), suggest a number of similarities between Noril'sk magmatism and Keweenawan magmatism which are explored below:

1. The presence of an early sequence of lavas with a plume-like trace element signature. Both the Keweenawan successions at Mamainse Point and on the Black Bay Peninsula contain possibly contemporaneous primitive lavas with elevated Gd/Yb and Ti/Y which broadly resemble the more primitive flows developed in the Lower Sequence of the Siberian Trap. Specifically, the Gudchichinsky tholeiites and picrites of the Siberian Trap have trace element ratios and chondrite-normalised trace element patterns resembling those of the ocean island basalts average of Sun and McDonough (1989) (Fig. 10a).

2. The presence of highly contaminated lava flows. Crustal contamination is recognised within the Central and Upper Formations of the OVG, and to a lesser extent within Groups 2b, 3, 5, and 9 at Mamainse Point. The main criteria for recognition of contamination are the elevated La/Sm ratios and the high SiO_2 content of the lavas (Figs. 11a,d). Unlike the OVG flows, where contamination is identified within a specific series of flows at two stratigraphic horizons ~500m wide, in the Mamainse sequence, it is erratically developed in only a very few thin flow units. In the OVG, La/Sm reaches 6 in the Central Formation and 4.5 in the Upper Formation, whereas SiO_2 reaches 54 wt.% in the Central Formation and 55 wt.% in the Upper Formation. These heavily contaminated sequences resemble the contaminated Bushe and Poladpur flows of the Deccan Trap (Lightfoot and Hawkesworth, 1988; Mahoney et al., 1982; Cox and Hawkesworth, 1984, 1985) and the Nadezhdinsky lava flows of the Noril'sk Region, Siberian Trap (Lightfoot et al., 1990).

An important similarity between the contamination shown by the Central Formation lavas in the OVG and that identified in the Nadezhdinsky through Mokulaevsky Formations of the Siberian Trap is illustrated by the direction in which contamination increases through the basalt stratigraphy. In the Central Formation of the OVG, SiO_2 , La/Sm, and Th/Y all increase upwards through the stratigraphy of the flows over a distance of about 500m (Lightfoot et al., 1991a). This increase is accompanied by a slight decline in Mg-number and an increase in Ni content (Lightfoot et al., 1991a). In both cases, the sudden entry of heavily contaminated lavas at the base of the sequence is associated with strong Ni depletion of the lavas. The interpretation of this depletion of Ni and increase in SiO_2 at Noril'sk is that sudden contamination resulted in the segregation of immiscible sulphides which stripped the magma of the Ni, Cu, and PGE inventory (Naldrett et al., 1992; Lightfoot et al., 1994).

3. Lavas with strong Ni and Cu depletion were complemented by the presence of magmatic sulphides within intrusions. A number of the OVG and MPVG flows illustrate quite low abundances of Ni and Cu. Whereas Cu tends to be mobile under relatively low grade metamorphic conditions, the observation that Ni declines with increasing La/Sm and SiO_2 at almost constant Mg-number is not readily explained by fractional crystallisation (Naldrett and Lightfoot, 1993). The similarity between this trend and the variation in Nadezhdinsky lavas at Noril'sk is quite striking. In both cases, there is a decline in Ni content at almost constant Mg-number, as La/Sm increases (Naldrett and Lightfoot, 1993). The important similarity between the two is that both the Nadezhdinsky flows at Norils'k and the Central Formation OVG flows, decrease in Ni context up-section.

4. The presence of intrusions which have undergone high level olivine and possibly sulphide fractionation. No picritic intrusions or intrusions with significant sulphide mineralisation have been recognised at Mamainse Point or within the area of St. Ignace Island and the Black Bay Peninsula. Very little work has been done on the intrusions of the Keweenawan in the region of the Black Bay Peninsula and St. Ignace Islands, but there are a large number of ring complexes and dykes which could represent suitable targets of economic importance. For example, the Ni-Cu-PGE sulphides of the Great Lakes Nickel deposit occur as a zone of disseminated sulphides at the base of the second cycle in the Crystal Lake Gabbro. This intrusion has many similarities in terms of size and composition with those of the Noril'sk District. Within the Nipigon Plate there are a number of diabase and picrite intrusions which might represent exploration targets (see Fig. 2a and Sutcliffe, 1987).

5. Variations in the Ni and Cu contents versus MgO of Maminse Point and Osler tholeiites are shown in Fig. 11c and d. Ni and MgO variations appear to be largely independent of alteration effects; variations in Cu reflect a stronger control by alteration. There is a broad spread of Cu content in rocks which have a limited range in Ni (Fig. 11b, c). Despite this observation, the general enrichment/depletion trends of Ni and Cu on this plot appear to be broadly related. Samples from Groups 3, 5a, and 5b are largely samples which have relatively low Ni (<100ppm) in the interval 6-8wt.% MgO. Interestingly, this is accompanied by low Cu (0-70ppm). It is the samples from Groups 3, 5a and 5b which are displaced to higher La/Sm, and this feature has been explained by the addition of sialic LREE enriched crustal material during high level crustal contamination (Klewin and Berg, 1991). The OVG lavas which show elevated La/Sm (Fig. 11d) also have low Ni (<120ppm), but Cu is very variable (20-300ppm), presumably because alteration has remobilised the Cu in these flows. The observation that the most contaminated flows are also depleted in Ni was made by Naldrett and Lightfoot (1992), and the coincidence presumably has some exploration value in the search for magmatic sulphides in the Keweenawan Midcontinent Rift.

6. Presence of mantle-penetrating faults. Major fault zones are both parallel to the margin of the rift and at a high angle to the rift. Many of these faults control the distribution of both major dykes and ring complexes (Giguere, 1975; Wallace, 1972;1981; McIlwaine and Wallace, 1976). Whereas ring complexes have not been recognised at Noril'sk, the association of small picritic intrusions and diabase intrusions proximal to major mantle-penetrating faults has been recognised (e.g. Naldrett et al., 1992).

7. Identification of the late eruption of large volumes of compositionally uniform flows. Throughout the Siberian Trap, the uppermost 2000 m of basalt stratigraphy is essentially monotonously uniform in composition. Within the Keweenawan, the uppermost flows tend to be derived from one magma type, but show a wide range in the degree of polybaric fractional crystallisation (MPVG) or crustal contamination (OVG).

8. Presence of basalt-hosted hydrothermally redeposited post-volcanic native copper mineralisation. Hydrothermal copper mineralisation is developed within the MPVG in the Copper Corp. Property (Richards and Spooner, 1989) and within the volcanics of the Keweenawan Peninsula.

9. Identification of compositional changes with time. Geochemically, young CFB show systematic changes in composition with time. The Siberian Trap sequence at Noril'sk demonstrates a compositional shift from magmas which have essentially an asthensopheric signature to lavas which contain a major contribution from the continental lithospheric mantle and sequentially smaller amounts of crustal contamination upwards through the stratigraphy (Naldrett et al., 1992; Lightfoot et al., 1993). The same sequence of chemical changes is evident in the OVG lavas where there is a transition from more mafic lavas with high Nb/La, Gd/Yb and Ti/Y towards tholeiitic low-Mg lavas with lower Nb/La and Gd/Yb (Fig. 5). In the OVG there are two cycles of lavas which show an upward decline in the degree of contamination of the lavas by sialic crust. Thus, the Noril'sk lavas, like the OVG lavas, show a tendency to shift from predominantly asthenospheric signatures to more lithospheric signatures with time. This is somewhat at odds with the conclusion of Shirey et. al. (1994) who proposed a mantle plume and lithospheric contribution to the lower part of the sequence with more prominent OIB contributions higher in the Mamainse Point stratigraphy. However, their model does not take into consideration the variations in the more important Osler Volcanic Group which is closer to the proposed triple junction (Sutcliffe et. al. 1987; Burke and Dewey, 1973). This is unlike the Deccan Trap where there is a very small contribution from the

lithospheric mantle (presumably because of the very thin keel of lithosphere beneath the drifting Indian subcontinent). It is also unlike the Parana insofar as the Parana records a transition from dominantly mantle lithosphere signatures to asthenospheric signatures. This is presumably a reflection of the similarity of the Keweenawan and Siberian settings where both CFB record magmatism in a failed rift zone, whereas the Deccan and Parana record magmatism at the margins of major oceanic basins (continent drifting over a plume, and continental break-up, respectively).

Summary and Conclusions

1. The OVG flows evidently belong to at least two different magma types (Lightfoot et. al., 1991a). The Lower Formation is a high-Ti series, whereas the Central and Upper Formations are low-Ti series. The high-Ti series lavas are also characterised by elevated Gd/Yb, Zr/Y, Ti/Y and Ce/Nb but low La/Sm; they are high-Cr lavas with very low Al_2O_3. The most primitive and least contaminated Central and Upper Formation OVG lavas have low La/Sm and Gd/Yb; they belong to a high-Al, low-Cr series with low Ti/Y and variable Ce/Nb.

2. The MPVG lavas include members which resemble the Lower Formation of the OVG; these include lavas of Groups 1 and 2a. However, the MPVG lavas of Groups 1 and 2a have lower Zr/Y, La/Lu and Gd/Yb than Lower Formation flows of the OVG. Groups 6 and 7 of the Upper Division of MPVG lavas are low-Cr, -La/Sm, -Gd/Yb, and -La/Lu flows which belong to a high-Al series. Lavas of Groups 2b, 3, and 9 are all probably contaminated versions of either Group 1+2a type magma, or Group 6+7 type magma. Only Group 5 of the MPVG lavas is entirely different in composition, with remarkably low Gd/Yb, Zr/Y, La/Lu, Cr, Zr, but variable MgO and La/Sm.

3. The rhyolites of the MPVG and OVG occur dominantly at discrete horizons in the stratigraphy, and these appear to be compositionally quite different at the two locations.

4. Table 7 summarises the petrogenesis of the OVG and MPVG. Major and trace element data suggest that the most basal members of the OVG and MPVG include, and evolved from, high-Mg primitive liquids, whereas the remainder of the stratigraphy records lavas of essentially tholeiitic composition. The depth of partial melting appears to be essentially deeper in the earlier lavas than the later series, whereas the degree of source melting appears to have achieved a maximum in the Group 5 lavas. Trace element data suggest that the OVG lavas have seen significantly more crustal contamination than the MPVG lavas, whereas the lower portion of the Upper Division of the MPVG record evidence for protracted polybaric fractionation evolution, much like the NSVG. AFC processes are recognised in Group 5 of the OVG, but appear less likely in the Central and Upper Formations of the OVG as the amount of assimilation relative to fractional crystallisation is insufficient to generate the required amount of latent heat in order to melt the crust. Rather, it is proposed that the OVG Central and Upper Formation lavas were generated by dominantly mixing between tholeiitic and rhyolitic melts. Group 3 lavas appear to record evidence of RTF processes (Klewin and Berg, 1991).

5. The trace element signatures of the Lower Formation OVG and most basal Group 2a MPVG lavas are similar to those of uncontaminated asthensopheric-mantle derived oceanic basalts sampled above mantle plumes. In the Group 5 MPVG lavas, elemental signatures of N-MORB derived magmas are recognised. The trace element signatures of least contaminated Central and Upper Formation OVG lavas are essentially similar to within-plate basalts, and probably sample wide-spread domains of the stable continental lithospheric mantle.

6. Compositionally, the Lower Formation of the OVG and the Lower Division of the MPVG series are similar to the primitive rocks of the Nipigon Plate (Sutcliffe, 1987), whereas the Central and Upper Formations of the OVG series and the Upper Division of the MPVG series record compositions similar to the Fe-Ti transitional basalts of the NSVG and may be extrusive equivalents of the Logan diabase sills (Sutcliffe, unpublished data).

7. Geological, petrological, and geochemical similarities exist between the Noril'sk Region of the Siberian Trap and the Keweenawan Midcontinent Rift. Although mantle-penetrating faults are presently not

recognised in the Keweenawan Midcontinent Rift other than in the Lake Superior Basin based on seismic studies, there are many petrochemical similarities between the Noril'sk Region and the Keweenawan Midcontinent Rift. Both develop sequences which appear to represent a transition from plume-induced rifting to lithospheric extension; both CFB record evidence of crustal contamination, and although the evidence is not as strong in the Keweenawan, both show variable degrees of Ni and Cu depletion which might be attributed to sulphide segregation. These features, together with the very large number of poorly understood Keweenawan intrusions in the Nipigon Plate and cutting the Osler Series (Wallace, 1972; McIlwaine and Wallace, 1976), and the presence of economically mineralised intrusions such as the Duluth Complex and smaller deposits and occurrences such as those of the Crystal Lake Gabbro (Great Lake Nickel Deposit) and Coldwell Complex (Marathon Deposit) suggest that exploration efforts should not dismiss the likelihood that the Keweenawan Midcontinent Rift hosts a giant Noril'sk type Ni-Cu-PGE sulphide deposit.

Acknowledgements

The staff of the Geoscience Laboratories are thanked for generating the data. For permission to publish this work, John Wood, the Director of the Ontario Geological Survey, is thanked. For drafting, Kerry Lacey and Steve Josey are thanked. Johanne Guindon is thanked for typing the manuscript corrections. The authors appreciate comments from Chris Hawkesworth, and Andy Fyon on an earlier draft of this manuscript.

References

Annells, R.N. (1973). Proterozoic flood basalts of eastern Lake Superior: the Keweenawan volcanic rocks of the Mamainse Point area, Ontario. Geological Survey of Canada, Paper 72-10. 51pp.

Basaltic Volcanism Study Project (1981). Basaltic Volcanism on the Terrestrial Planets; p. 30-77 *in* Pre-Tertiary Continental Flood Basalts. p.30-77. Lunar and Planetary Sciences Institute. Pergamon Press. Inc. New York, 1286pp.

Beane, J.E., Turner, C.A., Hooper, P.R., Subarao, K.W., and Walsh, J.N., (1986). Stratigraphy, composition and form of the Decan basalts, western Ghats, India. Bull. Volc., V. 48, p. G1-83.

Berg, J.H., and Klewin, K.W. (1988). High-MgO lavas from the Keweenawan midcontinent rift near Mamainse Point, Ontario. Geology, V.16, p.1003-1006.

Bradshaw, T.K., Hawkesworth, C.J., and Gallagher, K. (1993). Basaltic Volcanism in the Southern Basin and Range: No Role for a Mantle Plume. Earth Planet. Sci. Lett., V. 116, v. 1-4, pp. 45-62.

Brannon, J.C. (1984). Geochemistry of successive lava flows of the Keweenawan North Shore Volcanic Group. Ph.D. dissertation, Washington Univ., St. Louis, Mo.

Brugmann, G.E., Naldrett, A.J., Asif, M., Lightfoot, P.C., Gorbachev, N.S., and Fedorenko, V.A. (1993). Siderophile and chalcophile metals as tracers of the evolution of the Siberian Trap in the Noril'sk Region, Russia. Geochim. Cosmochim Acta. V. 57, pp. 2001-2018.

Burke, K. and Dewey, J.F. (1973). Plume-generated triple junctions: Key indicators in applying plate tectonics to older rocks. J. Geol. V. 81, pp. 406-433.

Campbell, I.H. and Griffiths, R.W., (1990). Implications of mantle plume structure for the evolution of flood basalts. Earth Planet Science Letter V. 99, pp. 79-93.

Cannon, W.F., Green, A.G., Hutchinson, D.R., Lee, M. Milkereit, B., Behrendt, J.C., Halls, H.C., Green, J.C., Dickas, A.B., Morey, G.B., Sutcliffe, R.H., and Spencer, C. (1989). The North American Midcontinent Rift Beneath Lake Superior from GLIMPCE Seismic Reflection Profiling. Tectonics, Vol 8., No. 2., pp. 305-332.

Cox, K.G. (1980). A model for flood basalt volcanism. J. Petrol. V. 21, pp. 629-650.

Cox, K.G. and Hawkesworth, C.J. (1984). Relative contribution of crust and mantle to flood basalt magmatism, Mahabaleshwar area, Deccan Traps. Philos. Trans. R. Soc. London. Ser. A, V. 310, pp. 627-641.

Cox, K.G. and Hawkesworth, C.J. (1985). Geochemical stratigraphy of the Deccan Traps at Mahabaleshwar, Western Ghats, India, with implications for open system magmatic processes. J. Petrology V. 26, pp. 355-377.

Davis, D.W. and Sutcliffe, R. H. (1985). U-Pb ages from the Nipigon Plate and northern Lake Superior. Geological Society of America Bulletin, V. 96, pp. 1572-1579.

DePaolo, D.J. (1981). Trace element and isotopic effects of combined wallrock assimilation and fractional crystallisation: Earth Planet. Sci. Lett. V. 53, pp. 189-202.

Devey, C.W., and Lightfoot, P.C. (1986). Volcanological and tectonic control of stratigraphy and structure in the western Deccan Traps, Bul. Volcanol V. 48, pp. 195-207.

Doherty, W. (1989a). An internal standardization procedure for the determination of yttrium and the rare earth elements in geological materials by inductively coupled plasma mass spectrometry; Spectrochimica Acta, V. 44B, pp. 263-280.

Doherty, W. (1989b). Developments in Geoanalytical Inductively Coupled Plasma Mass Spectrometry; pp. 216-220 *in* Summary of Field Work and Other Activities. Ontario Geological Survey. Miscellaneous Paper 157.

Doherty, W., Wong, P., and Hodges, A.H. (1990). Determination of 22 trace elements in geological materials by inductively coupled plasma mass spectrometry; pp. 235-238 *in* Summary of Field Work and Other Activities. Ontario Geological Survey Miscellaneous Publication 151.

Gallagher, K. and Hawkesworth, C.J. (1992). Dehydration melting and the generation of continental flood basalts. Nature V. pp. 358, 57-59.

Giblin, P.E. and Armsburst, G.A. (1964-1968). Batchawana, Ontario Department of Mines. Map 2251, scale 1:63 360.

Giguère, J.F. (1975). Geology of St. Ignace Island and adjacent islands, District of Thunder Bay. Ontario Division of Mines, Geological Report 118, 35p., Map 2285.

Green, J.C. (1971). The North Shore Volcanic Group; Program, 17th Ann. Inst. Lake Superior Geol.; Duluth, Minn., May 1971, pp. 73-96.

Green, J.C. (1972). North Shore Volcanic Group; pp. 294-332 *in* Geology of Minnesota: A Centennial Volume. Edited by P.K. Sims and G.B. Morey, Minnesota Geological Survey, St. Paul.

Green, J.C. (1977). Keweenawan plateau volcanism in the Lake Superior Region Volcanic Regimes in Canada. Edited W.R.A. Baragar, L.C. Coleman, and K.M. Hall, Special Paper Geological Association of Canada 16, V. pp. 407-422.

Green, J.C. (1982). Geology of Keweenawan extrusive rocks; pp. 47-56 *in* Geology and tectonics of the Lake Superior Basin: Wold, R.J., and Hinze, W.J. eds., Memoir 156, Geological Society of America.

Green, J.C. (1983). Geological and geochemical evidence for the nature and development of the Middle Proterozoic (Keweenawan) midcontinent rift of North America: Tectonophysics, V. 94, p. 413-437.

Halls, H.C. and Pesonen, L.J. (1982). Paleomagnetism of Keweenawan rocks; pp. 173-201 *in* Geology and Tectonics of the Lake Superior Basin. Edited by R.J. Wold and W.J. Hinze. Memoir 156 Geological Society of America.

Hawkesworth, C.J., Lightfoot, P.C., Fedorenko, V.A., Blake, S., Naldrett, A.J., Doherty, W. and Gorbachev, N.S. (1995). Magma differentiation and mineralisation in the Siberian continental flood basalts. Lithos, V. 34, V. 1-3, pp. 61-87..

Hawkesworth, C.J. and Gallagher, K. (1993).Mantle hotspots, plumes and regional tectonics as causes of intraplate magmatism. Terra Nova, V. 5, pp. 552-559.

Henderson, P. (1982). Inorganic Geochemistry. Pergamon Press Inc. Oxford. 353pp.

Hellman, P.L., Smith, R.E., and Henderson, P. (1979). The mobility of the rare earth elements: evidence and implications from selected terrains affected by burial metamorphism. Contrib. Mineral. Petrol. V. 71, pp. 23-44.

Hooper, P.R., (1982). The Columbia River Basalts. Science, V. 215, pp. 1463-1466.

Klasner, J.S., Canon, W. F. and Van Schmus W.R. (1982). The Pre-Keweenanwan tectonic history of southern Canadian Shield and its influence on formation of the midcontinent rift; pp. 27-46 *in* Geological Society of America Memoir 156.

Klewin, K.W. (1989). Polybaric fractionation in an evolving continental rift: evidence from the Keweenawan Mid-continent rift. J. Geology. V.97, p. 65-76.

Klewin, K.W. and Berg, J.H. (1990). Geochemistry of the Mamainse Point volcanics, Ontario, and implications for the Keweenawan paleomagnetic record. Can. J. Earth Sciences, V. 27, p. 1194-1199.

Klewin, K.W., and Berg, J.H. (1991). Petrology of the Keweenawan Mamainse Point Lavas, Ontario: Petrogenesis and continental rift evolution. J. Geophys. Res. V. 96, p. 457-474.

Klewin, K.W. and Shirey S.B. (1992). The igneous petrology and magmatic evolution of the Midcontinent rift system; Tectono-physics, V. 213, pp. 33-40.

Kristmannsdottir, H., and Tomasson, J. (1978). Zeolite zones in geothermal areas in Iceland; pp. 273-284 *in* Natural Zeolites: Occurerence, properties and use; Sand, L.B., and Mumpton, F.A., eds., Oxford, Pergamon Press.

Lightfoot, P.C. (1993). The interpretation of geoanalytic data; pp. 377-455 *in* A handbook of Geoanalysis. Ed. C. Riddle. Dekker, New York.

Lightfoot, P.C., Hawkesworth, C.J., and Sethna, S.F. (1987). Petrogenesis of rhyolites and trachytes from the Deccan Trap: Sr, Nd, and Pb isotope and trace element evidence. Contrib. Mineral. Petrol. V. 95: pp. 44-54.

Lightfoot, P.C., and Hawkesworth, C.J. (1988). Origin of Deccan Trap lavas: evidence from combined trace element and Sr-, Nd-, and Pb- isotope studies. Earth Planet Science Letters. V. 91, pp. 89-104.

Lightfoot, P.C., Doherty, W., and Sutcliffe, R.H. (1989). Precise Determination of Trace Element Abundances in basalts from the Black Bay Peninsula and Mamainse Point sections of the Keweenawan volcanic pile using inductively coupled plasma-mass spectrometry; *pp. 265-274 in* Summary of Field Work and Other Activities 1989; Ontario Geological Survey, Miscellaneous Paper 146.

Lightfoot, P.C., Naldrett A.J., Gorbachev, N.S., Doherty, W., and Fedorenko, V.A. (1990). Geochemistry of the Siberian Trap of the Noril'sk area, USSR, with implications for the relative contributions of crust and mantle to flood basalt magmatism. Contrib. Mineral. Petrol. V. 104, pp. 631-644.

Lightfoot, P.C., Doherty, W., and Sutcliffe, R.H. (1991a). Crustal contamination identified in Keweenawan Osler Group Tholeiites, Ontario: A trace element perspective. J. Geology V. 99, pp. 739-760.

Lightfoot, P.C. Chai, G., Hodges, A.E., and Rowell, D. (1991b). An update report on the certification of the OGS in-house MRB standard-reference materials; pp. 231-236 *in* Summary of Field Work and Other Activities. Ontario Geological Survey Miscellaneous Paper No. 157.

Lightfoot, P.C., Hawkesworth, C.J., Hergt, J. Naldrett, A.J., Gorbachev, N.S., Fedorenko, V.A., and Doherty, W. (1993). Remobilisation of the continental lithosphere by a mantle plume: major-, trace-element, and Sr-, Nd-, and Pb-isotope evidence from picritic and tholeiitic lavas of the Noril'sk District, Siberian Trap, Russia. Contrib. Mineral. Petrol. V. 114, pp. 171-188.

Lightfoot, P.C., Naldrett, A.J., Gorbachev, N.S., Fedorenko, V.A., Hawkesworth, C.J., Hergt, J., and Doherty, W. (1994). Chemostratigraphy of Siberian Trap lavas, Noril'sk District, Russia: implications for the source of flood basalt magmas and their associated Ni-Cu mineralisation; pp. 283-312 *in* Proceedings of the Sudbury-Noril'sk Symposium. Ontario Geological Survey. Special Volume No. 5.

Livnat, A., Kelly, W.C., Essene, E.J. and Rye, R. O. (1983). P-T-X conditions of sub-greenschist burial metamorphism and copper mineralization, Keweenaw peninsula, northern Michigan; *in* Geological Society America, Abstracts with Programs, V. 15, 629 p.

Mahoney, J., Macdougall, J.D., Lugmair, G.W., Murali, A.V., Sankar Das, M., and Gopalan, K. (1982). Origin of the Deccan Trap flows at Mahabaleshwar inferred from Nd and Sr isotopic and chemical evidence. Earth Planet. Sci. Letts., V. 60, pp. 47-60.

Massey, N.W.D. (1980). The geochemistry of some Keweenawan metabasites from Mamainse Point, Ontario. Ph.D. thesis. McMaster University, Hamilton, Ontario. 352p.

Massey, N.W.D. (1983). Magma genesis in a late Proterozoic proto-oceanic rift: REE and other trace-element data from the Keweenawan Mamainse Point Formation, Ontario, Canada. Precambrian Research V. 21, p. 81-100.

McIlwaine, W.H., and Wallace, H. (1976). Geology of the Black Bay Peninsula, District of Thunder Bay; Ontario Division of Mines, Geological Report 133, 54p., Map 2304.

McKenzie, D., and Bickle, M.J. (1988). The volume and composition of melt generated by extension of the lithsophere. J. Petrol. V. 29, pp. 625-679.

Merk, G.P. and Jirsa, M.A. (1982). Provenance and tectonic significance of the Keweenawan interflow sedimentary rockspp. 97-106 *in* Geology and Tectonics of the Lake Superior Basin, edited by R..J. Wold and W.J. Hinze, Memoir Geological Society America 156, 280p.

Morgan, W.J. (1981). Hotspot tracks and the opening of the Atlantic and Indian Oceans; pp. 443-487 *in* The Sea, Emiliani C (ed.) Vol. 7, Wiley, New York, pp. 443-487.

Nakamura, N. (1974). Determination of REF, Ba, Fe, Mg, Na, and K in carbonaceous and ordinary chondrites. Geochem. Cosmochim Acta V. 38, pp. 757-775.

Naldrett, A.J., Lightfoot, P.C., Fedorenko, V.A., Doherty, W., and Gorbachev, N.S. (1992). Geology and geochemistry of intrusions and flood basalts of the Noril'sk Region, USSR, with implications for the origin of the Ni-Cu Ores. Econ. Geol. V. 87, pp. 975-1004.

Naldrett, A.J. and Lightfoot, P.C. (1993). Ni-Cu-PGE ores of the Noril'sk Region, Siberia: a model for giant magmatic sulphide deposits associated with flood basalts. In: Giant Ore Deposits. Ed. B.H. Whiting, C.J. Hodgson, and R. Mason. SEG Special Publication Number 2. pp. 81-124.

Nickolson, S.W., and Shirey, S.B. (1990). Evidence for a Precambrian mantle plume: A Sr, Nd, and Pb isotopic study of the Midcontinent Rift System in the Lake Superior Region, J. Geophys. Res. V. 95, pp. 10851-10868.

O'Hara, M.J. (1977). Geochemical evolution during fractional crystallisation of a periodically refilled magma chamber. Nature V. 266, pp. 503-507.

Ontario Geological Survey. (1990). The analysis of Geological Materials. Volume II: A Manual of Methods. Ontario Geological Survey. Miscellaneous Publication No. 149.

Paces, J.B. (1988). Magmatic processes, evolution and mantle source characteristics contributing to the petrogenesis of Midcontinent Rift basalts: Portage Lake Volcanics, Keweenaw Peninsula, Michigan. Ph.D. dissertation. Mich. Technol. Univ. Houghton, Mich.

Palmer, H.C. (1970) Paleomagnetism and correlation of some Middle Keweenawan rocks, Lake Superior. Can. J. Earth Sci. V. 7, pp. 1410-1436.

Peate, D.W., Hawkesworth, C.J., and Mantovani, M.S.M. (1992). Chemical stratigraphy of the Pacana lavas (South America): classification of magma types and their spatial distribution Bull. Volc. V. 55, pp. 119-139.

Pearce, J.A., and Norry, M.J. (1979) Petrogenetic implications of Ti, Zr, Y, and Nb variations in volcanic rocks. Contrib. Mineral. Petrol. V. 69: pp. 33-47.

Richards, J.P. and Spooner, E.T.C. (1989). Evidence for Cu-(Ag) Mineralization by Magmatic-Meteoric Mixing in Keweenawan Fissure Veins, Mamainse Point, Ontario. Economic Geology V. 84, pp. 360-385.

Sage, R. P. (1994). Geology of the Michipicoten Greenstone Belt. Ontario Geological Survey, Open File Report 5888, 592 p.

Sage, R. P. Lightfoot, P.C., and Doherty, W. (1996) Bimodal cyclical Archean basalts and rhyolites from the Michipicoten (Wawa) Greenstone Belt, Ontario: Geochemical evidence for magma contributions from ancient lithosphere at the southern margin of the Superior Province. Precambrian Research, V. 76, pp. 119-153.

Sethna, S.F., and Battiwala, H.K. (1980) Major element geochemistry of the intermediate and acidic rocks associated with the Deccan Trap basalts. Proc. 3rd Ind Geol. Cong. Poona, India, pp. 281-294.

Shirey, S.B., Klewin, K.W., Berg, J.H. and Carlson, R.W. (1994Temporal changes in the sources of flood basalts: Isotopic and trace element evidence from the 1100 Ma old Keewenawan Mamainse Point Formation, Ontario, Canada; Geochemica et Cosmochimica Acta 58, pp. 4475-4490.

Sutcliffe, R.H. (1987). Petrology of Middle Proterozoic diabases and picrites from Lake Nipigon, Canada. Contribs. Mineral. Petrol. V. 96, pp. 201-211.

Sutcliffe, R.H. (1991). Proterozoic Geology of the Lake Superior Area. Chapter 16; pp. 627-658 *in* Geology of Ontario. OGS Special Volume No. 1, Part 4, 711 p.

Sun, S.S. (1980). Lead isotopic study of young volcanic rocks from the mid-ocean ridges, ocean islands and island arcs; Philosophical Transactions Royal Society of London, A297, pp. 409-445.

Sun, S.S. and McDonough, W.F., (1989). Chemical and isotopic systematics of oceanic basalts: implications for mantle composition and processes pp. 313-345 *in* Magmatism in the Ocean Basins, Edited A.D. Saunders and M.J. Norry, Geological Society Special Publication 42.

Taylor, S.R. and McLennan, S.M. (1985). The continental crust: its composition and evolution. Blackwell Scientific Publications. 312pp.

Thompson, R.N. (1982). Magmatism of the British Tertiary Volcanic Province. Scotland Journal Geology V. 18, pp. 49-107.

Ujike, O., and Goodwin, A.M. (1987) Geochemistry and origin of Archean felsic metavolcanic rocks, Central Noranda Area, Quebec, Canada, Canadian Journal Earth Science V. 24, pp. 2551-2567.

Van Schmus, W.R., and Hinze, W.J. (1985) The Midcontinent Rift System, Annual Review of Earth and Planetary Sciences, V. 13, pp. 345-383.

Wallace, H. 1972. Differentiation trends in Osler Volcanics, Shesheeb Bay Section. MSc. dissertation. University of Toronto. 109 p.

Wallace, H. (1981). Keweenawan geology of the Lake Superior Region. Geological Survey of Canada, Paper 81-10, pp. 399-417.

Watts, A.B. and Cox, K.G. 1989. The Deccan Traps: an interpretation in terms of progressive lithospheric flexure in response to a migrating load. Earth Planet. Sci. Letts. V. 93: pp. 85-97.

Wold, R.J., and Hinze, W.J. (eds.) (1982) Geology and tectonics of the Lake Superior Basin. Memoir Geological Society America, V. 156, 280p.

Table 1. Average composition and route mean standard deviation (1σ) of 10 basalts collected at one location in a 16m thick flow from Group 2a, MPVG. Also shown are the mean and route mean standard deviation (1σ) of in-house basalt standard MRB25-29 determined during the course of these analyses, and comparison values from the compilation of results (Lightfoot et al., 1991b).

Analyte	n	Range Average (variation within one flow)		%RSD(1σ)	MRB25-29 Observed (In-house standard)	(1σ)	MRB25-29 Expected
SiO_2	10	47.2-52.6	49.1	2.7	49.1	*	49.11
TiO_2	10	1.82-1.97	1.88	2.1	1.90	*	1.96
Al_2O_3	10	12.9-14.1	13.6	2.9	12.50	*	12.65
$Fe2O_3$	10	11.9-13.9	13.3	4.?	13.60	*	13.61
MgO	10	8.3-10.3	9.3	7.5	5.94	*	6.13
MnO	10	0.16-0.20	0.17	5.8	0.20	*	0.19
CaO	10	8.0-11.0	9.2	9.7	9.10	*	9.53
Na_2O	10	1.92-3.64	2.8	21.4	2.40	*	2.45
K_2O	10	0.20-0.82	0.56	33.9	0.71	*	0.69
P_2O_5	10	0.18-0.20	0.19	5.3	0.26	*	0.25
LOI	10	2.8-8.9	4.0	45	3.00	*	2.97
Ba	10	165-1450	688	56.8	270	*	289
Rb		not detected			14	*	13.9
Sr	10	316-549	388	17.8	315	*	312
Y	10	16-19	17	5.9	25.3	*	25.1
Zr	10	100-117	112	4.5	175	*	174
Hf					4.8	*	4.72
Nb					14	*	13.9
Ta					0.85	*	0.83
Ni	10	208-356	279	12.9	97	*	91
Cu	10	50-136	91	36.3	148	*	150
Cr	10	399-560	498	8.6	244	*	255
Sc	10	20-25	23	4.3	31	*	29
V	10	214-285	264	7.2	294	*	312
Zn	10	78-95	87	6.8	111	*	117
Co	10	42-55	51	7.8	45	*	47
La	10	10-12	11.6	6.0	21.3	0.6	20.38
Ce	10	25-29	28.3	4.6	51.3	1.2	48.85
Pr	10	3.3-3.9	3.8	5.3	6.57	0.06	6.30
Nd	10	15-19	17.8	6.2	29.3	0.6	27.68
Sm	10	4.0-4.8	4.5	4.4	6.60	0.10	6.21
Eu	10	1.5-1.7	1.7	5.5	2.03	0.11	1.94
Gd	10	3.8-4.4	4.2	4.8	5.73	0.21	5.46
Tb	10	0.55-0.69	0.64	6.3	0.88	0.02	0.83
Dy	10	3.4-4.0	3.8	5.3	5.33	0.06	5.10
Ho	10	0.63-0.78	0.73	5.5	1.00	0.01	1.00
Er	10	1.6-1.9	1.8	5.6	2.67	0.06	2.55
Tm	10	0.21-0.27	0.24	8.3	0.37	0.02	0.37
Yb	10	1.4-1.6	1.5	6.7	2.47	0.06	2.35
Lu	10	0.19-0.22	0.21	4.8	0.35	0.01	0.35

Note: Samples included in the average of one flow: 8, 92,93, 94, 95, 96, 97, 98, 99, 100, 101.

* - precision for major element standards is typically 5% rsd 2σ, or better for all major element oxides. For trace element standards, except where shown, precision is typically 5% or better.

RSD = Root Mean Square Deviation

Table 2: Representative analysis of samples from the Mamainse Point sequence sorted by stratigraphic position.

SAMPLE NUMBER	STRATI-GRAPHIC POSITION (M)	GROUP	SiO_2	TiO_2	Al_2O_3	Fe_2O_3	MgO	MnO	CaO	Na_2O	K_2O	P_2O_5	LOI	Mg-Number
5	40	1	49.2	1.15	12.82	12.93	12.70	0.12	9.71	1.04	0.22	0.08	10.7	0.696
1	105	2a	50.2	1.38	13.43	11.91	10.54	0.25	8.23	3.25	0.64	0.13	6.9	0.673
2	175	1	50.8	1.20	14.03	11.60	9.50	0.18	9.49	2.30	0.76	0.09	5.2	0.656
3	255	1	49.6	1.30	14.31	12.15	9.00	0.19	9.91	2.67	0.74	0.11	2.4	0.633
4	305	Daisystone	50.0	1.68	19.02	10.40	4.53	0.20	7.71	5.28	1.02	0.14	5.1	0.503
6	350	2a	47.8	1.72	12.78	14.17	11.08	0.17	9.88	1.93	0.28	0.16	4.6	0.645
7	460	2a	46.9	1.81	12.00	14.78	12.32	0.17	9.33	2.08	0.42	0.19	5.2	0.660
9	530	2a	47.2	2.02	12.66	14.70	12.23	0.17	8.47	1.87	0.45	0.24	5.3	0.659
92	605	2a	50.3	1.69	14.13	12.45	9.04	0.16	9.12	2.30	0.45	0.35	4.8	0.628
8	655	2a	49.5	1.85	13.90	13.70	8.82	0.16	9.21	2.01	0.62	0.19	2.8	0.600
93	655	2a	51.6	1.87	12.88	11.89	9.49	0.17	8.04	3.63	0.20	0.18	8.9	0.650
94	655	2a	47.2	1.97	14.09	13.46	10.30	0.20	8.83	3.07	0.72	0.19	3.9	0.640
95	655	2a	48.2	1.87	13.85	13.33	9.91	0.18	9.49	2.53	0.47	0.18	3.9	0.634
96	655	2a	48.5	1.87	13.70	13.08	9.85	0.19	9.76	2.44	0.44	0.19	3.5	0.637
97	655	2a	50.7	1.87	13.08	12.56	9.25	0.17	9.90	1.92	0.40	0.20	3.4	0.631
98	655	2a	48.2	1.88	13.81	13.39	8.25	0.18	10.98	2.54	0.53	0.20	4.0	0.589
99	655	2a	49.7	1.82	13.44	13.76	9.25	0.18	8.25	2.63	0.82	0.18	3.2	0.610
100	655	2a	48.1	1.89	13.45	13.87	9.77	0.18	8.59	3.19	0.76	0.18	3.3	0.621
101	655	2a	49.2	1.89	13.51	13.51	8.55	0.16	8.66	3.64	0.65	0.19	3.1	0.595
10	720	2b	54.4	1.13	15.22	11.44	5.63	0.18	6.86	3.21	1.80	0.17	1.9	0.534
11	760	2b	54.0	1.16	15.34	11.22	6.26	0.16	6.11	3.46	2.06	0.19	2.5	0.565
72	840	2c	49.0	2.38	14.98	14.14	8.42	0.17	5.21	3.87	1.64	0.23	4.0	0.581
12	915	2c	50.6	2.26	15.12	13.41	8.44	0.17	5.38	3.63	0.73	0.23	6.6	0.594
13	1005	2c	49.5	2.16	15.03	13.32	7.63	0.21	7.32	3.77	0.90	0.20	5.9	0.571
14	1105	2c	50.6	2.00	15.65	12.78	8.31	0.26	4.58	3.59	2.02	0.23	5.4	0.602
15	1200	3	49.1	1.43	16.19	12.25	8.21	0.21	9.28	2.42	0.69	0.20	7.5	0.609
16	1380	3	48.4	1.91	15.58	11.77	6.36	0.22	10.69	3.44	1.45	0.21	7.3	0.557
17	1430	3	50.2	1.34	16.55	12.00	6.13	0.30	7.99	4.18	1.21	0.13	2.4	0.543
18	1480	3	49.9	1.37	15.77	11.83	7.80	0.26	7.49	4.05	1.36	0.17	3.6	0.606
73	1535	3	50.2	1.22	16.53	11.67	6.98	0.21	7.30	4.73	1.02	0.12	7.4	0.582
74	1575	3	50.0	1.22	16.13	11.91	6.75	0.30	7.39	5.10	1.05	0.12	6.3	0.569
76	1595	3	49.1	1.57	15.93	12.08	6.91	0.20	10.69	2.64	0.74	0.17	6.2	0.571
19	1760	3b	48.1	1.52	19.23	12.72	6.67	0.16	4.31	5.45	1.63	0.22	6.3	0.550
20	1785	3c	48.1	1.43	15.78	13.34	8.22	0.21	8.38	2.99	1.31	0.21	9.8	0.589
21	1860	5a	54.5	0.64	15.92	10.35	7.15	0.23	5.49	2.70	2.95	0.04	4.2	0.617
22	1945	5a	55.7	0.65	16.56	9.64	7.28	0.19	6.17	2.86	0.91	0.06	5.9	0.637
23	2065	5b	49.2	0.60	15.61	11.99	7.28	0.25	13.01	1.38	0.62	0.06	11.6	0.586
24	2160	5b	49.1	0.71	17.51	12.58	5.83	0.18	12.05	1.83	0.18	0.07	4.4	0.519
25	2210	5b	48.6	0.68	16.76	13.16	7.99	0.15	9.25	3.12	0.20	0.05	2.7	0.586
77	2280	5b	44.8	0.85	17.97	11.36	5.24	0.24	16.70	1.45	1.30	0.07	12.6	0.518
78	2310	5c	52.4	1.38	13.59	16.57	3.89	0.18	7.93	2.84	1.07	0.20	5.6	0.353
26	2370	5b	49.5	0.61	16.74	11.78	7.67	0.19	11.26	1.86	0.33	0.06	2.7	0.602
27	3040	6a	50.3	2.15	13.94	17.38	5.50	0.19	6.90	3.05	0.36	0.23	6.5	0.424
07	3080	6b	49.1	3.14	12.23	18.78	4.66	0.42	8.79	2.26	0.21	0.36	6.3	0.366
08	3095	6a	48.9	2.22	16.67	13.91	3.59	0.27	11.82	2.14	0.22	0.24	7.9	0.375
28	3105	6a	50.2	1.98	14.97	14.20	3.99	0.26	11.89	2.05	0.23	0.23	8.7	0.395
29	3115	6a	50.4	2.18	14.85	15.18	4.75	0.24	8.92	3.08	0.15	0.27	8.6	0.421
30	3180	6a	49.5	2.29	14.73	17.56	4.72	0.19	7.27	3.12	0.35	0.24	8.0	0.385
31	3190	6b	47.9	2.69	13.38	17.98	4.86	0.29	9.55	2.76	0.32	0.29	4.0	0.386
32	3220	6b	48.9	3.02	12.83	17.94	4.22	0.30	9.03	3.10	0.33	0.32	3.7	0.354
33	3240	6b	49.2	3.13	12.61	18.65	5.42	0.26	6.99	3.13	0.34	0.31	3.5	0.403
34	3270	6b	49.5	3.14	11.79	20.33	4.45	0.25	7.66	2.33	0.17	0.36	7.0	0.337
35	3305	6a	49.1	1.80	16.34	12.29	4.70	0.23	12.85	2.01	0.45	0.19	10.9	0.471
79	3385	6a	49.8	1.87	15.65	13.22	5.26	0.20	9.79	3.63	0.33	0.23	4.9	0.481
80	3505	6b	49.6	2.44	13.85	17.56	5.52	0.21	6.51	3.09	0.86	0.33	6.9	0.422
36	3610	6a	50.2	1.92	15.53	14.38	5.38	0.22	10.42	1.22	0.50	0.21	11.1	0.465
81	3750	6a	49.4	2.26	14.36	15.58	4.92	0.22	9.37	2.55	1.09	0.25	8.9	0.423
37	3800	6a	48.3	1.96	15.55	15.33	4.10	0.20	11.85	2.29	0.17	0.26	7.8	0.384

Table 2: Representative analysis of samples from the Mamainse Point sequence (continued)

SAMPLE NUMBER	STRATI-GRAPHIC POSITION (M)	GROUP	SiO_2	TiO_2	Al_2O_3	Fe_2O_3	MgO	MnO	CaO	Na_2O	K_2O	P_2O_5	LOI	Mg-Number
82	3840	6a	48.8	2.31	14.01	17.12	1.95	0.22	10.66	2.67	2.00	0.27	9.7	0.209
38	3880	6c	50.8	3.27	10.89	21.34	4.03	0.28	6.39	1.61	0.81	0.54	7.8	0.305
39	3960	6a	48.5	2.02	16.17	14.96	5.90	0.16	9.35	2.41	0.27	0.25	7.6	0.478
83	3990	6a	47.8	2.07	16.24	16.02	5.50	0.17	8.87	2.65	0.39	0.24	8.2	0.444
84	4020	6c	48.1	2.75	14.10	16.48	3.22	0.25	11.48	2.46	0.83	0.34	11.4	0.312
40	4040	6c	49.0	3.00	16.06	15.32	3.70	0.18	6.96	2.97	1.86	0.93	4.0	0.360
41	4095	6c	43.3	2.87	14.82	24.74	4.41	0.26	8.95	0.18	0.11	0.33	11.8	0.293
42	4180	7a	48.8	1.07	18.11	9.81	9.04	0.18	10.89	1.81	0.22	0.10	4.4	0.682
43	4240	7a	48.5	1.07	18.23	9.93	8.33	0.17	10.92	2.43	0.26	0.12	4.3	0.661
44	4270	7a	48.5	0.98	16.89	10.49	9.82	0.15	11.22	1.76	0.16	0.08	4.3	0.685
85	4305	7a	48.8	0.96	17.19	10.13	8.86	0.14	11.36	2.34	0.19	0.08	3.9	0.671
45	4370	7a	49.4	0.94	17.27	9.93	9.66	0.18	8.81	3.41	0.35	0.07	4.8	0.694
47	4500	7c	48.4	2.30	15.53	14.50	7.27	0.21	8.32	2.34	0.78	0.40	3.2	0.539
46	4505	7a	48.6	0.99	17.49	10.23	8.55	0.24	11.30	2.29	0.24	0.10	7.5	0.660
64	4510	7b	49.1	1.33	16.81	11.77	7.55	0.14	10.61	2.28	0.28	0.15	3.6	0.599
90	4510	7a	47.9	0.87	17.44	10.72	9.46	0.14	11.35	1.84	0.17	0.09	4.5	0.672
91	4510	7a	48.6	1.04	17.46	10.87	8.18	0.19	11.35	1.36	0.91	0.09	8.3	0.637
86	4540	7b	48.3	1.42	17.41	11.64	8.99	0.15	9.45	2.30	0.20	0.14	6.3	0.643
48	4560	7a	48.3	1.09	17.22	10.75	8.82	0.18	11.38	1.93	0.20	0.13	3.9	0.656
49	4560	7b	48.3	1.25	17.56	11.18	7.89	0.18	10.56	2.69	0.28	0.13	4.1	0.622
63	4595	7b	48.2	1.56	17.16	11.93	6.64	0.16	10.88	3.03	0.27	0.15	3.2	0.565
50	4640	7d	43.1	3.80	15.68	14.93	4.53	0.20	12.68	2.98	1.31	0.81	6.3	0.414
51	4750	7b	47.1	1.46	16.61	13.75	9.02	0.26	9.51	1.83	0.34	0.14	5.2	0.604
52	5000	7b	47.9	1.88	16.94	13.59	6.76	0.20	9.33	2.89	0.31	0.21	3.7	0.537
53	5100	7b	47.3	1.58	17.08	12.88	7.86	0.16	10.32	2.39	0.22	0.17	4.5	0.587
54	5160	7b	46.7	1.60	16.44	13.39	8.43	0.18	10.29	2.56	0.25	0.16	4.3	0.594
55	5180	7b	47.4	1.64	16.36	13.40	8.08	0.21	10.02	2.37	0.37	0.17	4.1	0.584
56	5230	7b	48.8	1.63	16.44	13.28	7.99	0.22	6.75	4.02	0.75	0.14	4.8	0.583
57	5260	7b	48.3	1.40	16.80	12.54	7.53	0.15	10.11	2.65	0.41	0.15	4.9	0.583
59	5310	7b	45.3	1.94	16.01	14.32	2.88	0.24	14.32	4.01	0.74	0.20	9.9	0.318
60	5430	9	46.2	3.66	14.44	16.22	6.06	0.33	6.74	4.42	1.02	0.95	3.5	0.465
61	5530	9	46.5	3.73	14.52	16.59	4.83	0.20	8.66	2.69	1.41	0.91	2.3	0.404

FOOTNOTES:

-All analysis recalculated to 100% free of LOI

-Mg-number = $MgO/40.404/(MgO/40.404)+85/100*(Fe_2O_3/79.9226)$.

Table 2: Total Fe expressed as Fe_2O_3 (continued)

Sample number	Stratigraphic position (m)	Group	Ba (ppm)	Rb (ppm)	Sr (ppm)	Zr (ppm)	Hf (ppm)	Nb (ppm)	Ta (ppm)	Y (ppm)	Ni (ppm)	Cu (ppm)	Cr (ppm)	Co (ppm)	Sc (ppm)	V (ppm)	Zn (ppm)
5	40.0	1	112	5	125	69	1.9	3.3	0.22	13	460	21	1190	67	23.0	205	87
1	105	2a	267	14	275	99	2.7	6.5	0.39	16	223	132	415	53	27.0	245	103
2	175	1	418	18	220	78	2.2	3.9	0.23	15	165	33	500	45	28.0	256	80
3	255	1	540	20	260	91	2.6	4.7	0.29	17	170	65	500	45	28.0	266	87
4	305	Daisy-stone	441	33	650	91	2.6	5.2	0.35	14	109	114	98	38	18.0	228	204
6	350	2a	215	2	255	110	3.1	8.2	0.47	18	400	33	915	60	26.0	267	94
7	460	2a	190	7	275	105	3.0	8.4	1.20	17	540	59	845	66	23.0	246	90
9	530	2a	231	6	330	125	3.4	12.0	0.73	18	530	63	835	65	19.0	238	95
92	605	2a	306	n.a.	364	104	n.a.	n.a.	n.a.	17	191	173	550	46	23.0	236	89
8	655	2a	684	10	390	110	3.0	9.6	0.59	18	290	50	520	55	25.0	276	95
93	655	2a	165	n.a.	340	100	n.a.	n.a.	n.a.	16	208	67	399	42	20.0	214	78
94	655	2a	397	n.a.	360	117	n.a.	n.a.	n.a.	19	288	132	510	54	24.0	285	94
95	655	2a	463	n.a.	339	111	n.a.	n.a.	n.a.	18	277	91	475	51	23.0	260	88
96	655	2a	403	n.a.	316	111	n.a.	n.a.	n.a.	18	356	134	560	52	23.0	263	92
97	655	2a	541	n.a.	338	111	n.a.	n.a.	n.a.	17	265	136	535	48	23.0	261	83
98	655	2a	682	n.a.	400	115	n.a.	n.a.	n.a.	17	273	100	500	51	23.0	264	81
99	655	2a	1450	n.a.	443	114	n.a.	n.a.	n.a.	17	273	73	485	50	24.0	271	87
100	655	2a	935	n.a.	411	113	n.a.	n.a.	n.a.	18	283	64	515	52	24.0	276	92
101	655	2a	1160	n.a.	549	116	n.a.	n.a.	n.a.	18	276	60	485	51	24.0	267	83
10	720	2b	700	39	350	165	4.1	27.0	1.50	23	34	98	56	36	30.0	226	89
11	760	2b	716	38	310	170	4.4	26.0	1.60	25	37	144	49	39	34.0	257	95
72	840	2c	1095	n.a.	396	130	n.a.	n.a.	n.a.	19	223	32	305	44	20.0	267	137
12	915	2c	161	27	175	155	4.0	14.0	0.76	22	99	18	150	45	25.0	278	158
13	1005	2c	777	24	375	135	3.7	12.0	0.77	20	107	43	142	41	24.0	239	117
14	1105	2c	885	39	275	145	3.9	15.0	0.94	21	142	128	137	42	23.0	276	217
15	1200	3	288	13	275	93	2.5	12.0	0.77	17	71	62	102	42	30.0	245	171
16	1380	3	773	39	375	105	2.9	9.5	0.59	17	106	46	209	35	27.0	246	103
17	1430	3	1230	24	720	96	2.5	12.0	0.75	18	73	41	105	41	32.0	248	155
18	1480	3	750	32	365	99	2.7	12.0	0.75	19	73	67	108	43	31.0	255	177
73	1535	3	616	n.a.	292	82	n.a.	n.a.	n.a.	n.a.	87	5	230	45	29.0	227	143
74	1575	3	548	n.a.	316	85	n.a.	n.a.	n.a.	n.a.	76	40	145	38	28.0	217	236
76	1595	3	376	n.a.	300	96	n.a.	n.a.	n.a.	18	61	70	87	39	28.0	237	114
19	1760	3b	491	44	165	44	1.4	7.6	0.49	17	100	15	207	39	32.0	236	140
20	1785	3c	243	60	150	125	3.1	11.0	0.70	22	91	26	95	54	37.0	241	126
21	1860	5a	723	93	275	83	2.7	14.0	0.92	26	28	43	94	40	24.5	164	162
22	1945	5a	321	22	240	85	2.7	15.0	1.00	28	31	105	77	39	22.3	167	162
23	2065	5b	128	26	125	27	0.8	1.6	0.10	16	42	6	230	43	11.1	213	135
24	2160	5b	160	2	170	48	1.4	4.0	0.27	18	37	124	109	48	15.8	210	79
25	2210	5b	141	4	375	39	1.2	2.3	0.15	17	39	38	135	49	33.3	217	73
77	2280	5b	124	n.a.	126	37	n.a.	n.a.	n.a.	14	142	23	108	59	33.0	202	110
78	2310	5c	437	n.a.	241	117	n.a.	n.a.	n.a.	33	35	121	33	41	41.0	302	88
26	2370	5b	288	6	220	43	1.3	2.8	0.19	17	35	24	109	47	18.6	196	74
27	3040	6a	229	12	210	140	4.0	10.0	0.63	29	33	100	78	42	19.3	282	138
107	3080	6b	163	n.a.	210	194	n.a.	n.a.	n.a.	37	26	189	365	42	44.0	395	207
108	3095	6a	176	n.a.	251	127	n.a.	n.a.	n.a.	24	52	351	106	37	32.0	271	156
28	3105	6a	134	6	235	145	3.7	10.0	0.61	27	33	75	99	34	20.3	291	131
29	3115	6a	111	4	265	155	3.9	11.0	0.63	28	33	141	89	40	23.8	287	132
30	3180	6a	121	11	210	130	3.4	9.1	0.60	26	32	21	91	38	20.4	287	119
31	3190	6b	216	4	245	200	5.3	14.0	0.84	35	39	200	78	44	21.5	352	143
32	3220	6b	338	3	235	195	5.4	14.0	1.20	38	44	337	69	41	21.6	414	161
33	3240	6b	318	5	300	215	5.7	16.0	0.94	40	43	174	65	41	26.3	402	147
34	3270	6b	160	3	260	195	5.3	15.0	0.86	37	39	229	44	40	22.3	394	173
35	3305	6a	154	10	210	115	3.0	8.0	0.46	21	28	292	140	41	17.4	236	105
79	3385	6a	267	n.a.	443	130	n.a.	n.a.	n.a.	26	47	249	152	34	31.0	272	93
80	3505	6b	415	n.a.	222	184	n.a.	n.a.	n.a.	37	32	106	122	37	39.0	319	120
36	3610	6a	134	14	160	125	3.2	8.3	0.49	22	29	251	155	44	14.3	250	221
81	3750	6a	264	n.a.	165	132	n.a.	n.a.	n.a.	28	35	89	139	37	36.0	319	132
37	3800	6a	150	2	240	130	3.3	9.7	0.55	23	27	141	80	45	20.9	234	113
82	3840	6a	219	n.a.	169	148	n.a.	n.a.	n.a.	30	30	115	119	25	33.0	323	69
38	3880	6c	272	24	130	305	8.1	22.0	1.50	54	31	121	0	33	11.2	89	195
39	3960	6a	197	14	245	145	3.5	10.0	0.59	24	29	214	75	44	21.2	249	107
83	3990	6a	200	n.a.	229	126	n.a.	n.a.	n.a.	24	116	74	88	50	30.0	251	125
84	4020	6c	345	n.a.	164	174	n.a.	n.a.	n.a.	34	34	126	95	40	37.0	309	127
40	4040	6c	760	59	275	390	8.6	110.0	7.00	38	21	20	0	27	24.2	106	133

Table 2: Total Fe expressed as Fe_2O_3 (continued)

Sample number	Strati-graphic position (m)	Group	Ba (ppm)	Rb (ppm)	Sr (ppm)	Zr (ppm)	Hf (ppm)	Nb (ppm)	Ta (ppm)	Y (ppm)	Ni (ppm)	Cu (ppm)	Cr (ppm)	Co (ppm)	Sc (ppm)	V (ppm)	Zn (ppm)
41	4095	6c	86	5	53	205	5.4	14.0	0.82	35	60	78	158	75	45.0	359	508
42	4180	7a	120	4	305	69	1.8	4.7	0.28	16	217	50	235	42	29.0	194	64
43	4240	7a	141	6	280	68	1.9	4.6	0.28	15	217	42	226	42	29.0	194	68
44	4270	7a	123	3	235	62	1.6	4.0	0.44	13	240	99	260	46	32.0	182	66
85	4305	7a	118	n.a.	246	58	n.a.	n.a.	n.a.	14	190	41	262	43	27.0	192	70
45	4370	7a	350	11	770	66	1.6	4.1	0.25	14	201	40	237	42	25.0	182	63
47	4500	7c	471	16	305	195	4.6	27.0	1.70	27	105	70	155	45	28.0	262	113
46	4505	7a	157	4	245	63	1.6	4.3	0.25	13	206	103	251	42	24.0	187	116
64	4510	7b	118	n.a.	222	86	n.a.	n.a.	n.a.	18	158	81	196	43	26.0	204	77
90	4510	7a	103	n.a.	208	56	n.a.	n.a.	n.a.	13	278	34	287	47	24.0	175	64
91	4510	7a	318	n.a.	186	48	n.a.	n.a.	n.a.	13	206	26	273	44	25.0	186	114
86	4540	7b	121	n.a.	230	88	n.a.	n.a.	n.a.	18	160	101	218	47	27.0	206	99
48	4560	7a	130	3	245	71	1.9	4.9	0.29	15	203	123	258	46	26.0	186	71
49	4560	7b	114	7	320	94	2.4	6.7	0.38	18	170	101	210	45	26.0	203	75
63	4595	7b	121	n.a.	237	93	n.a.	n.a.	n.a.	20	89	43	230	41	31.0	248	81
50	4640	7d	643	35	385	295	6.7	51.0	3.20	27	120	229	63	44	26.0	310	197
51	4750	7b	140	6	240	100	2.6	7.3	0.46	20	135	107	140	51	28.0	230	90
52	5000	7b	219	4	250	135	3.4	10.0	0.59	26	74	98	85	46	30.0	242	114
53	5100	7b	130	2	240	105	2.9	7.9	0.48	21	169	52	189	47	22.0	222	81
54	5160	7b	140	4	260	100	2.5	7.9	0.45	20	172	50	179	51	26.0	223	91
55	5180	7b	160	n.a.	241	96	n.a.	n.a.	n.a.	20	159	37	166	47	26.0	217	85
56	5230	7b	422	n.a.	402	101	n.a.	n.a.	n.a.	21	120	38	193	45	28.0	227	89
57	5260	7b	150	n.a.	245	93	n.a.	n.a.	n.a.	19	125	88	156	44	26.0	210	82
59	5310	7b	261	n.a.	296	117	n.a.	n.a.	n.a.	n.a.	65	49	106	44	29.0	242	143
60	5430	9	436	n.a.	274	332	n.a.	n.a.	n.a.	37	96	81	51	44	26.0	340	198
61	5530	9	647	n.a.	421	320	n.a.	n.a.	n.a.	37	91	199	51	42	25.0	357	113

n.a. - not available

Table 2. (continued)

Sample	Stratigraphic position (m)	Group	La (ppm)	Ce (ppm)	Pr (ppm)	Nd (ppm)	Sm (ppm)	Eu (ppm)	Gd (ppm)	Tb (ppm)	Dy (ppm)	Ho (ppm)	Er (ppm)	Tm (ppm)	Yb (ppm)	Lu (ppm)
5	40.0	1	7	15	1.9	9	2.4	0.9	2.5	0.44	2.7	0.50	1.4	0.17	1.2	0.17
1	105	2a	12	27	3.3	15	3.5	1.2	3.5	0.56	3.3	0.66	1.6	0.21	1.4	0.22
2	175	1	8	18	2.4	11	3.0	1.1	3.0	0.49	3.0	0.60	1.7	0.21	1.3	0.20
3	255	1	9	20	2.6	13	3.5	1.2	3.5	0.57	3.5	0.68	1.8	0.25	1.5	0.23
4	305	Daisy-stone	8	20	2.7	13	3.3	1.3	3.3	0.50	3.1	0.56	1.4	0.18	1.2	0.16
6	350	2a	12	27	3.5	17	4.3	1.4	4.1	0.66	3.9	0.72	1.8	0.24	1.6	0.21
7	460	2a	13	28	3.8	18	4.5	1.5	4.2	0.63	3.7	0.67	1.7	0.22	1.4	0.21
9	530	2a	14	33	4.2	20	4.9	1.8	4.4	0.67	3.8	0.69	1.8	0.22	1.5	0.20
92	605	2a	14	33	4.1	19	4.4	1.7	4.0	0.60	3.6	0.69	1.7	0.23	1.3	0.21
8	655	2a	12	29	3.8	18	4.4	1.6	4.4	0.63	3.7	0.68	1.7	0.22	1.5	0.21
93	655	2a	10	25	3.3	15	4.0	1.5	3.8	0.55	3.4	0.63	1.6	0.21	1.4	0.19
94	655	2a	12	29	3.8	18	4.6	1.7	4.3	0.64	4.0	0.74	1.8	0.25	1.5	0.22
95	655	2a	12	29	3.8	18	4.8	1.7	4.2	0.65	3.8	0.76	1.8	0.25	1.6	0.21
96	655	2a	12	29	3.9	19	4.8	1.7	4.3	0.65	3.9	0.77	1.9	0.25	1.6	0.22
97	655	2a	11	28	3.8	18	4.7	1.7	4.3	0.65	3.7	0.73	1.7	0.23	1.5	0.21
98	655	2a	12	28	3.7	18	4.5	1.7	4.1	0.64	3.7	0.72	1.8	0.23	1.4	0.21
99	655	2a	11	28	3.8	17	4.4	1.6	4.0	0.62	3.7	0.74	1.7	0.24	1.4	0.21
100	655	2a	12	29	3.8	18	4.5	1.7	4.3	0.64	3.8	0.72	1.8	0.25	1.5	0.22
101	655	2a	12	29	3.9	19	4.7	1.7	4.4	0.69	4.0	0.78	1.8	0.27	1.5	0.22
10	720	2b	28	60	6.7	26	5.3	1.7	4.9	0.77	4.7	0.94	2.5	0.38	2.4	0.37
11	760	2b	30	62	6.9	28	5.6	1.7	4.9	0.77	4.9	0.98	2.6	0.38	2.6	0.38
72	840	2c	14	33	4.3	20	4.8	1.8	4.5	0.67	4.1	0.78	1.8	0.26	1.6	0.23
12	915	2c	16	39	5.0	24	5.8	2.0	5.6	0.79	4.5	0.88	2.1	0.29	1.7	0.26
13	1005	2c	17	39	5.0	23	5.4	1.9	4.9	0.75	4.3	0.80	1.9	0.27	1.6	0.23
14	1105	2c	20	45	5.5	25	5.6	1.8	5.1	0.76	4.4	0.82	2.0	0.27	1.7	0.25
15	1200	3	14	31	3.6	16	3.7	1.3	3.4	0.56	3.5	0.71	1.8	0.24	1.6	0.25
16	1380	3	13	31	3.9	19	4.4	1.6	4.2	0.62	3.6	0.70	1.7	0.24	1.4	0.21
17	1430	3	14	30	3.7	16	3.8	1.4	3.5	0.55	3.5	0.69	1.8	0.27	1.6	0.26
18	1480	3	15	31	3.8	17	4.0	1.3	3.9	0.59	3.7	0.75	1.8	0.27	1.7	0.28
73	1535	3	n.a.	n.a.	n.a.	n.a	n.a.	n.a.	n.a.	n.a.	n.a.	n.a.	n.a.	n.a.	n.a.	n.a.
74	1575	3	n.a.	n.a.	n.a.	n.a.	n.a.	n.a.	n.a.	n.a.	n.a.	n.a.	n.a.	n.a.	n.a.	n.a.
76	1595	3	13	30	3.7	16	3.7	1.3	3.5	0.57	3.5	0.65	1.8	0.25	1.7	0.25
19	1760	3b	7	17	2.2	11	2.8	1.2	2.7	0.49	3.2	0.64	1.8	0.25	1.7	0.25
20	1785	3c	15	33	4.1	16	4.0	1.2	3.7	0.63	4.2	0.88	2.4	0.37	2.3	0.36
21	1860	5a	23	45	4.7	18	3.6	0.7	3.5	0.65	4.3	0.98	2.8	0.44	2.9	0.47
22	1945	5a	25	49	4.9	19	3.9	0.8	4.0	0.69	4.5	1.00	2.8	0.45	3.1	0.49
23	2065	5b	3	7	1.0	5	1.5	0.6	2.1	0.39	2.8	0.63	1.9	0.29	1.9	0.28
24	2160	5b	7	14	1.7	8	2.1	0.8	2.4	0.42	3.1	0.71	1.9	0.30	2.1	0.31
25	2210	5b	4	9	1.2	6	1.9	0.8	2.4	0.44	3.1	0.68	2.0	0.29	2.1	0.33
77	2280	5b	4	9	1.1	5	1.7	0.7	2.0	0.36	2.6	0.57	1.6	0.26	1.8	0.26
78	2310	5c	19	40	4.6	19	4.4	1.5	4.6	0.83	5.6	1.20	3.4	0.53	3.6	0.53
26	2370	5b	5	11	1.3	6	1.8	0.8	2.3	0.42	3.0	0.67	1.9	0.29	1.9	0.31
27	3040	6a	14	33	4.5	21	5.5	1.8	5.6	0.92	5.8	1.20	3.1	0.44	2.9	0.44
107	3080	6b	17	44	5.8	26	7.1	2.3	7.3	1.20	7.7	1.60	4.2	0.60	4.0	0.58
108	3095	6a	13	32	4.1	19	5.0	1.8	4.7	0.81	5.1	1.10	2.8	0.41	2.7	0.39
28	3105	6a	13	32	4.1	20	5.0	1.8	5.1	0.79	5.3	1.00	2.7	0.41	2.6	0.38
29	3115	6a	14	34	4.4	20	5.4	1.7	5.3	0.85	5.5	1.10	3.2	0.44	2.8	0.42
30	3180	6a	13	31	4.0	19	4.9	1.7	5.1	0.80	5.4	1.10	2.9	0.41	2.6	0.40
31	3190	6b	16	41	5.5	27	6.9	2.2	7.1	1.20	7.2	1.50	4.3	0.59	3.7	0.57
32	3220	6b	17	42	5.5	27	7.3	2.2	6.7	1.20	7.7	1.40	4.1	0.56	3.8	0.54
33	3240	6b	18	45	6.0	29	7.6	2.3	7.4	1.20	7.8	1.60	4.2	0.64	3.9	0.62
34	3270	6b	20	44	6.0	28	7.5	2.3	7.5	1.20	7.6	1.60	4.3	0.62	4.0	0.58
35	3305	6a	14	29	3.8	17	4.2	1.6	4.2	0.64	4.2	0.81	2.3	0.34	2.2	0.30
79	3385	6a	13	31	4.0	19	4.7	1.7	4.9	0.77	5.0	1.00	2.6	0.40	2.6	0.38
80	3505	6b	17	43	5.7	26	6.8	2.4	7.1	1.20	7.3	1.50	3.9	0.57	3.9	0.57

Table 2. (continued)

Sample	Stratigraphic position (m)	Group	La (ppm)	Ce (ppm)	Pr (ppm)	Nd (ppm)	Sm (ppm)	Eu (ppm)	Gd (ppm)	Tb (ppm)	Dy (ppm)	Ho (ppm)	Er (ppm)	Tm (ppm)	Yb (ppm)	Lu (ppm)
36	3610	6a	12	28	3.5	16	4.3	1.5	4.0	0.67	4.3	0.88	2.5	0.31	2.4	0.32
81	3750	6a	13	32	4.2	20	5.2	1.8	5.1	0.83	5.4	1.10	2.9	0.41	2.8	0.42
37	3800	6a	12	29	3.8	17	4.4	1.6	4.6	0.73	4.5	0.92	2.4	0.37	2.4	0.38
82	3840	6a	15	37	4.7	21	5.5	1.8	5.6	0.86	5.8	1.20	3.1	0.44	2.8	0.44
38	3880	6c	26	65	8.5	39	10.0	3.0	10.0	1.70	11.0	2.10	6.1	0.84	5.6	0.87
39	3960	6a	13	31	4.0	18	4.9	1.7	4.5	0.82	5.2	0.98	2.8	0.36	2.6	0.39
83	3990	6a	13	31	3.9	18	4.6	1.6	4.5	0.71	4.7	0.96	2.5	0.38	2.5	0.37
84	4020	6c	17	41	5.3	24	6.2	2.1	6.4	1.00	6.2	1.30	3.5	0.50	3.4	0.51
40	4040	6c	56	115	13.0	54	10.0	3.2	9.0	1.20	7.7	1.60	4.1	0.60	4.1	0.63
41	4095	6c	16	39	5.2	24	6.5	1.8	6.5	1.10	7.1	1.50	4.3	0.62	4.1	0.60
42	4180	7a	5	13	1.9	9	2.4	1.0	2.8	0.46	2.8	0.62	1.6	0.22	1.5	0.22
43	4240	7a	5	13	1.8	9	2.4	1.1	2.8	0.43	2.8	0.58	1.5	0.21	1.5	0.21
44	4270	7a	5	12	1.6	8	2.1	0.9	2.4	0.38	2.5	0.54	1.4	0.21	1.3	0.19
85	4305	7a	5	13	1.8	9	2.4	0.9	2.4	0.42	2.8	0.53	1.5	0.20	1.4	0.20
45	4370	7a	5	11	1.6	8	2.1	0.9	2.5	0.38	2.6	0.54	1.4	0.22	1.4	0.18
47	4500	7c	25	56	6.9	30	6.3	2.1	5.7	0.85	5.1	1.00	2.8	0.41	2.6	0.37
46	4505	7a	5	12	1.7	8	2.3	1.0	2.5	0.40	2.6	0.53	1.4	0.22	1.4	0.21
64	4510	7b	8	20	2.6	12	3.2	1.2	3.2	0.51	3.5	0.72	1.8	0.27	1.8	0.27
90	4510	7a	5	13	1.7	8	2.2	0.9	2.4	0.40	2.5	0.52	1.3	0.20	1.3	0.19
91	4510	7a	5	13	1.7	8	2.1	1.0	2.4	0.38	2.5	0.49	1.3	0.19	1.2	0.19
86	4540	7b	8	21	2.7	12	3.2	1.2	3.3	0.55	3.5	0.69	1.9	0.28	1.9	0.27
48	4560	7a	5	13	1.9	9	2.5	1.0	2.7	0.46	2.8	0.62	1.6	0.23	1.6	0.23
49	4560	7b	8	18	2.5	12	3.1	1.2	3.2	0.53	3.4	0.71	1.9	0.27	1.8	0.26
63	4595	7b	8	20	2.8	13	3.5	1.3	3.6	0.57	3.9	0.76	2.0	0.31	2.0	0.29
50	4640	7d	42	96	12.0	49	9.9	2.9	8.4	1.00	6.2	1.10	2.7	0.38	2.5	0.38
51	4750	7b	8	20	2.7	13	3.4	1.4	3.8	0.60	3.9	0.81	2.1	0.31	2.2	0.30
52	5000	7b	11	27	3.8	17	4.5	1.7	5.0	0.80	5.0	1.10	2.7	0.41	2.6	0.38
53	5100	7b	9	24	3.1	15	3.8	1.4	4.1	0.63	4.1	0.83	2.1	0.31	2.1	0.28
54	5160	7b	9	23	2.9	14	3.8	1.4	3.8	0.62	3.9	0.80	2.2	0.31	2.0	0.28
55	5180	7b	9	23	2.9	14	3.5	1.3	3.8	0.62	3.8	0.78	2.1	0.31	1.9	0.29
56	5230	7b	10	23	3.0	14	3.7	1.3	3.8	0.63	3.9	0.81	2.0	0.30	2.0	0.31
57	5260	7b	9	21	2.8	13	3.4	1.3	3.7	0.58	3.6	0.76	2.0	0.29	1.8	0.28
59	5310	7b	n.a.	n.a.	n.a.	n.a.	n.a.	n.a.	n.a.	n.a.	n.a.	n.a.	n.a.	n.a.	n.a.	n.a.
60	5430	9	52	120	15.0	60	12.0	3.4	9.4	1.30	7.7	1.50	3.8	0.53	3.4	0.52
61	5530	9	52	120	14.0	58	11.0	3.3	9.2	1.30	7.7	1.50	3.6	0.53	3.4	0.50

Table 3. Summary of compositional features of OVG and MPVG.

Group/ Formation	Stratigraphic interval	Petrography	MgO wt.%	Al_2O_3 wt.%	TiO_2 wt.%	Cr, Ni, Cu (ppm)	Zr (ppm)	La/Sm	Gd/Yb	La/Lu	Ce/Nb	Ti/Y	Zr/Y
MAMAINSE POINT GROUP													
1, 2a, 2c, 3b, 3c	40-255, 350-655, 840-1105, 1760-1785	Olivine-phyric and plagioclase spherulitic basalt	7.5-12.5	12-16	1.2-2.6	High Cr		2.2-3.5	2.0-3.1	35-85	2.1-5.0		5.8-7.0
2b	720-760	Olivine-phyric basalt	5.5-6.5		1.1			5.1-5.2	1.9-2.0				
3	1200-1595	Plagioclase -phyric basalt	5.5-8.0		1.1-2.0			3.5-3.8	2.0-2.3				
5a,b,c	1860-2370	Optiitic basalt	3.8-8.0		0.7-1.3	Low Cr	30-125	2-6.5	1.0-1.3	10-90	2.8-4.5	120-400	2.8-3.5
6a,b,c	3040-4095	Tholeitic basalt	3.0-6.0	3-6	1.8-3.2			2-2.7	1.5-2.1	22-40	2.2-4.2	350-550	4-6
7a,b,c,d	4180-5310		5.50	5-10	0.9-2.1								
9	5430-5530	Diabase textured tholeiite	4.5-6.0		3.7-3.8		310-330	4.1-4.4	2.7-2.8	100	2		
OSLER FORMATION													
LOWER	0-800	Olivine and augite porphyritic basalt	7.3-10.0	7-12	1.5-3.2	High Cr	200-300	2.0-3.8	3.2-4.3	3-7		>500	>6
CENTRAL	800-2400	Plagioclase porphyritic and aphyric basalt	3.0-7.5		1.0-1.5			3.1-6.2	1.5-2.2	32-90	2.1-5.0	<380	
UPPER	2400-3100	Plagioclase porphyritic and aphyric basalt	3.0-7.0		1.3-2.4			2.3-4.8	1.7-2.7	25-100	2.7-8.0	<380	

Table 4. Average compositions of the main Osler Group and Mamainse Point lava groups.

Group/ Formation	Osler Group Lower Formation	Osler Group Central Formation	Osler Group Upper Formation	Mamainse Pt. Sequence Group 2a	Mamainse Pt. Sequence Group 3	Group 5a	Group 6a	Group 7a	Group 9
n	4	4	4	15	7	2	13	9	2
SiO_2	49.8	51.2	49.6	48.9	49.5	55.1	49.3	48.6	46.3
TiO_2	2.50	1.28	1.62	1.82	1.43	0.64	2.07	1.00	3.70
Al_2O_3	10.3	14.8	15.6	13.4	16.1	16.3	15.3	17.5	14.5
Fe_2O_3	13.8	13.3	13.0	13.4	11.9	10.0	15.2	10.3	16.4
MgO	9.7	6.1	6.2	9.9	7.0	7.2	4.6	8.9	5.5
MnO	0.17	0.19	0.19	0.17	0.24	0.21	0.21	0.17	0.26
CaO	9.9	10.4	10.4	9.1	8.7	5.8	10.0	11.0	7.7
Na_2O	2.8	2.2	2.7	2.6	3.8	2.8	2.5	2.1	3.6
K_2O	0.70	0.46	0.49	0.52	1.07	1.93	0.50	0.29	1.21
P_2O_5	0.54	0.18	0.17	0.19	0.15	0.05	0.24	0.10	0.93
LOI	2.45	3.00	2.63	4.45	5.81	5.05	8.4	5.10	2.90
Ba	307	264	167	539	654	522	181	173	541
Rb	12.2	7.6	10.7	7.7	27.0	57.5	9.0	5.1	n.a.
Sr	379	217	214	359	377	257	233	302	347
Y	23	24	28	17.5	17.8	27.0	25.5	14.0	37.0
Zr	226	128	154	111	94	84	134	62	326
Hf	5.35	2.88	3.66	3.04	2.65	2.70	3.50	1.73	n.a.
Nb	16.9	9.3	9.6	8.9	11.4	14.5	9.5	4.4	n.a.
Ta	1.0	0.57	0.60	0.67	0.71	0.96	0.57	0.29	n.a.
Th	1.8	3.0	1.7	n.a.	n.a.	n.a.	n.a.	n.a.	n.a.
U	0.45	0.73	0.48	n.a.	n.a.	n.a.	n.a.	n.a.	n.a.
Ni	202	93	116	311	78	29	40	217	94
Cu	130	144	139	91	47	74	162	62	140
Cr	824	138	122	570	140	85	108	254	51
Sc	31.3	31.8	30.5	23.4	29.3	23.4	24.5	26.8	25.5
V	320	281	278	258	239	166	273	186	348
Zn	108	110	115	89	157	162	126	77	156
Co	54	47	46	53	40	39	39	43	43
La	24.5	15.3	13.2	12.1	13.8	24.0	13.2	5.04	52
Ce	60.9	33.5	31.4	287	30.6	47.0	31.5	12.55	120
Pr	8.6	4.1	4.4	3.76	3.74	4.80	4.08	1.74	14.5
Nd	39.4	16.7	19.3	17.8	16.8	18.5	18.8	8.33	59
Sm	8.7	4.2	5.1	4.47	3.92	3.75	4.89	2.28	11.5
Eu	2.63	1.34	1.65	1.61	1.38	0.73	1.70	0.96	3.35
Gd	7.15	4.29	5.49	4.15	3.70	3.75	4.86	2.54	9.30
Tb	0.97	0.70	0.90	0.63	0.56	0.67	0.78	0.41	1.30
Dy	5.22	4.32	5.62	3.73	3.56	4.40	5.09	2.65	7.70
Ho	0.93	0.94	1.15	0.71	0.70	0.99	1.03	0.55	1.70
Er	2.33	2.68	3.21	1.75	1.78	2.80	2.75	1.44	3.70
Tm	0.29	0.38	0.47	0.23	0.25	0.45	0.39	0.21	0.53
Yb	1.78	2.47	3.00	1.47	1.60	3.00	2.61	1.40	3.40
Lu	0.24	0.37	0.45	0.21	0.25	0.48	0.38	0.20	0.51

Table 5. Compositional data for rhyolites from the Mamainse Point and Osler sequences.

Sample	88ARS2024	88ARS2027	88PCL071	88PCL087	88PCL088	88PCL089	88PCL106	88PCL056
Group/ Formation	Osler	Osler	Mamainse Point	Mamainse Point	Mamainse Point	Mamainse Point	Mamainse Point	Mamainse Point
(m)	n.a.	n.a.	5570	2850	4320	4320	3360	5570
SiO_2	68.0	71.6	71.9	79.9	75.9	78.1	80.8	77.4
TiO_2	0.78	0.59	0.16	0.07	0.06	0.05	0.06	0.05
Al_2O_3	15.37	14.15	14.8	12.4	12.5	12.7	11.3	12.2
Fe_2O_3	5.66	3.39	1.40	1.41	1.06	0.54	1.68	1.65
MgO	1.29	0.60	0.40	0.22	n.d.	n.d.	0.40	0.04
MnO	0.09	0.05	0.03	0.03	0.03	0.01	0.03	0.02
CaO	2.21	2.27	7.7	0.26	3.43	0.49	0.81	5.12
Na_2O	3.26	2.96	0.02	n.d.	1.05	1.54	0.19	2.06
K_2O	4.03	4.27	3.52	5.73	5.93	6.54	4.77	1.37
P_2O_5	0.11	0.08	0.06	n.d.	0.01	0.01	0.01	0.03
LOI	1.90	2.70	9.30	2.10	3.70	1.10	3.20	6.30
Ba	n.a.	n.a.	185	300	584	805	n.a.	n.a.
Rb	109	108	98	263	345	377	n.a.	72
Sr	150	121	33	16	38	20	n.a.	37
Y	23	27	13	16	58	48	n.a.	45
Zr	296	289	64	86	123	125	n.a.	96
Hf	7.54	7.49	n.a.	n.a.	n.a.	n.a.	n.a.	n.a.
Nb	22.7	23.9	12	47	110	113	n.a.	81
Ta	0.93	0.95	n.a.	n.a.	n.a.	n.a.	n.a.	n.a.
Th	n.a.	n.a.	n.a.	n.a.	n.a.	n.a.	n.a.	n.a.
U	n.a.	n.a.	n.a.	n.a.	n.a.	n.a.	n.a.	n.a.
Ni	23	16	n.d.	n.d.	n.d.	n.d.	n.d.	n.d.
Cu	43	20	21	16	15	20	51	48
Cr	12	10	n.d.	n.d.	n.d.	12	n.a.	n.a.
Sc	6	5	3	n.d.	n.d.	n.d.	n.d.	n.d.
V	69	39	8	n.d.	n.d.	n.d.	n.d.	n.d.
Zn	74	75	57	80	49	23	73	22
Co	14	10	n.d.	n.d.	n.d.	n.d.	n.d.	n.d.
La	79	96	16	26	32	33	18	26
Ce	165	195	32	40	81	72	30	64
Pr	18	21	3.3	4.2	9.3	9.5	4.2	7.4
Nd	63	75	12	13	36	36	13	25
Sm	10	12	2.3	2.5	9.8	10.0	2.6	6.1
Eu	1.80	2.30	0.55	0.10	0.22	0.19	0.14	0.50
Gd	6.10	7.80	2.0	2.2	9.2	8.8	2.0	5.6
Tb	0.88	1.00	0.32	0.48	1.7	1.70	0.36	1.00
Dy	4.7	5.30	1.9	3.5	11	11	2.6	6.4
Ho	0.88	1.00	0.43	0.78	2.20	2.10	0.53	1.4
Er	2.4	2.50	1.1	2.2	6.0	5.5	1.6	3.9
Tm	0.35	0.37	0.18	0.38	0.95	0.86	0.28	0.63
Yb	2.2	2.30	1.20	2.6	6.3	5.5	2.1	4.4
Lu	0.31	0.34	0.17	0.40	0.90	0.83	0.29	0.66

Table 6. Differentiation, depth of origin, source, tectonic setting and possible origin of the Mamainse Point and Osler group lavas.

Group/ Formation	Differentiation	Partial melting	Open system behaviour	Contamination history	Source	Magma type	Tectonic setting	Affinities to other Keweenawan rocks and CFB
MAMAINSE POINT GROUP								
9				EXTENSIVE	Asthenospheric and Lithospheric mantle		CFB in rift	
7a-c	60% fractionation	Spinel lherzolite source, 8-12 kbar		NONE RECOGNISED		Type 6-7	CFB in rift with melting of mantle.	Like Keweenawan high-Al tholeiites of NSVG
6a-d	87% fractionation							
5a-c	50% fractionation	High degrees of melting	AFC, r=0.2-0.5, 50% fractionation	EXTENSIVE	N-to T-type MORB source	Type 5	Embryonic MORB(?)	Like N-MORB
3			RTF magma chamber	MODERATE	Deep asthenopsheric mantle; possible plume contribution to chemistry; lithospheric mantle contribution	Type 1-3	Plume impinging on continental crust	Like OIB and Lower Formation Osler lavas. Similar to picrite intrusions of Nipigon Plate
2b	2 stages of fractionation			MODERATE				
1,2a,2c,3b,3c	Primitive magma	15-30 kbar melting		NONE RECOGNISED				
OSLER GROUP								
UPPER	<8% fractionation		Mixing with crustal melts	EXTENSIVE	Shallow mantle lithosphere	Central/upper Type (=Type 5-7)	CFB in rift with much crustal melting	Like Mamainse Point high-Al tholeiites, but with much contamination
CENTRAL	<8% fractionation		Mixing with crustal melts	EXTENSIVE				
LOWER	Primitive liquid	15-30 kbar melting		NONE RECOGNISED	Deep asthenopsheric mantle; possible plume contribution to chemistry	Lower Type (=Type 1-3)	Plume impinging on continental crust close to aulacogen	Like OIB and Types 1-3 Mamainse Point lavas. Similar to picrite intrusions of Nipigon Plate

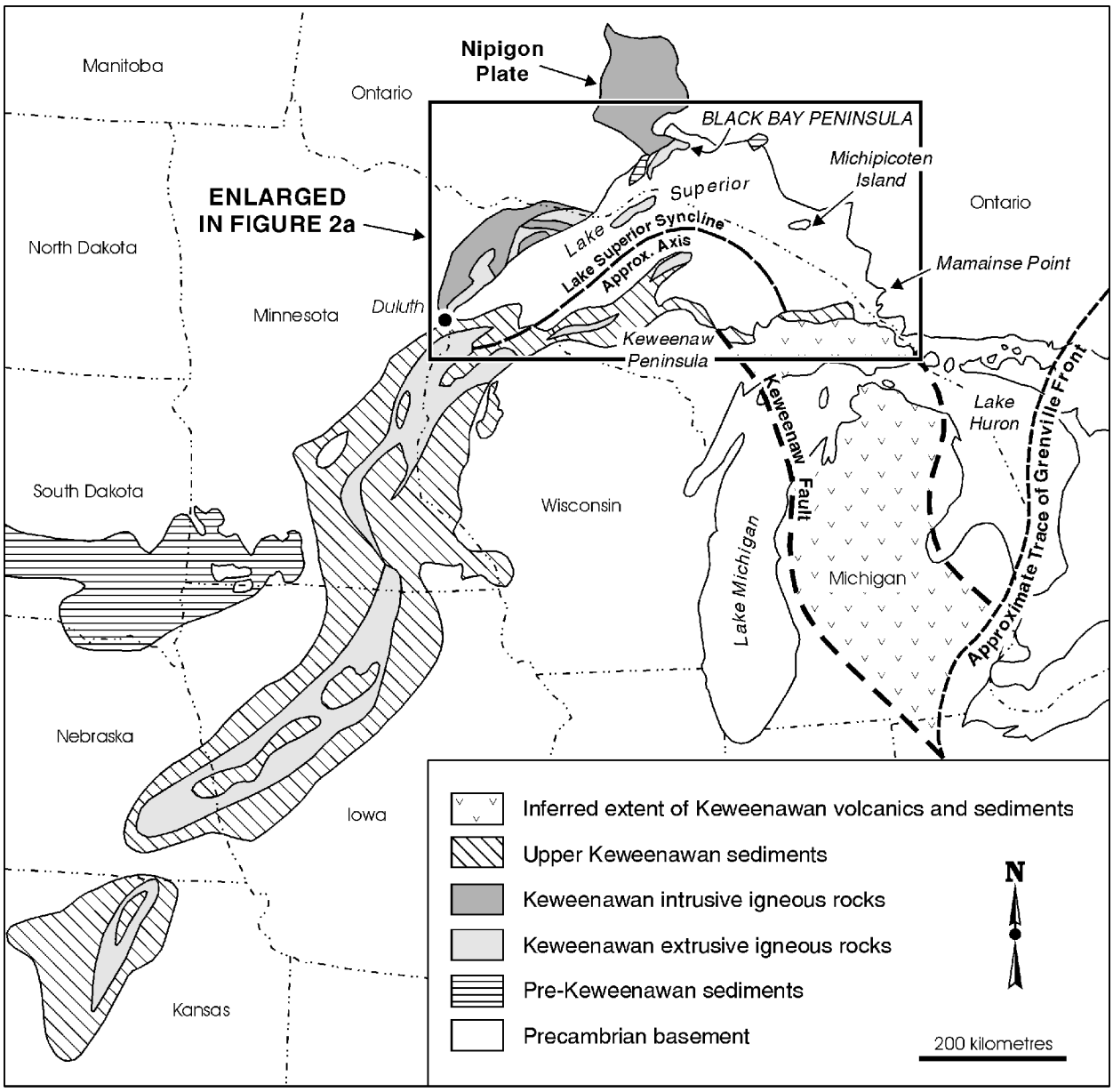

Figure 1. Map showing the Midcontinent Rift System and some of the major geological features of the region. Inset box is enlarged in Figure 2a, where the location of Keweenawan volcanic and plutonic units in the Lake Superior region are shown. The Keweenawan Mid-continent gravity high follows the trend of exposed and buried Keweenawan-aged rocks. Based on Basaltic Volcanism Study Project (1981).

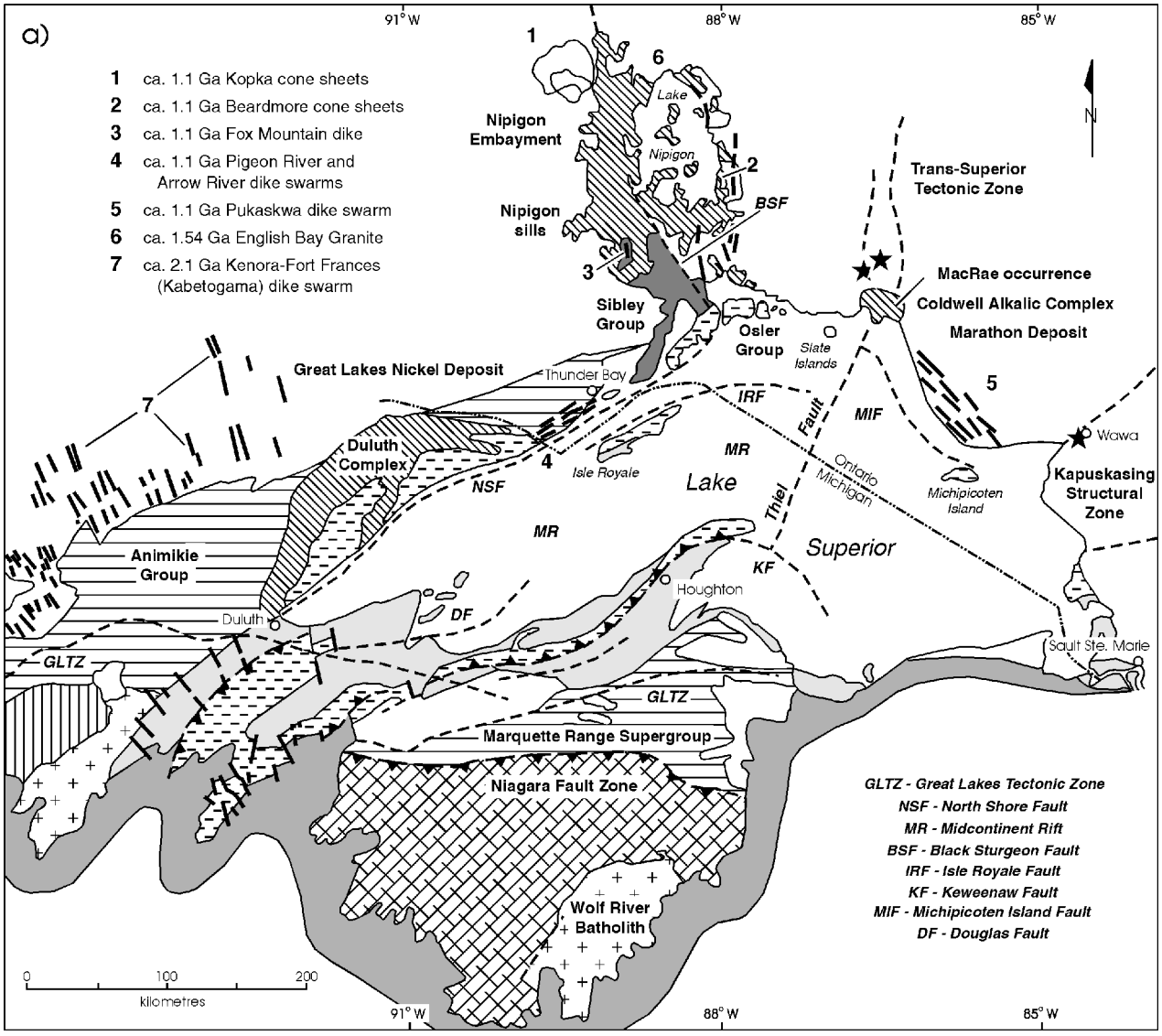

Figure 2a. Geological map of the Lake Superior basis showing the locations of the study areas, and the map enlarged in Fig. 2b. Detailed geology of the Osler Group is given in Lightfoot et al., (1991a). Based on Sutcliffe (1991).

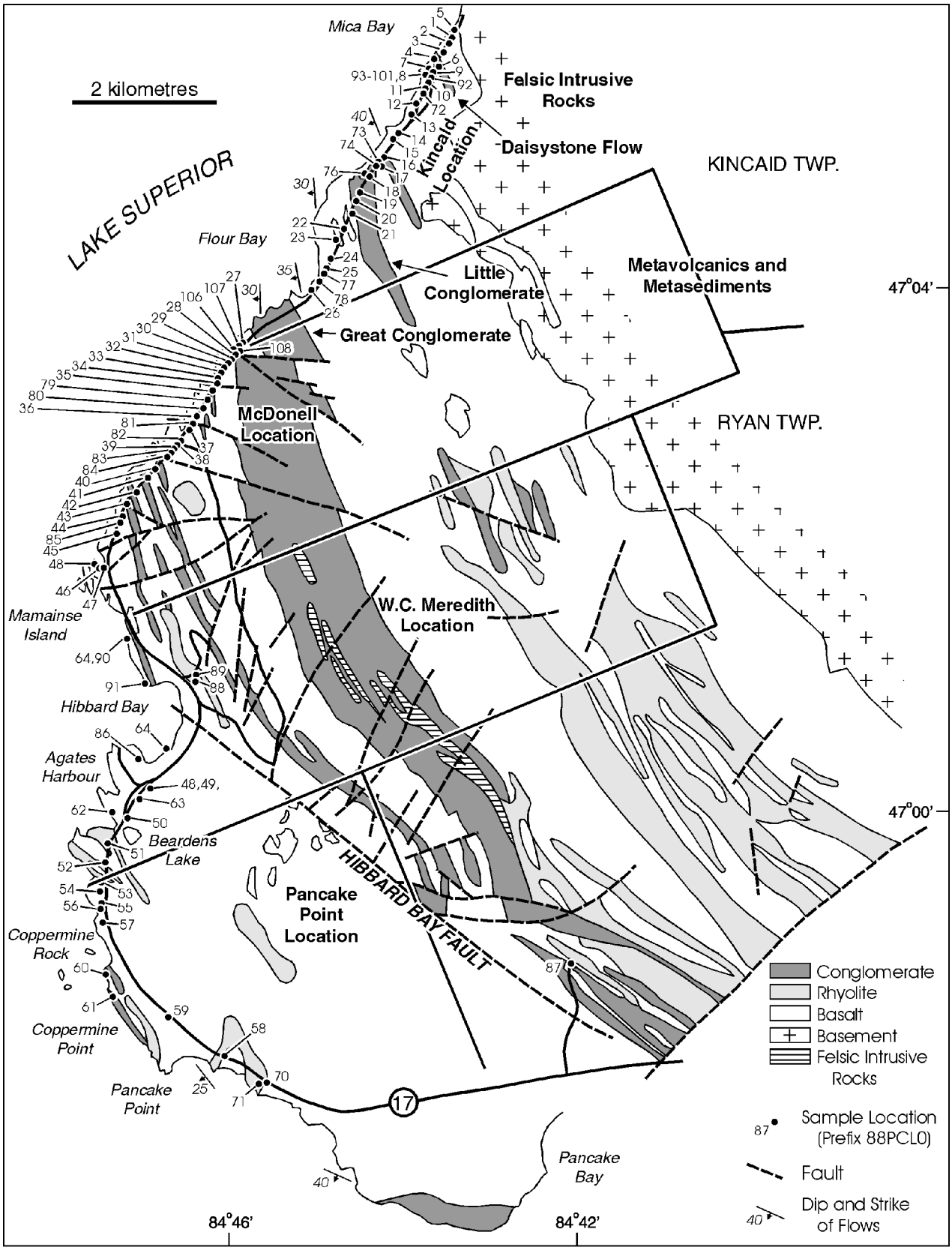

Figure 2b. Geological map of the MPVG sequence and the locations of samples collected for this study. Samples carry prefix 88PCL0. Based on OGS Map 2251 (Giblin and Armburst, 1964-68) and Lightfoot et al., (1991a).

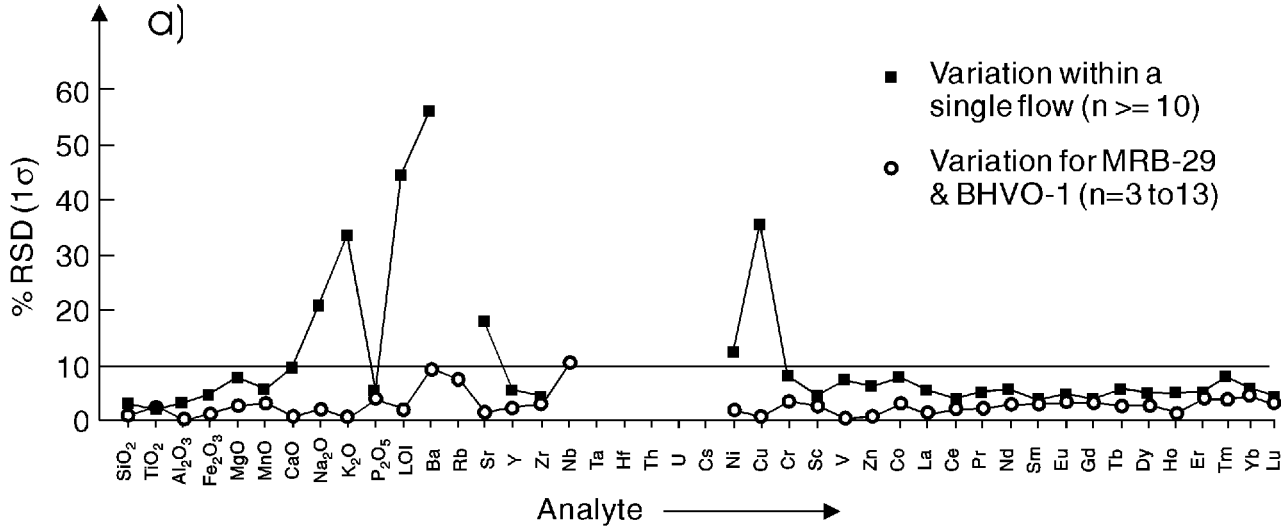

Figure 3a. Comparison of errors associated with analysis (based on multiple analyses of in-house standard MRB-29) and variations due to within-flow heterogeneity (based on 10 analysis of samples from within a single MPVG flow). The horizontal line is shown at an RSD (1 sigma) of 10%.

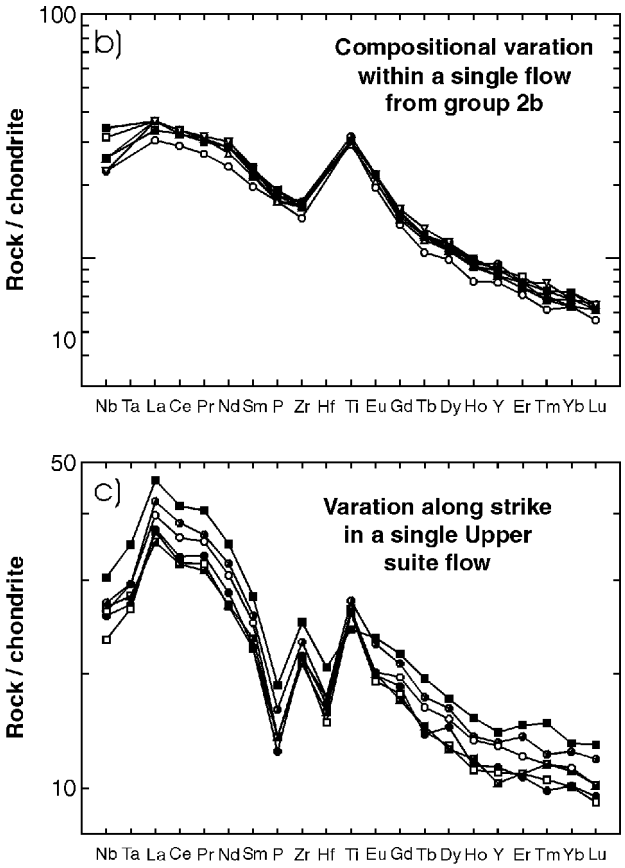

Figure 3b. Chondrite normalized (Sun, 1980) variations in incompatible element content within a series of samples taken from a single Group 2a flow from the MPVG. **3c)** Chondrite-normalized variations in a series of samples collected along strike from the core of a simple flow unit from the Upper Formation of the OVG lava series (data from Lighfoot et al., 1991a).

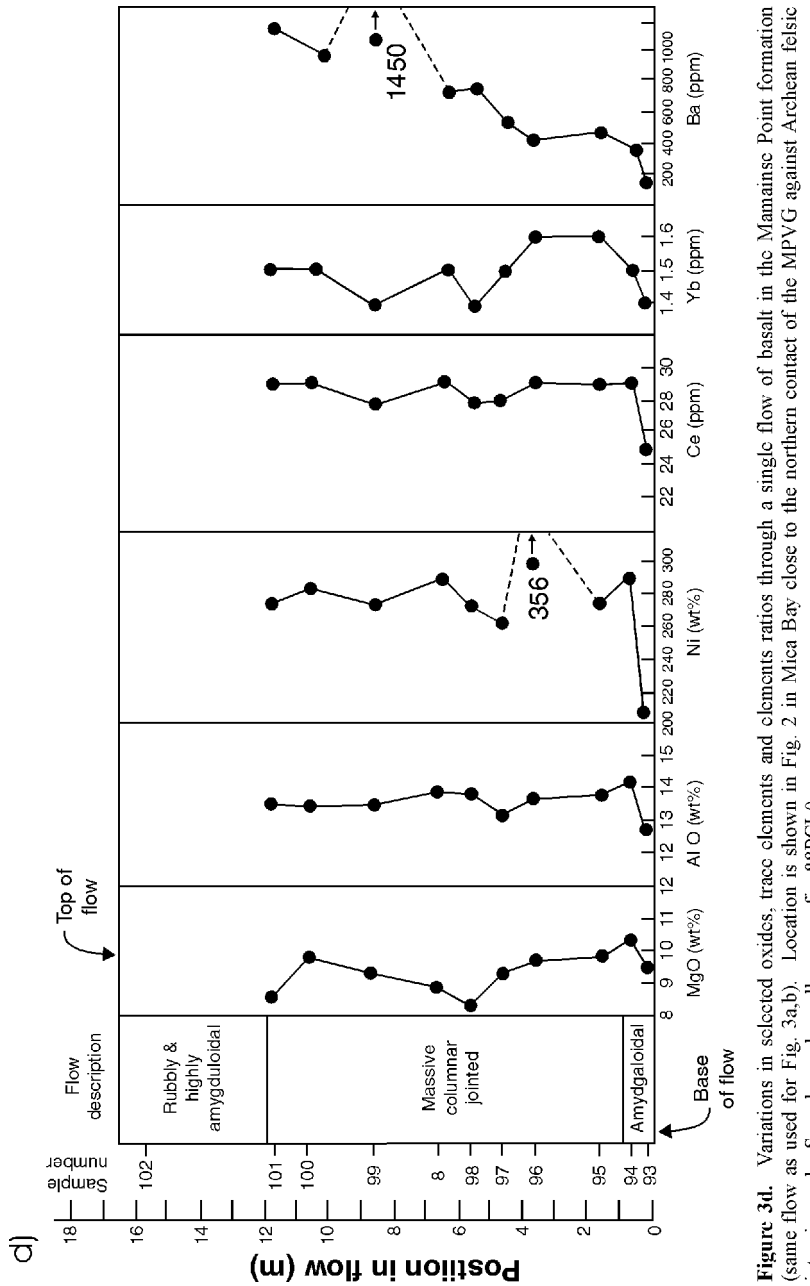

Figure 3d. Variations in selected oxides, trace elements and elements ratios through a single flow of basalt in the Mamainse Point formation (same flow as used for Fig. 3a,b). Location is shown in Fig. 2 in Mica Bay close to the northern contact of the MPVG against Archean felsic intrusive rocks. Sample numbers all carry prefix: 88PCL0.

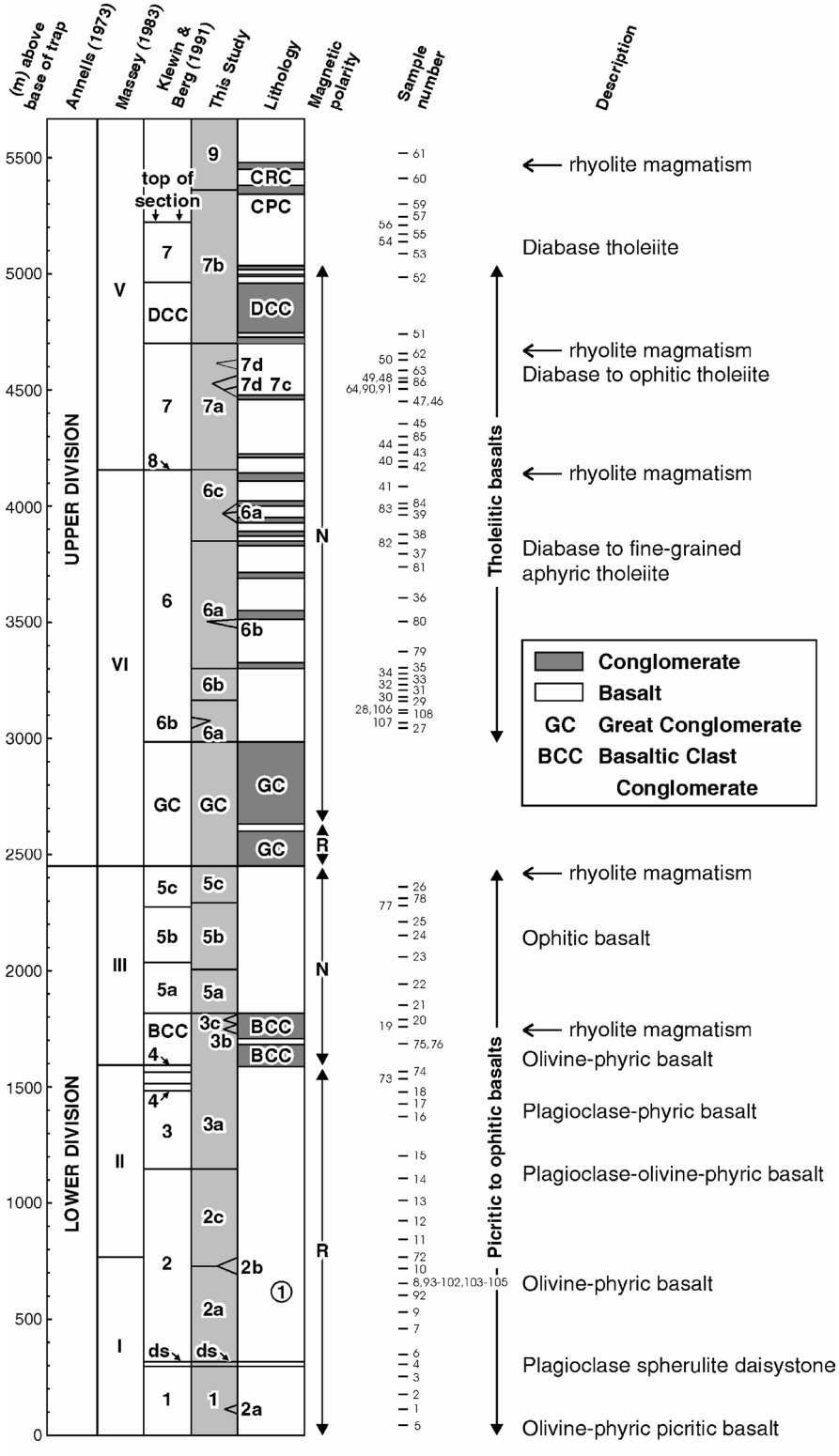

Figure 4. Petrographic variations through the MPVG, and approximate locations of samples shown in Figure 2b. Subdivisions of basalt stratigraphy are from Annells (1973), Massey (1983) and Klewin and Berg (1991); we follow the nomenclature of Klewin and Berg (1991), modified to reflect additional flow types which do not correlate with Klewin and Berg (1991) as shown under column heading "This study". Magnetic polarity is based on Halls and Pesonen (1982). Position of rhyolite magmatism is annotated based on position within observed stratigraphy.

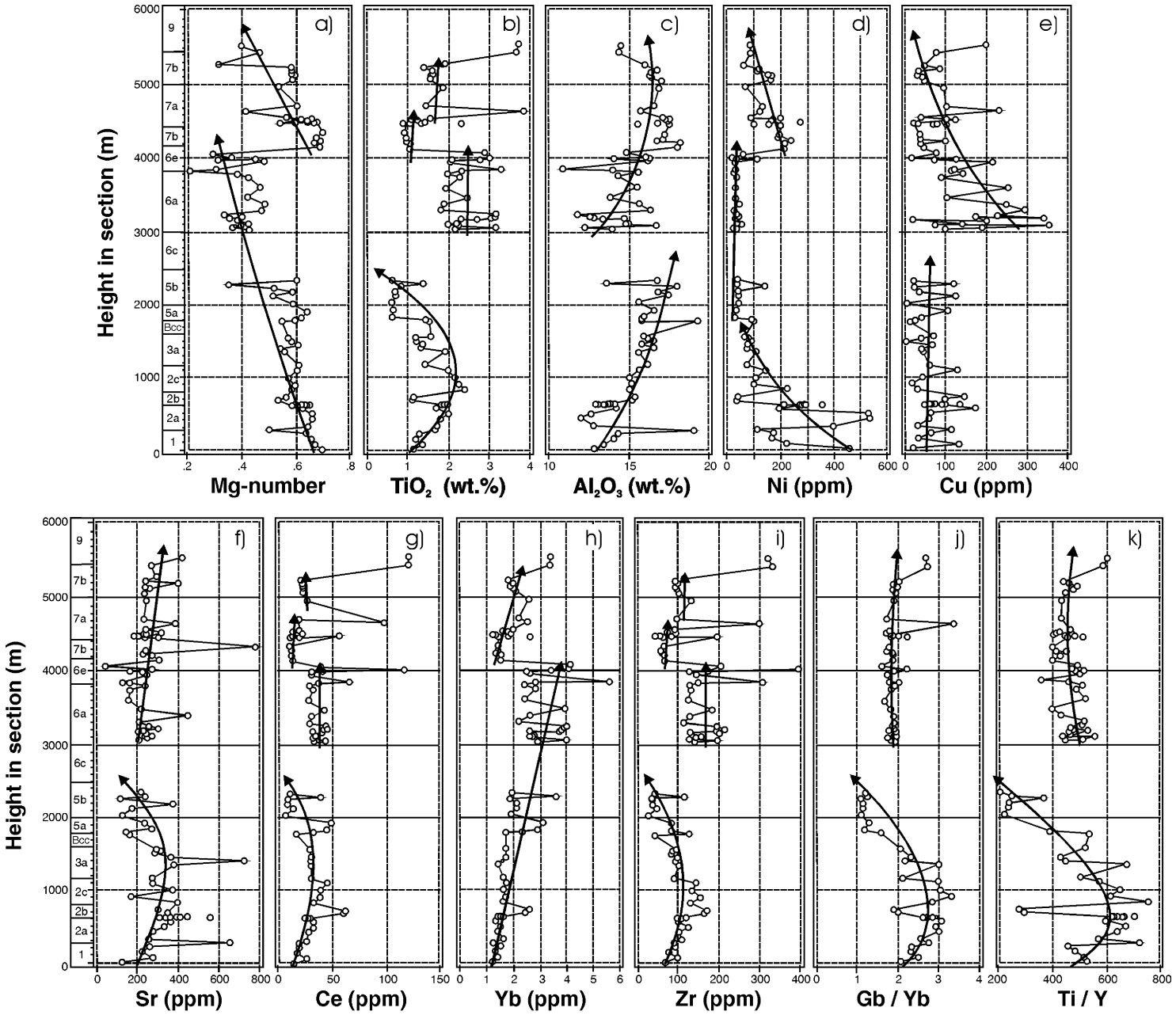

Figure 5a-k. Chemostratigraphy of the MPVG. Variations in selected analytes with stratigraphic position in the MPVG. Stratigraphic position has been calculated following Klewin and Berg (1991). Major elements are recalculated to 100% free of LOI. GC - Great conglomerate; BCC - basalt clast conglomerate. Position of sample is given in metres above the base based on the recalculation of the positions using the average dip of the lava flows and the supposition that the sequence is not disrupted by faulting. Diagram **a)** shows the variation in Mg-number and MgO. Arrows show the general direction of geochemical evolution.

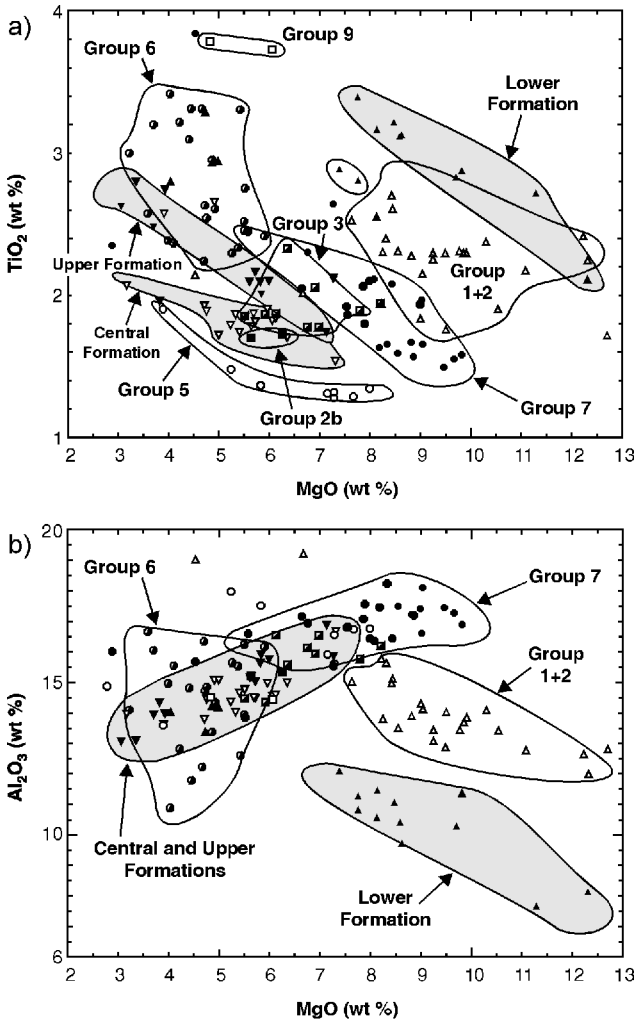

Figure 6a. Variation in TiO_2 versus MgO in MPVG and OVG (shaded area) lavas. **6b)** Variation in Al_2O_3 versus MgO in MPVG and OVG lavas. Major elements oxides are recalculated to 100% free of LOI. Figure 5 shows the symbols used to represent samples from different groups in the MPVG; these are summarized in the caption to Figure 6.

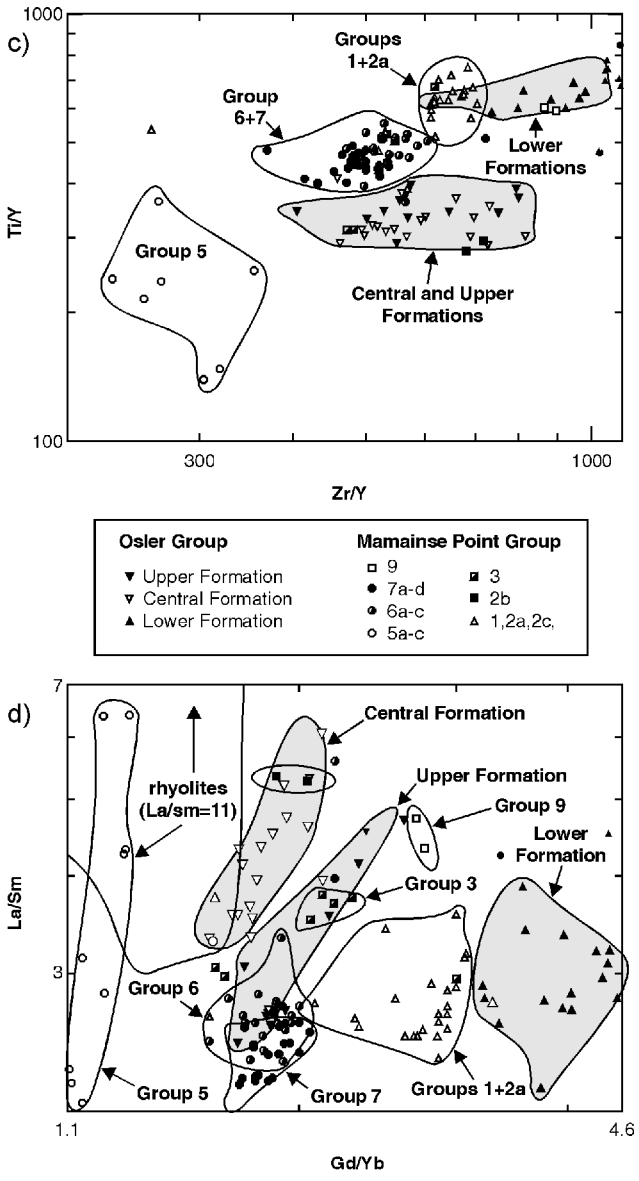

Figure 6c. Variation in La/Sm versus Gd/Yb in MPVG and OVG lavas. **6d)** Variation in Ti/Y versus Zr/Y in MPVG and OVG lavas. Figure 5 shows the symbols used to represent samples from different groups in the MPVG; these are summarized in the caption to Figure 6.

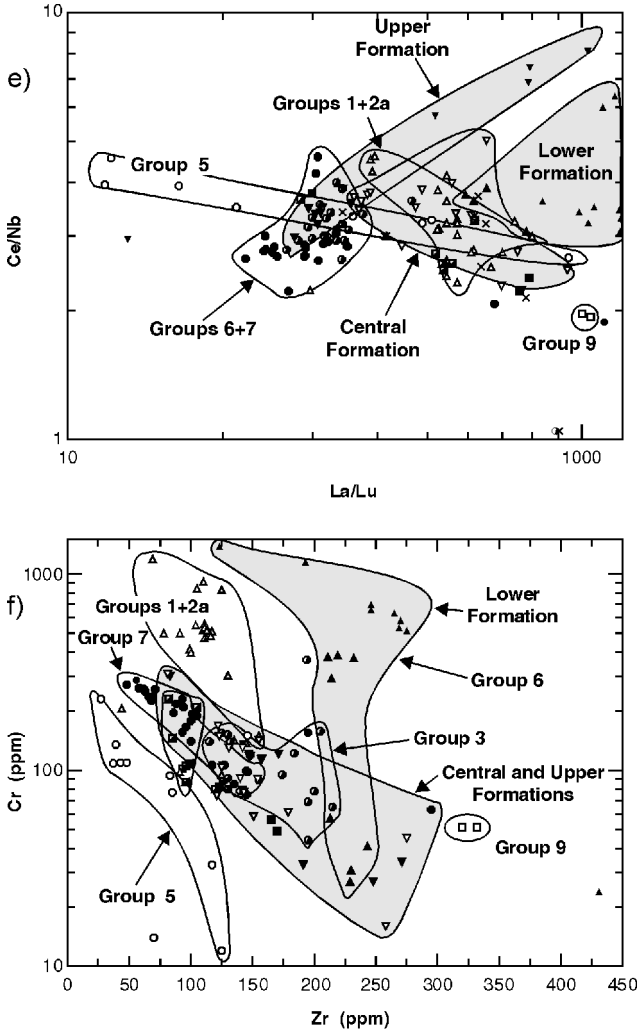

Figure 6e. Variation in Ce/Nb versus La/Lu in MPVG and OVG lavas. **6f)** Variation in Cr versus Zr in MPVG and OVG lavas. Figure 5 shows the symbols used to represent samples from different groups in the MPVG; these are summarized in the caption to Figure 6.

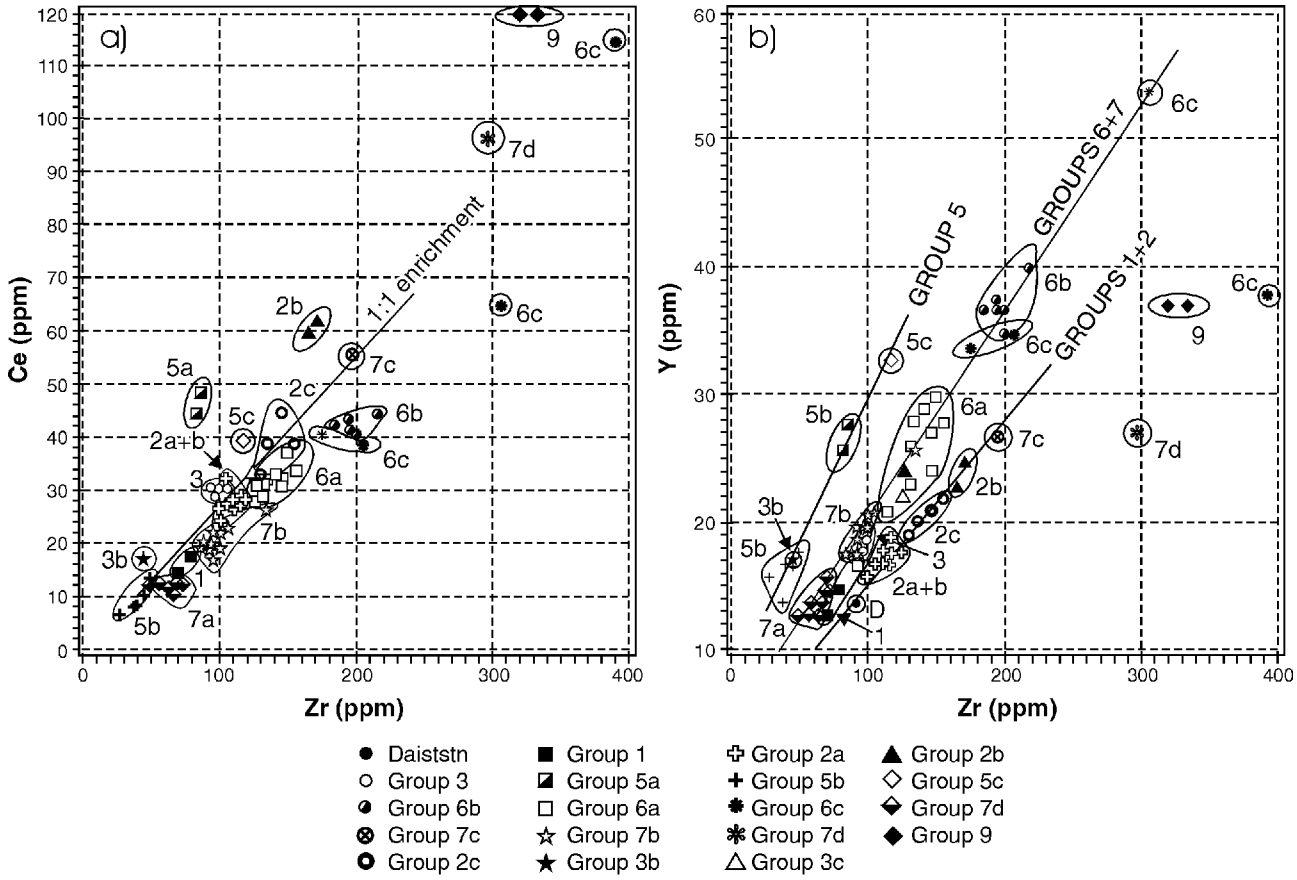

Figure 7a. Variation in Ce versus Zr in MPVG and OVG lavas. **b)** Variation in Y versus Zr in MPVG and OVG flows. Note the good linear correlation of Ce versus Zr, but wide range in Y/Zr.

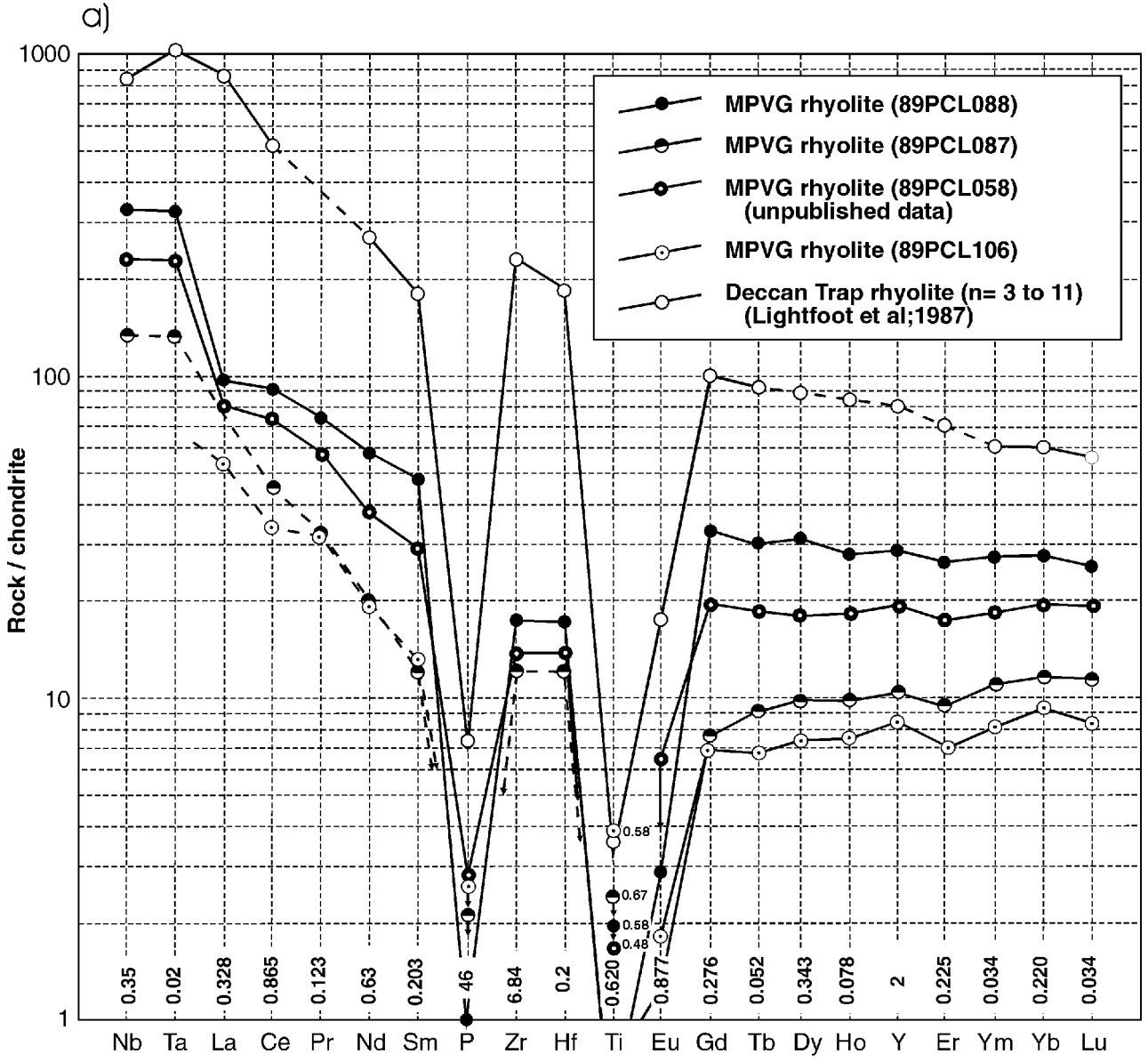

Figure 8a. Chondrite-normalized spiderdiagram (Thompson, 1982; Nakamura, 1974) for Lower Division MPVG rhyolites and Central-Upper Formation OVG rhyolites. Data are compared with averate of Deccan Trap rhyolites (Lightfoot et al., 1987).

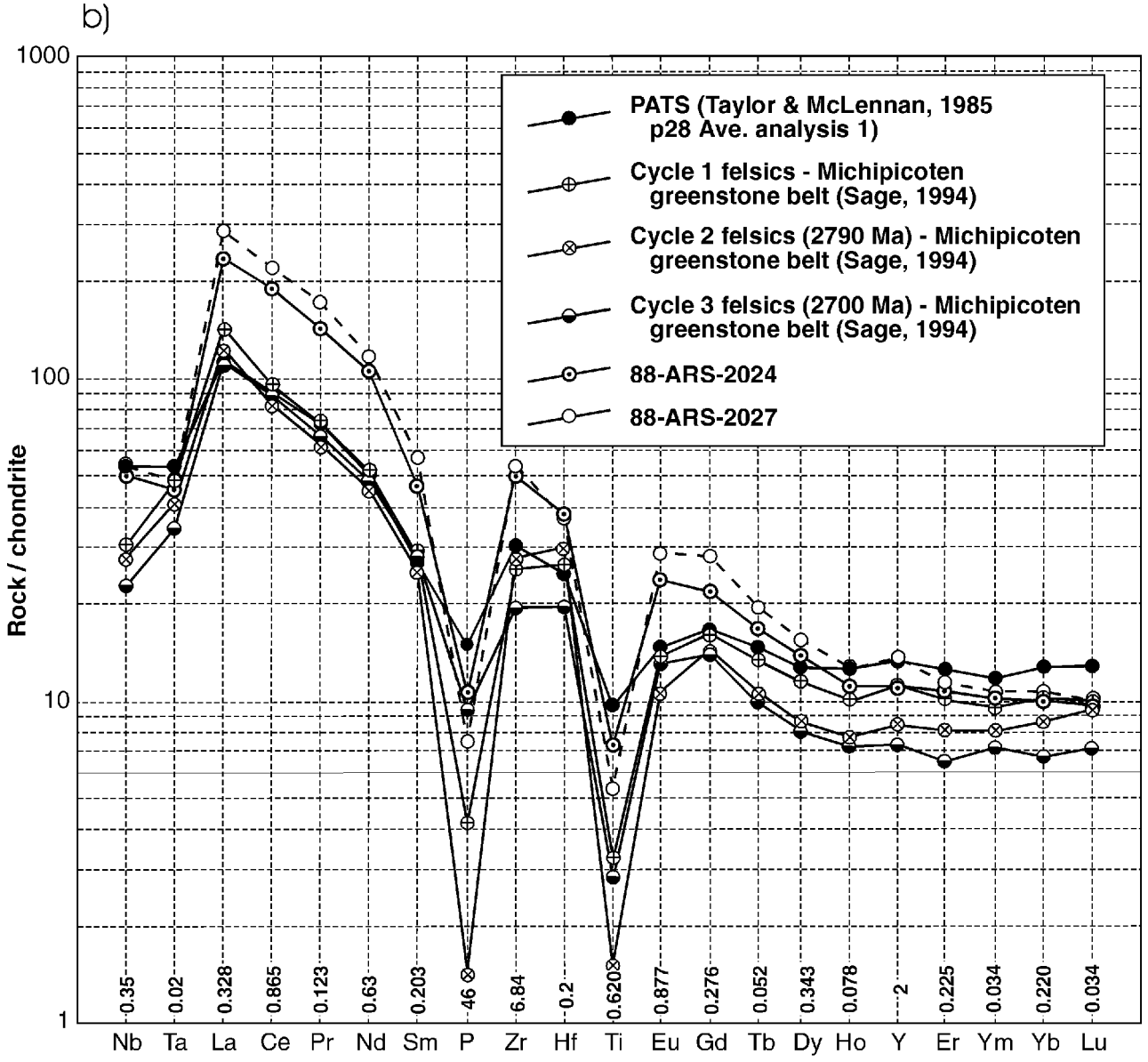

Figure 8b. Comparison of MPVG and OVG rhyolites with felsic volcanic rocks of the Michipicoten Greenstone Belt (Sage, 1994; Sage et al., in prep.) and average Archean shale (PATS) (analysis from, p28, Taylor and McLennan, 1985).

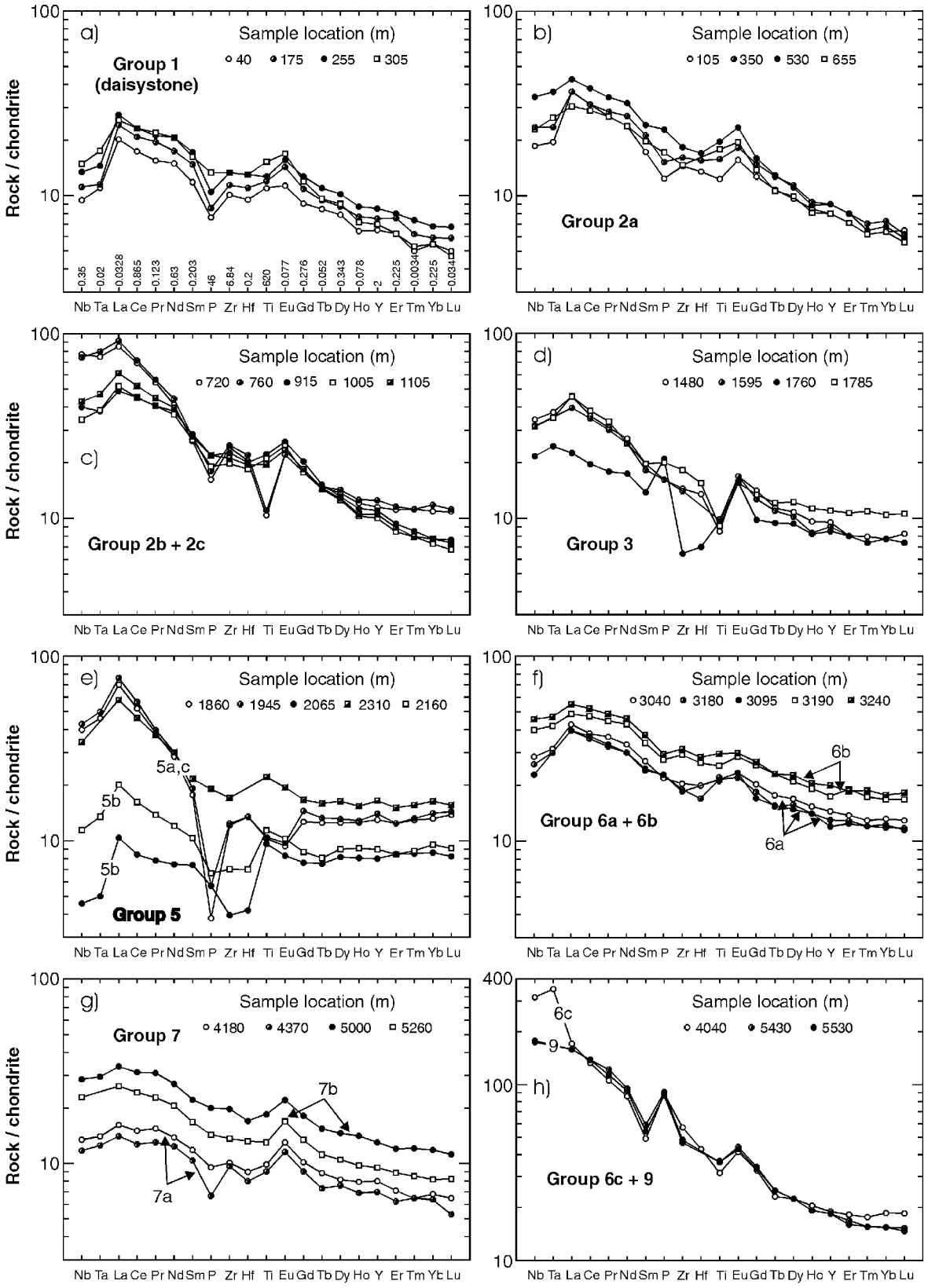

Figure 9. Representative chondrite-normalized (Thompson, 1982; Nakamura, 1974) spiderdiagrams for NPVG and OVG lavas. Representative analyses of lavas are shown. MPVG: **a)** Group 1; **b)** Group 2a; **c)** Group 2b and 2c; **d)** Group 3; **e)** Group 5; **f)** Group 6a and b; **g)** Group 7a and b; **h)** Groups 6 and 9. OVG. Sample identifies correspond to elevation above base of sequence in metres. OVG data from Lightfoot et al.l, (1991a).

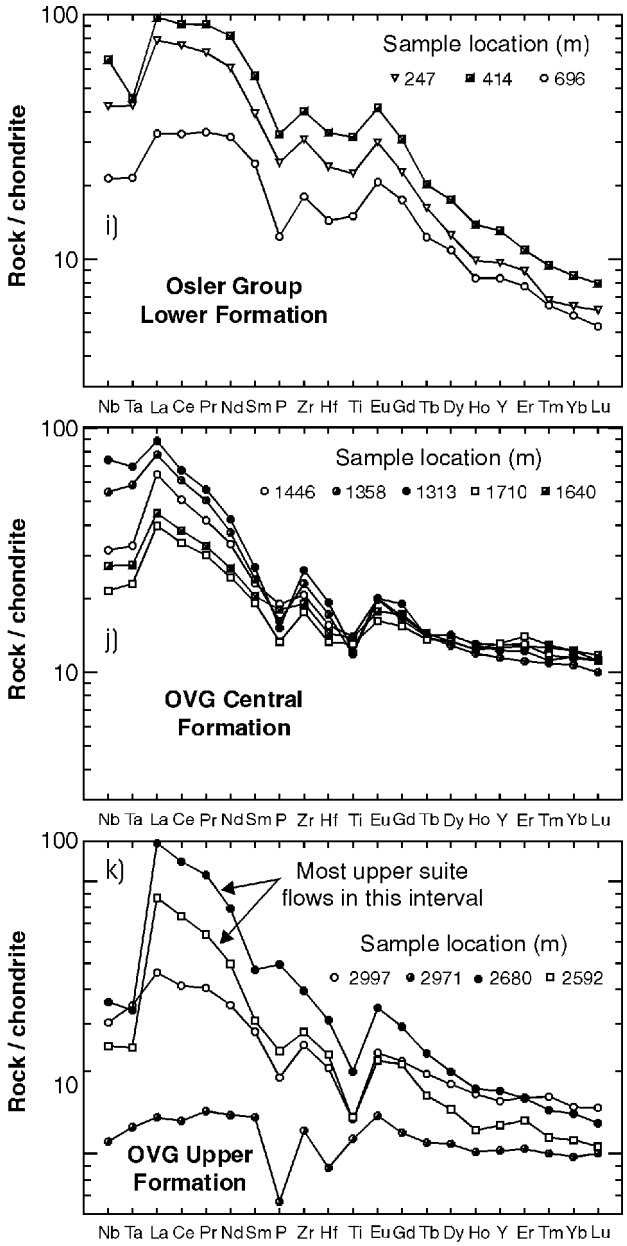

Figure 9 (con't). i) Lower Formation; **j)** Central Formation; **k)** Upper Formation. Sample identifies correspond to elevation above base of sequence in metres. OVG data from Lightfoot et al., (1991a).

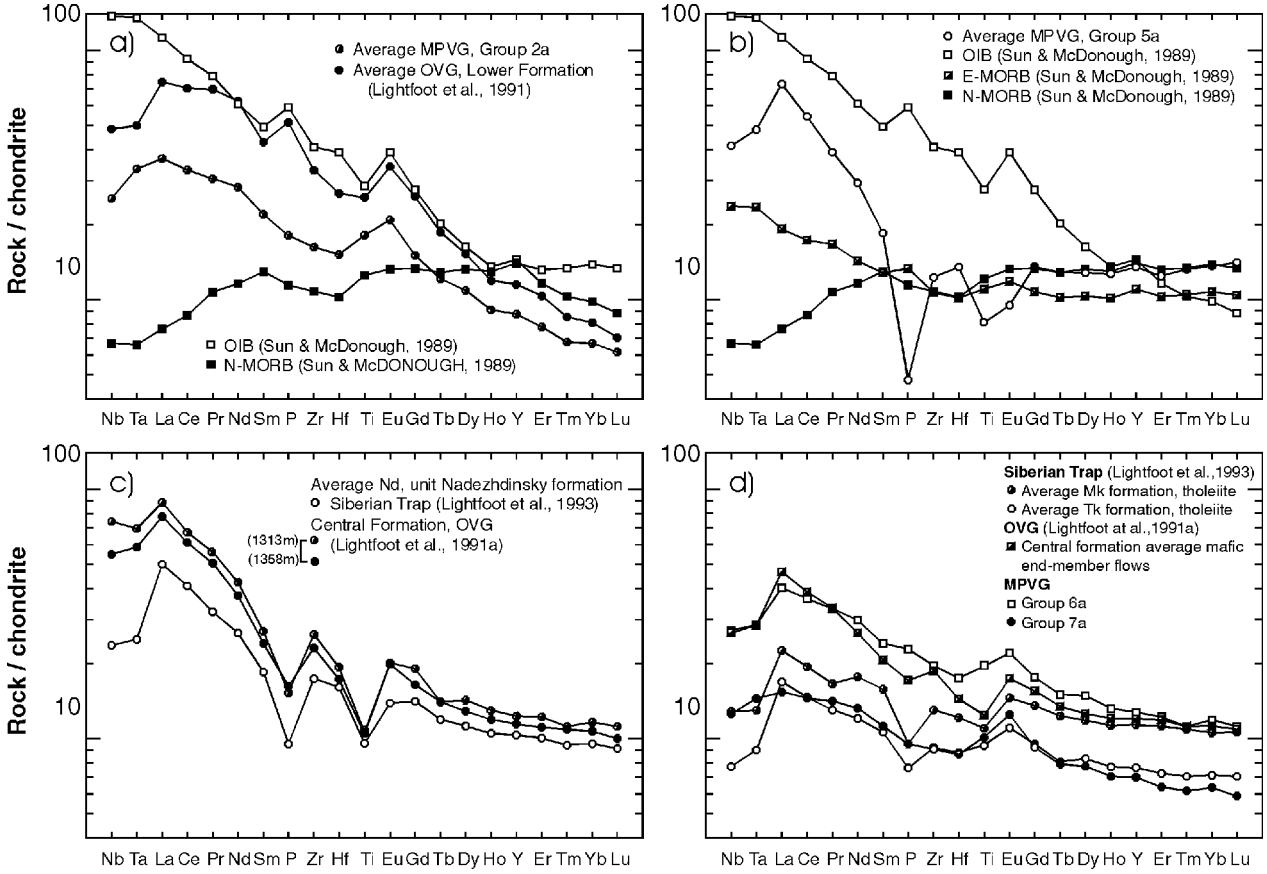

Figure 10. Chondrite-normalized plots comparing the compositions of Keweenawan lavas with Phanerozoic oceanic basalts and CFB. N-MORb = normal type MORB. OIB-ocean island basalt. Data for OVG lavas from Lighfoot et al., (1991a). Data for Siberian Trap lavas from Lightfoot et al., (1993). Data for N-MORB and OIB (Sun and McDonough, 19989). **a)** Comparison of average MPVG 2a and average OVG Lower Formation lavas (Table 3) with OIB and N-MORB. **b)** Comparison of average MPVG 5a with OIB, E-MORBand N-MORB. Comparison of average Siberian Trap, OVG and MPVG least - contaminated lavas.

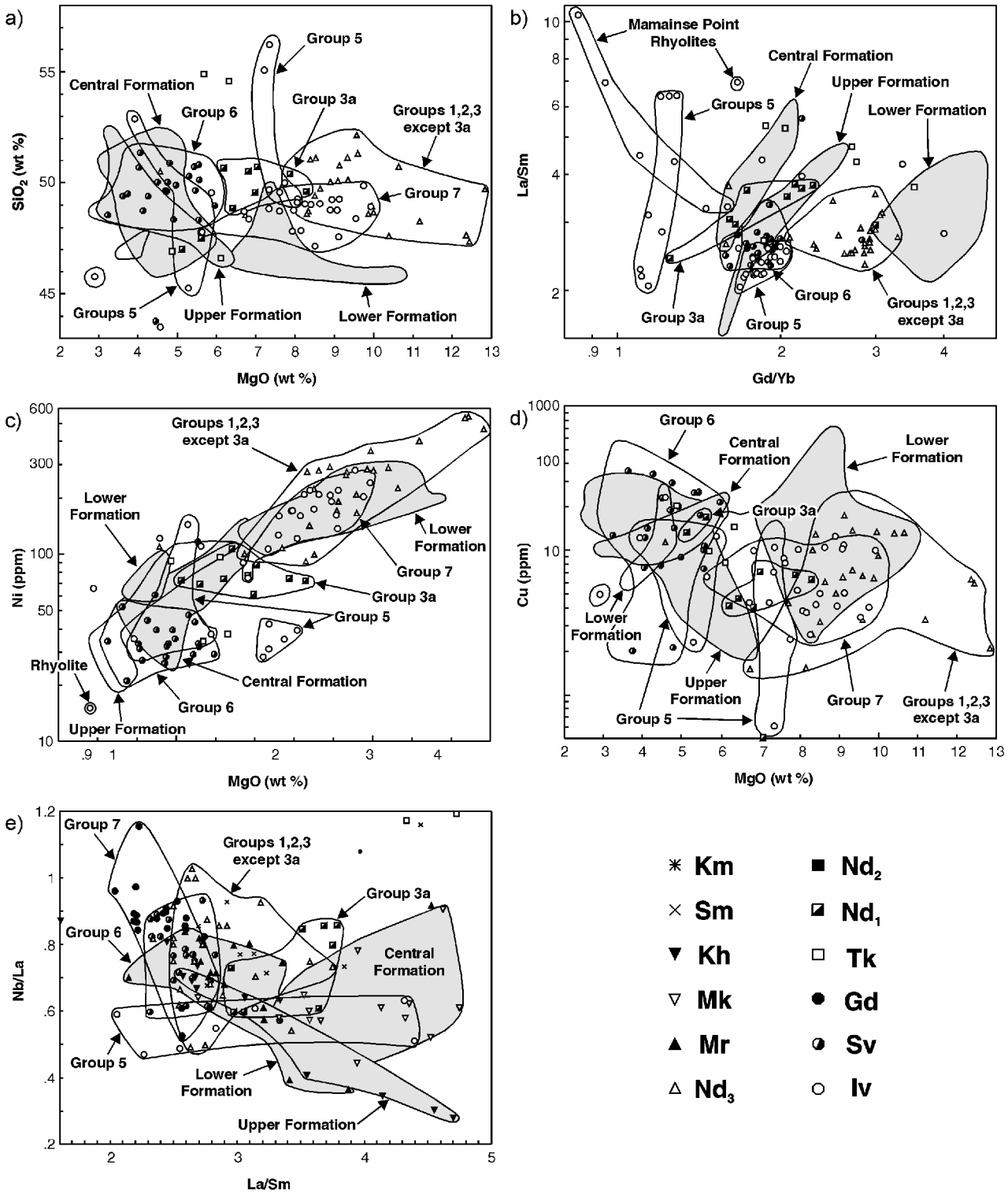

Figure 11. Geochemical variations in Keweenawan and Siberian Trap lavas. Data from Lightfoot et al., (1991a, 1993, 1994, Hawkesworth et al., 1995). **Iv** - Ivakinsky Formation; **Sv** - Sjverminsky Formation; **Gd** - Gudchichinsky Formation; **Tk** - Tuklonsky Formatioin; **Nd** - Nadezhdinsky Formation; **Mr** - Morongovsky Formation; **Mk** - Mokulaevsky Formation; **Kh** - Kharaelakhsky Formation; **Ku** - Kumginsky Formation; **Sm** - Samoedsky Formation; **Nd_{1-3}** - units of Nd showing progressively less contamination from Nd_1 to Nd_3.
Keweenawan: a) SiO_2 vs MgO; **b)** Cu vs MgO; **c)** Ni vs MgO; **d)** La/Sm vs Cd/Yb; **e)** Nb/La vs La/Sm. Shaded areas are for Osler Volcanic Group (OVG).

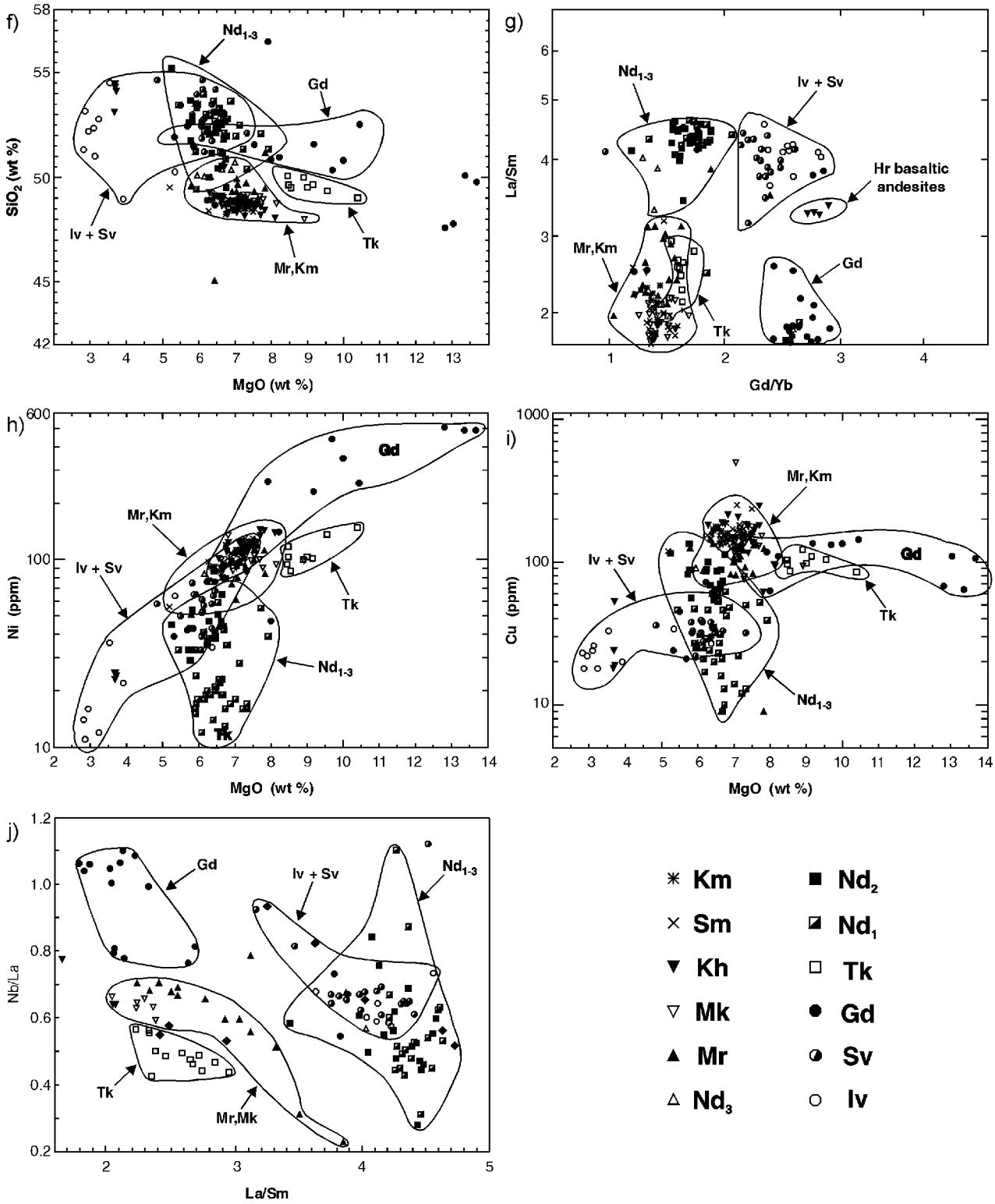

Figure 11. Geochemical variations in Keweenawan and Siberian Trap lavas. Data from Lightfoot et al., (1991a, 1993, 1994, Hawkesworth et al., 1995). **Iv** - Ivakinsky Formation; **Sv** - Sjverminsky Formation; **Gd** - Gudchichinsky Formation; **Tk** - Tuklonsky Formatioin; **Nd** - Nadezhdinsky Formation; **Mr** - Morongovsky Formation; **Mk** - Mokulaevsky Formation; **Kh** - Kharaelakhsky Formation; **Ku** - Kumginsky Formation; **Sm** - Samoedsky Formation; **Nd_{1-3}** - units of Nd showing progressively less contamination from Nd_1 to Nd_3.

Siberian Trap: f) SiO_2 vs MgO; **g)** La/Sm vs Gd/Yb; **h)** Ni vs MgO; **i)** Cu vs MgO; **j)** Nb/La vs La/Sm.

Data sources: this study; Lightfoot et al., (1991a,b, 1993, 1994); Lightfoot et al., (in prep - unpublished data); Hawkesworth et al., (1994).

Metric Conversion Table

Conversion from SI to Imperial			Conversion from Imperial to SI		
SI Unit	*Multiplied by*	*Gives*	*Imperial Unit*	*Multiplied by*	*Gives*
		LENGTH			
1 mm	0.039 37	inches	1 inch	**25.4**	mm
1 cm	0.393 70	inches	1 inch	**2.54**	cm
1 m	3.280 84	feet	1 foot	**0.304 8**	m
1 m	0.049 709	chains	1 chain	20.116 8	m
1 km	0.621 371	miles (statute)	1 mile (statute)	**1.609 344**	km
		AREA			
1 cm^2	0.155 0	square inches	1 square inch	**6.451 6**	cm^2
1 m^2	10.763 9	square feet	1 square foot	**0.092 903 04**	m^2
1 km^2	0.386 10	square miles	1 square mile	2.589 988	km^2
1 ha	2.471 054	acres	1 acre	0.404 685 6	ha
		VOLUME			
1 cm^3	0.061 023	cubic inches	1 cubic inch	**16.387 064**	cm^3
1 m^3	35.314 7	cubic feet	1 cubic foot	0.028 316 85	m^3
1 m^3	1.307 951	cubic yards	1 cubic yard	0.764 554 86	m^3
		CAPACITY			
1 L	1.759 755	pints	1 pint	0.568 261	L
1 L	0.879 877	quarts	1 quart	1.136 522	L
1 L	0.219 969	gallons	1 gallon	**4.546 090**	L
		MASS			
1 g	0.035 273 962	ounces (avdp)	1 ounce (avdp)	28.349 523	g
1 g	0.032 150 747	ounces (troy)	1 ounce (troy)	**31.103 476 8**	g
1 kg	2.204 622 6	pounds (avdp)	1 pound (avdp)	**0.453 592 37**	kg
1 kg	0.001 102 3	tons (short)	1 ton (short)	**907.184 74**	kg
1 t	1.102 311 3	tons (short)	1 ton (short)	**0.907 184 74**	t
1 kg	0.000 984 21	tons (long)	1 ton (long)	**1016.046 908 8**	kg
1 t	0.984 206 5	tons (long)	1 ton (long)	**1.016 046 90**	t
		CONCENTRATION			
1 g/t	0.029 166 6	ounce (troy)/ ton (short)	1 ounce (troy)/ ton (short)	34.285 714 2	g/t
1 g/t	0.583 333 33	pennyweights/ ton (short)	1 pennyweight/ ton (short)	1.714 285 7	g/t

OTHER USEFUL CONVERSION FACTORS

	Multiplied by	
1 ounce (troy) per ton (short)	31.103 477	grams per ton (short)
1 gram per ton (short)	0.032 151	ounces (troy) per ton (short)
1 ounce (troy) per ton (short)	20.0	pennyweights per ton (short)
1 pennyweight per ton (short)	0.05	ounces (troy) per ton (short)

Note: Conversion factors which are in bold type are exact. The conversion factors have been taken from or have been derived from factors given in the Metric Practice Guide for the Canadian Mining and Metallurgical Industries, published by the Mining Association of Canada in co-operation with the Coal Association of Canada.

ISSN 0826-9580
ISBN 0-7778-8984-6